Aalto University
School of Chemical
Technology

CHEM E5125 Thin Film Technology

Lecture 3 PVD 1

Plasma and ion bombardment

Jari Koskinen
jari.koskinen@aalto.fi

19.1.2021

Contents

- Plasma types
- Generation of plasma
- Ion solid interaction
- Thin film microstructure in PVD

Plasma

- Plasma
  - Gas of positive ions, electrons and (mostly) neutral atoms
  - Etymology: Greek: “moulded” - plasma fills the chamber
  - Charge neutrality $n_e = n_i$
  - Colliding electrons ionise atoms
  - Ions and electrons accelerate in electric field
  - Collisions excite atoms
  -

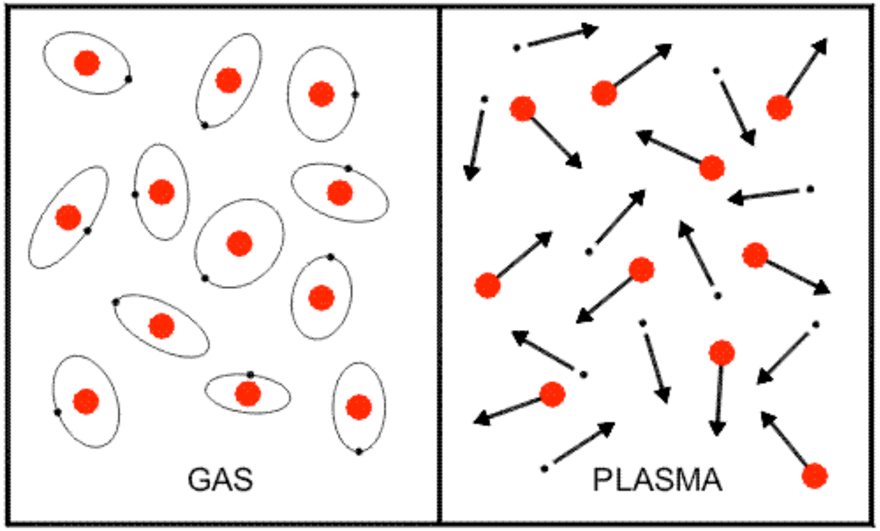

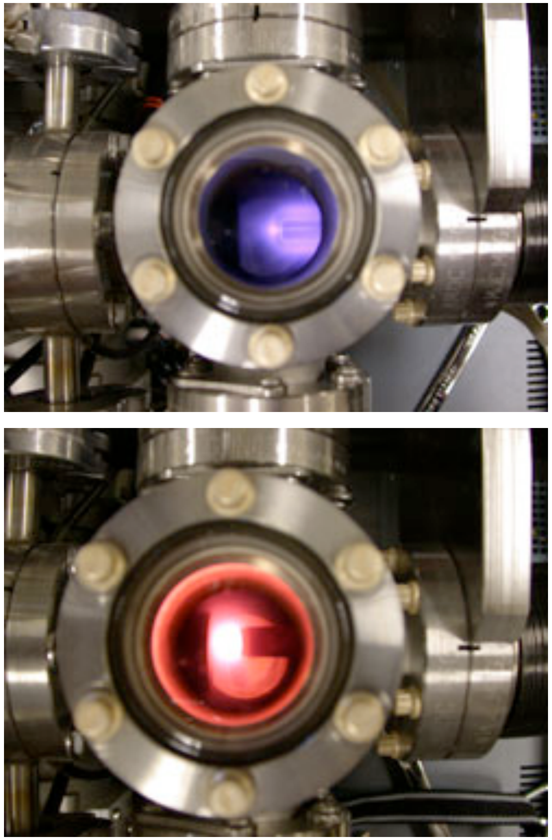

Glow discharge

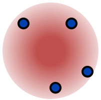

Glow discharge

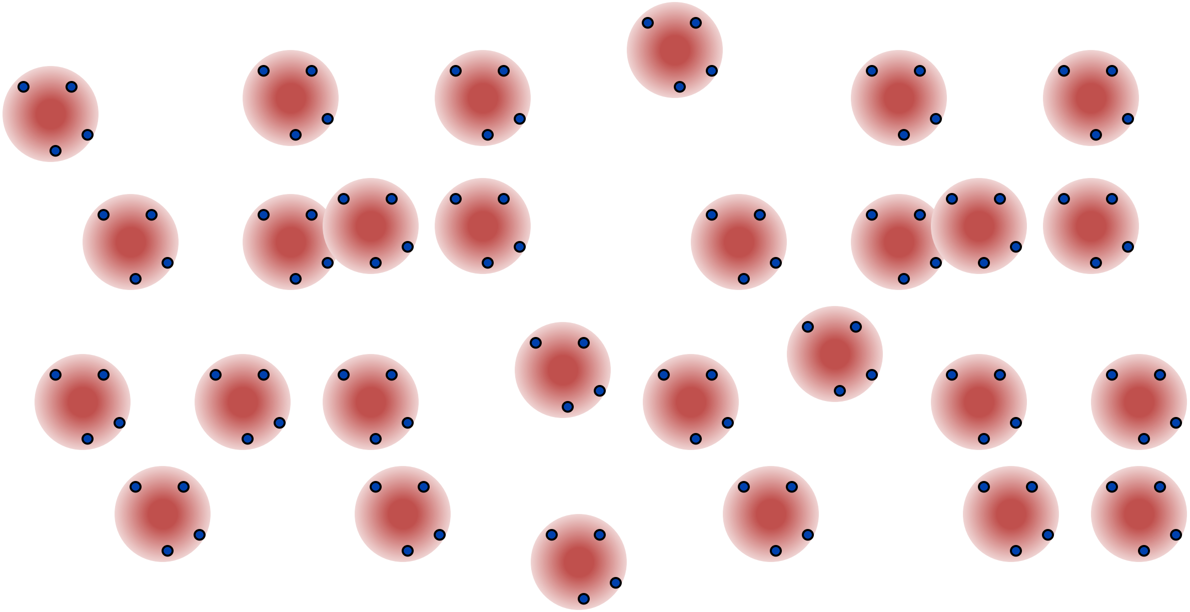

Glow discharge

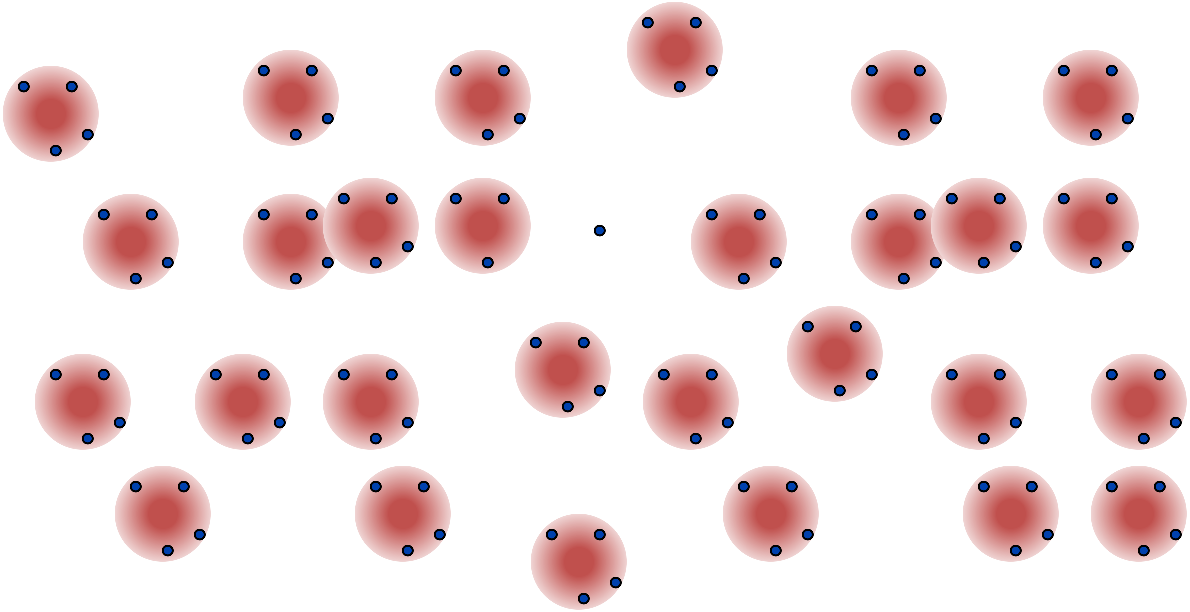

Glow discharge

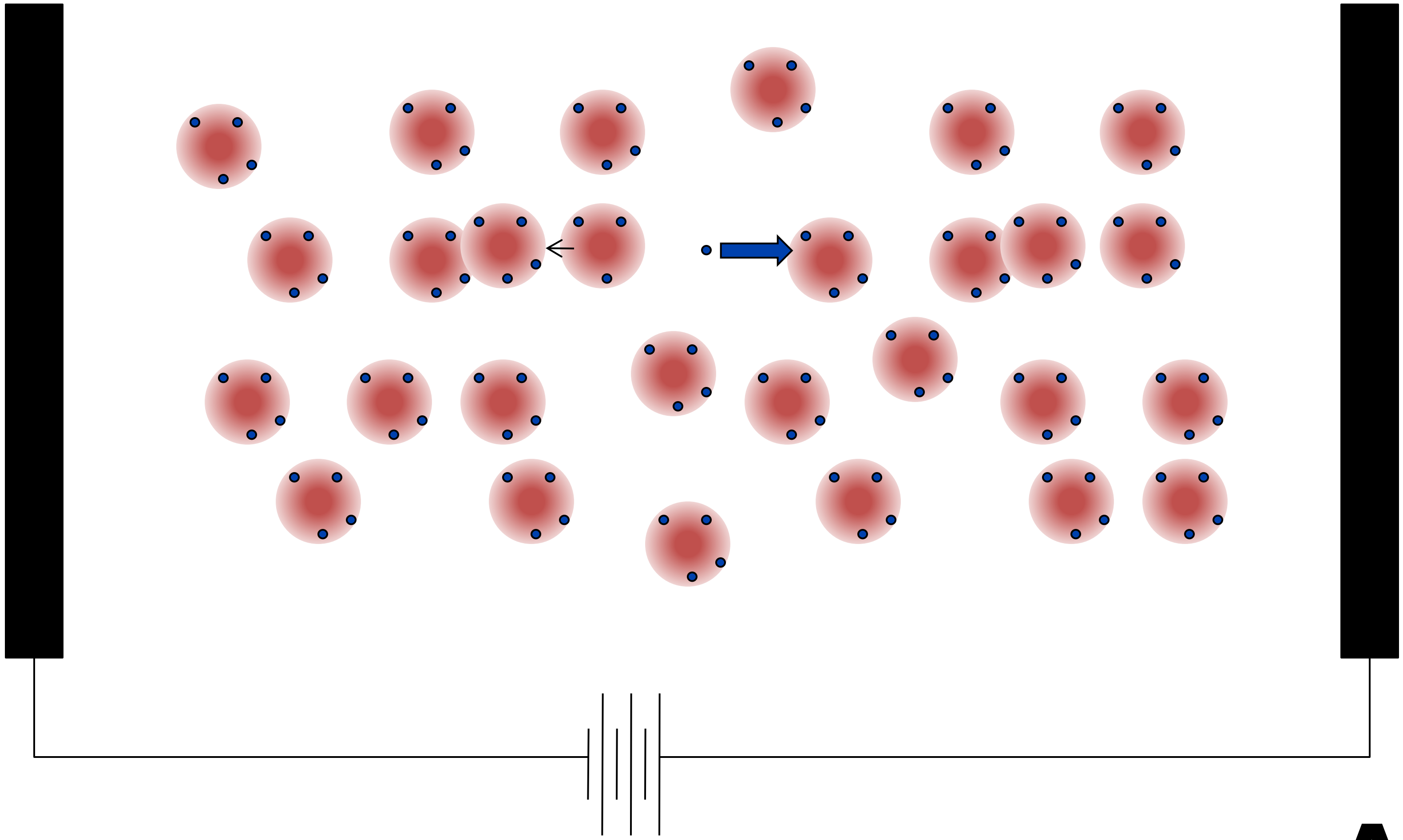

Jari Koskinen, Aalto University 2016

Aalto-yliopisto
Teknillinen korkeakoulu

Glow discharge

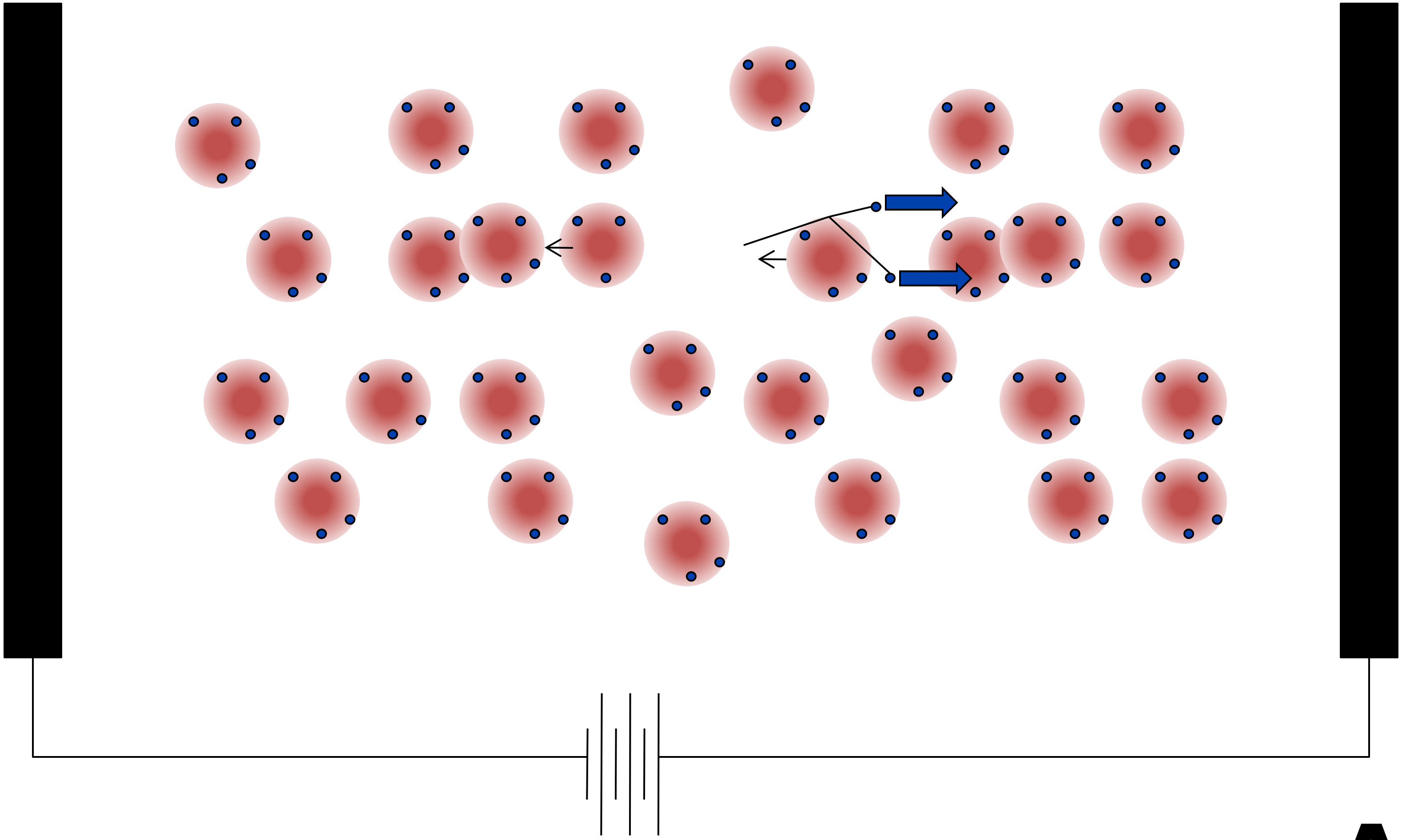

Glow discharge

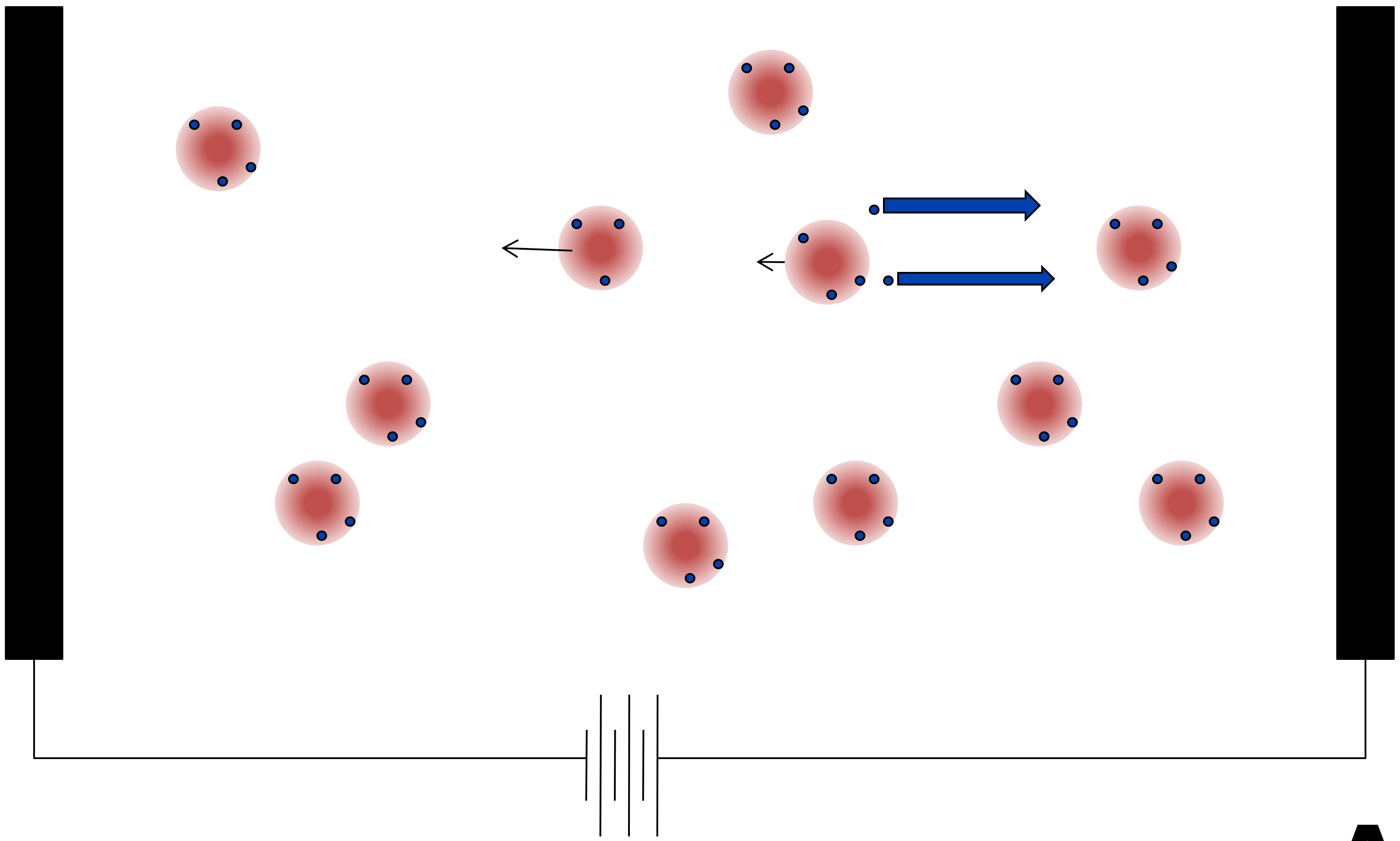

Glow discharge

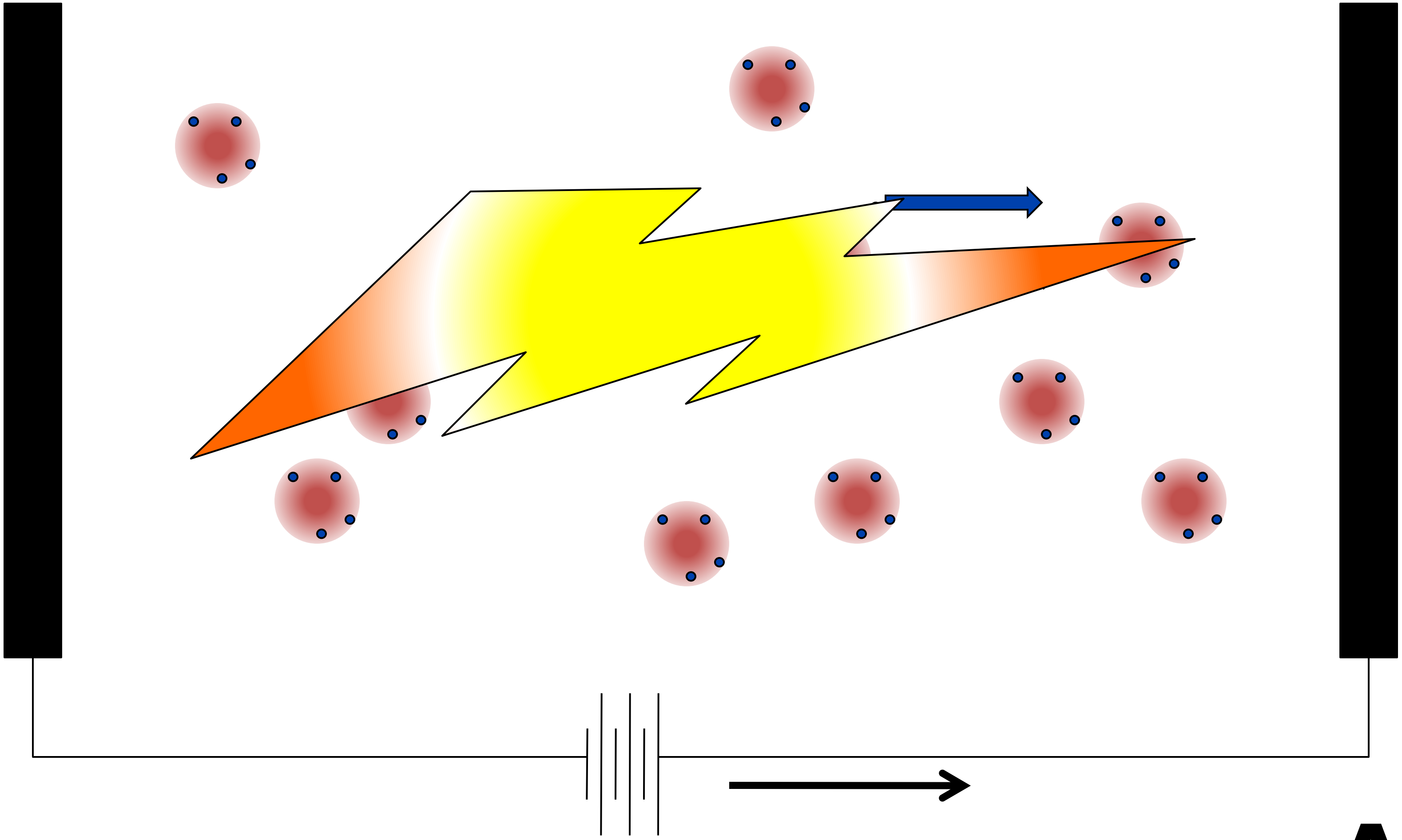

Jari Koskinen, Aalto University 2016

Aalto-yliopisto
Teknillinen korkeakoulu

DC Plasma glow discharge and arc

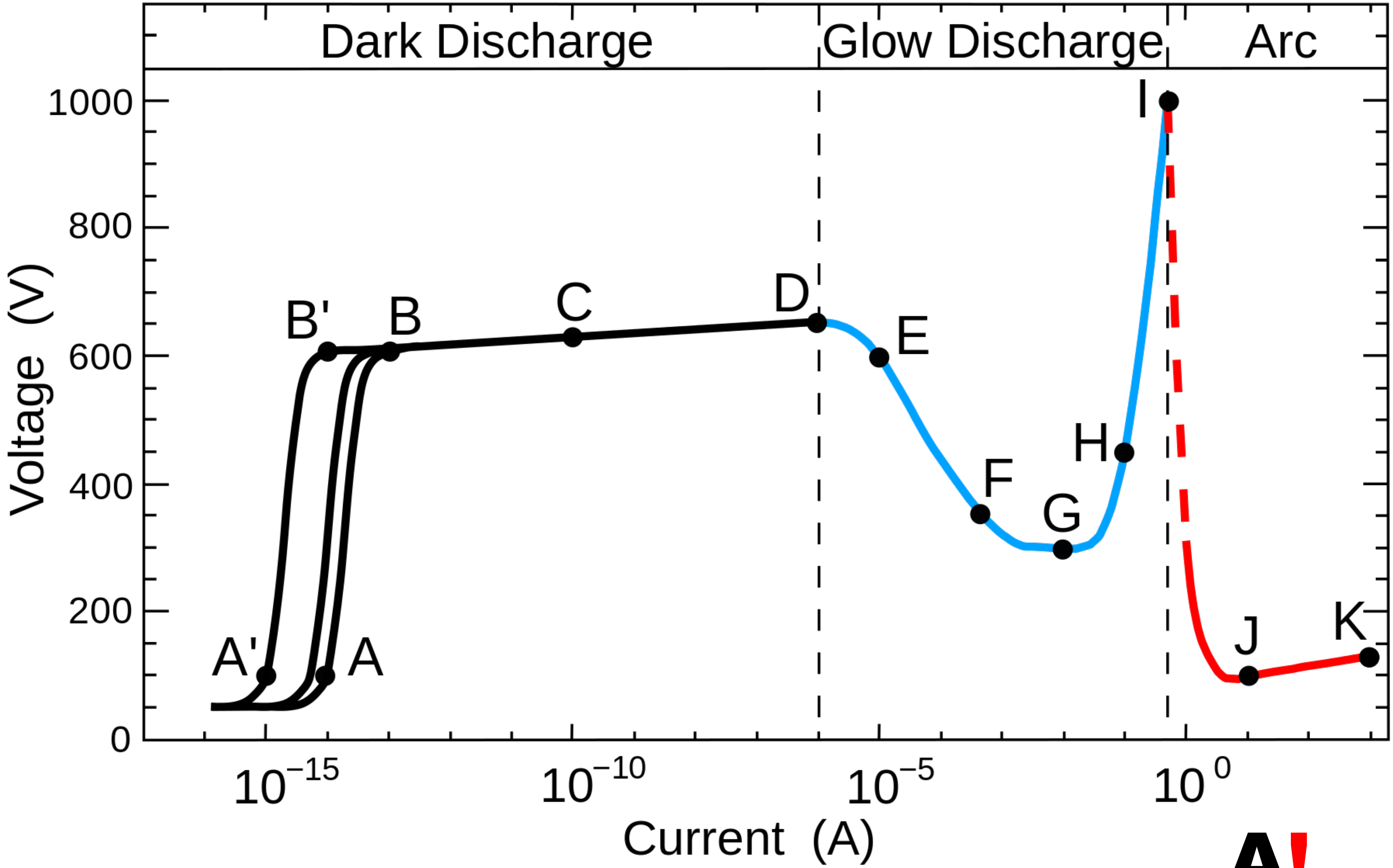

DC Plasma glow discharge and arc

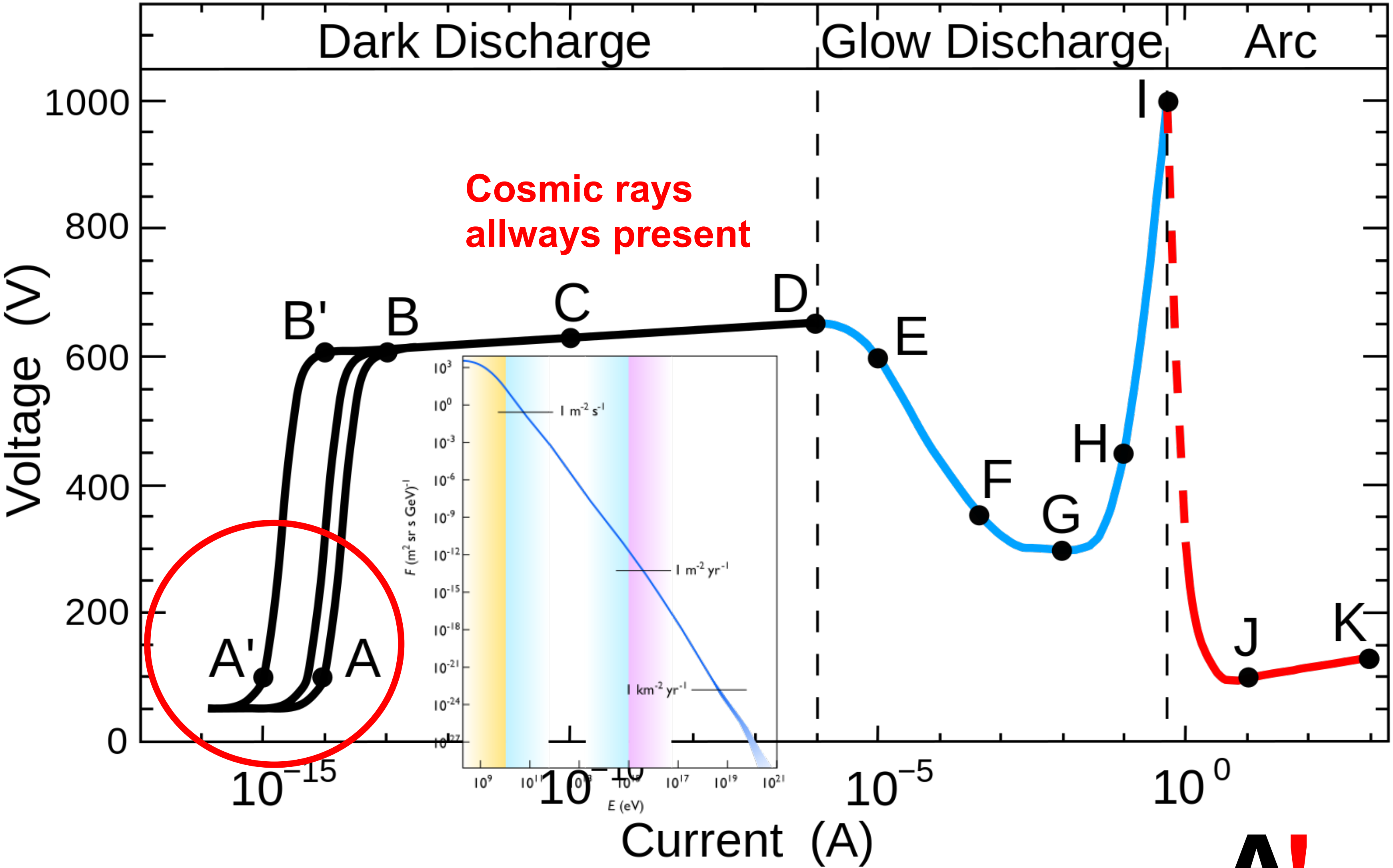

Cosmic rays allways present

DC Plasma glow discharge and arc

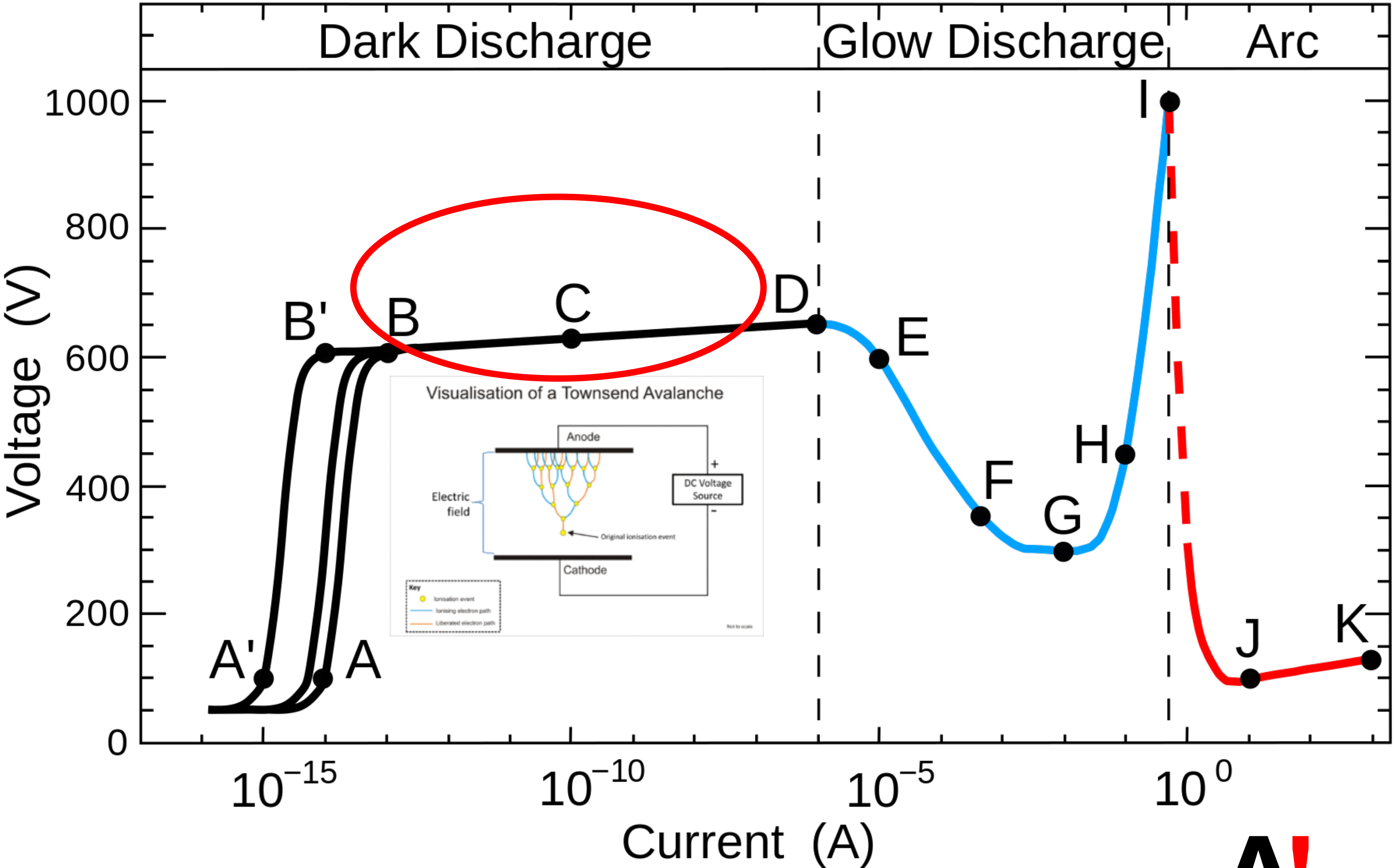

DC Plasma glow discharge and arc

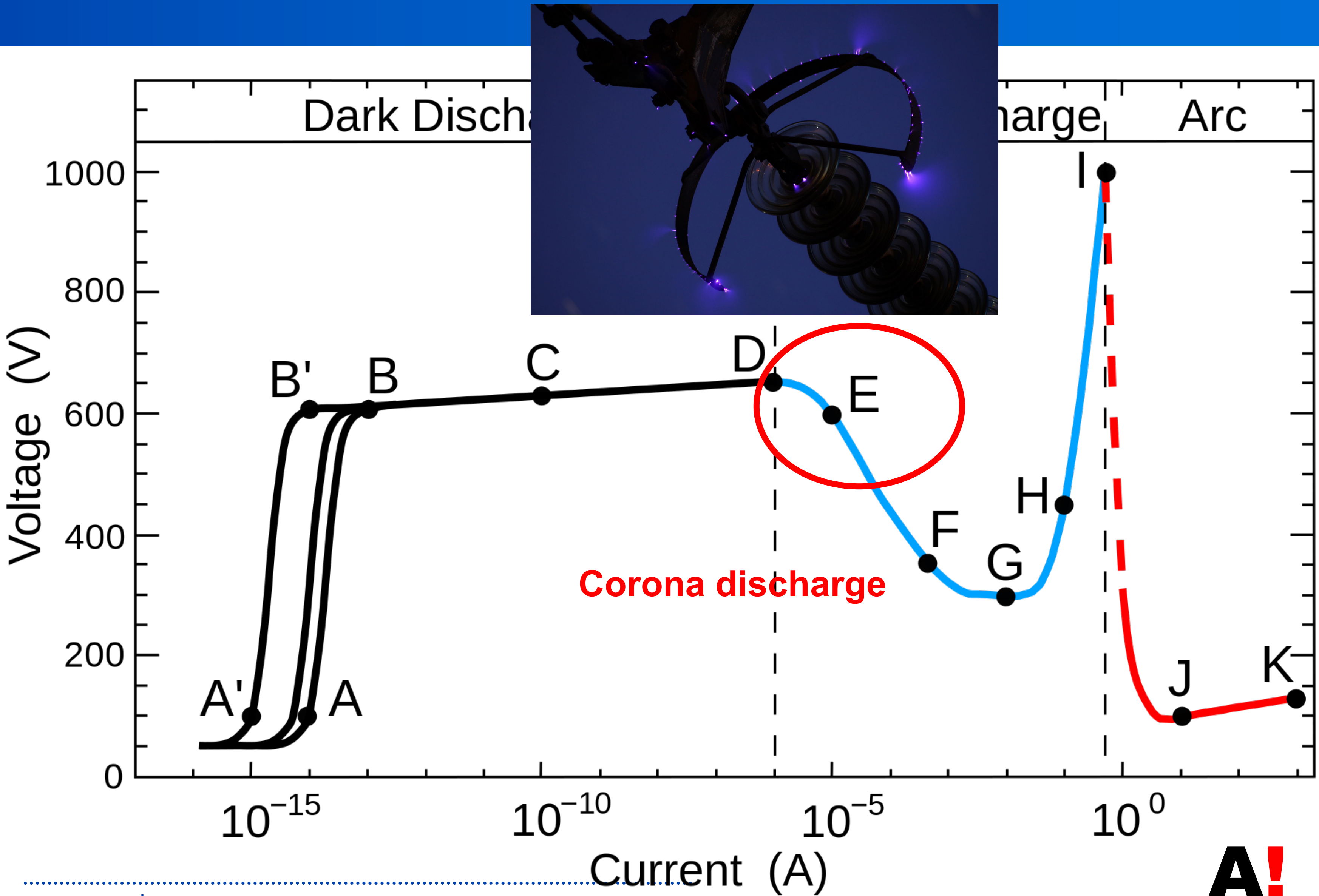

Corona discharge

DC Plasma glow discharge and arc

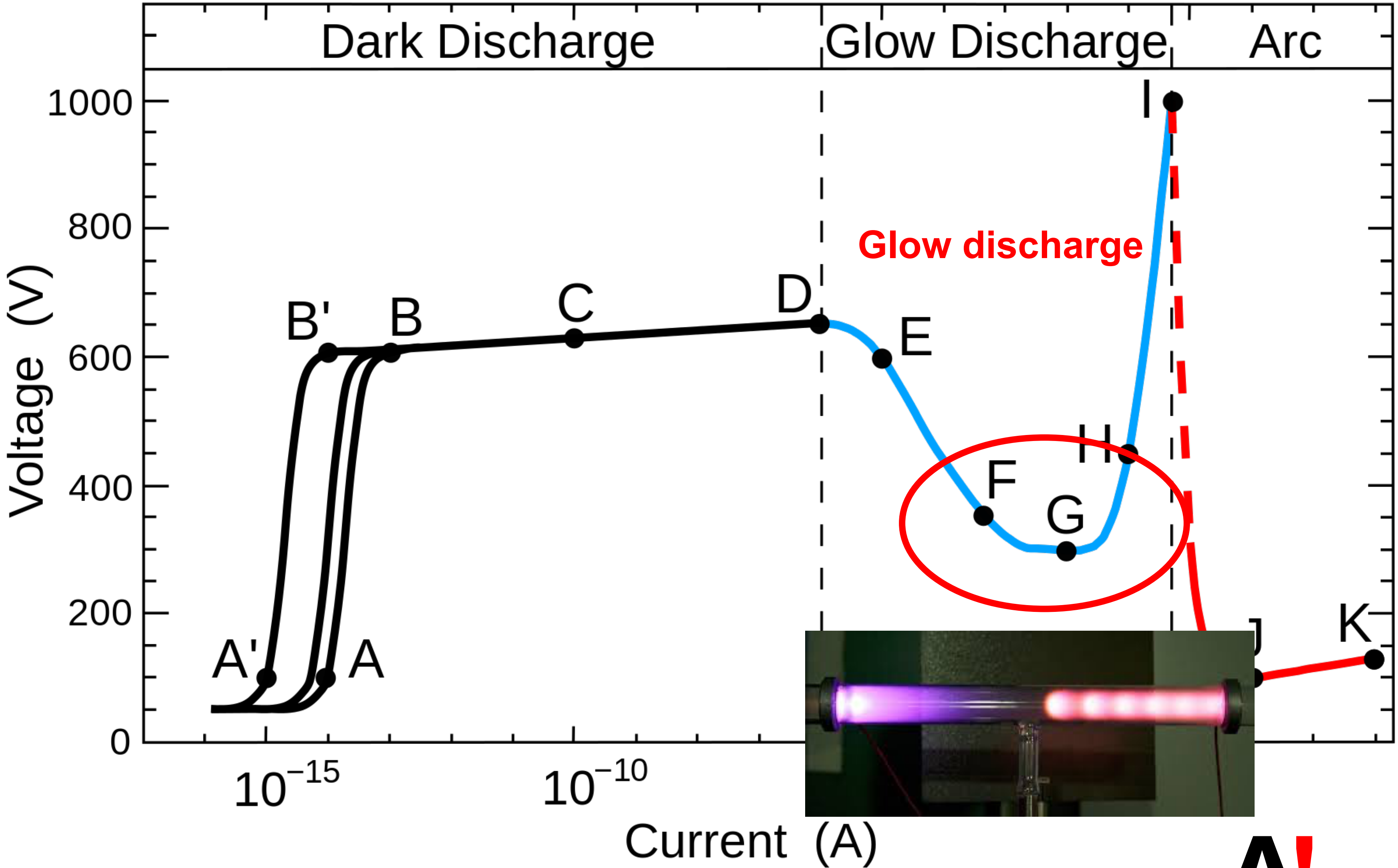

DC Plasma glow discharge and arc

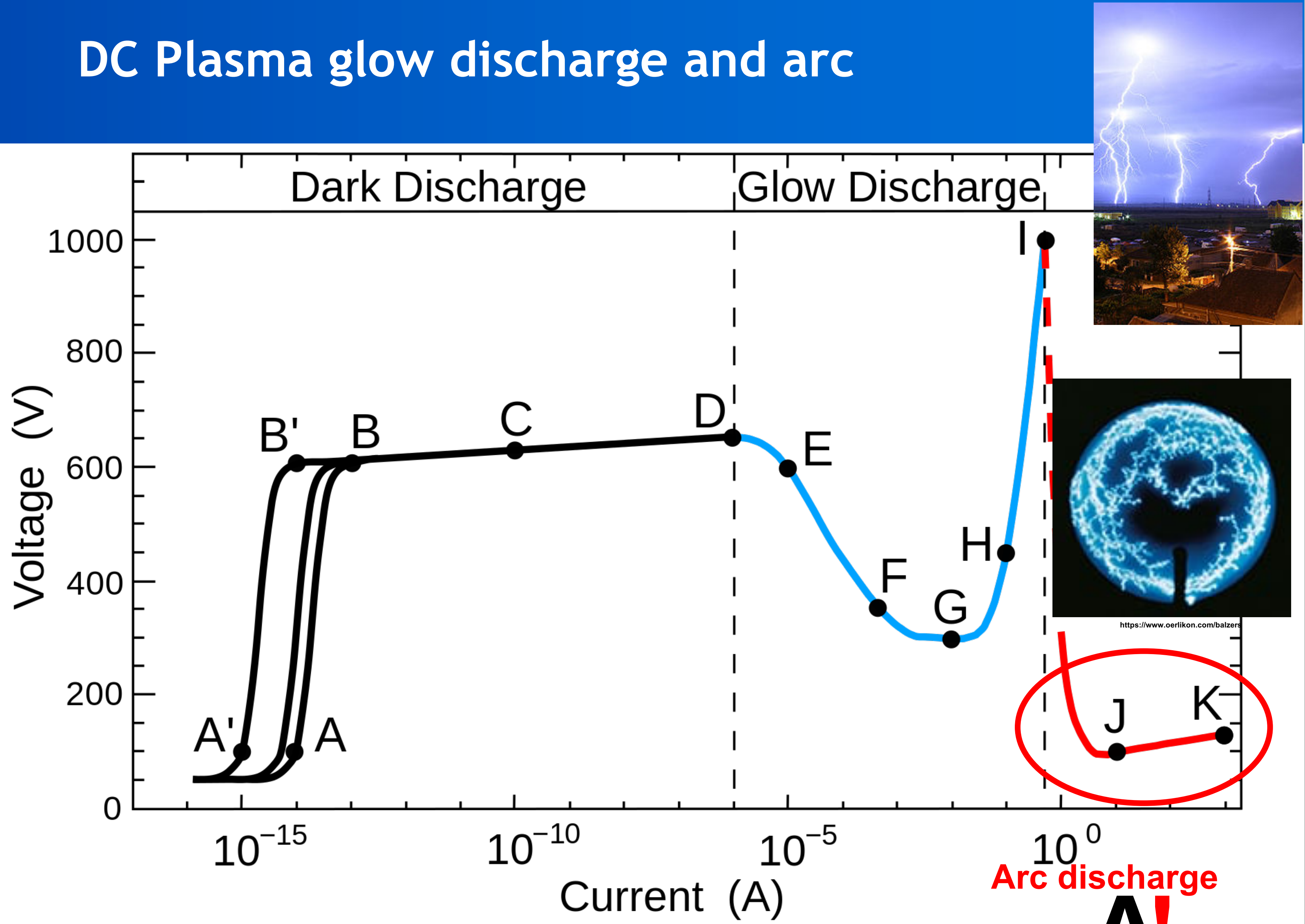

https://www.oerlikon.com/balzers

Glow discharge plasma

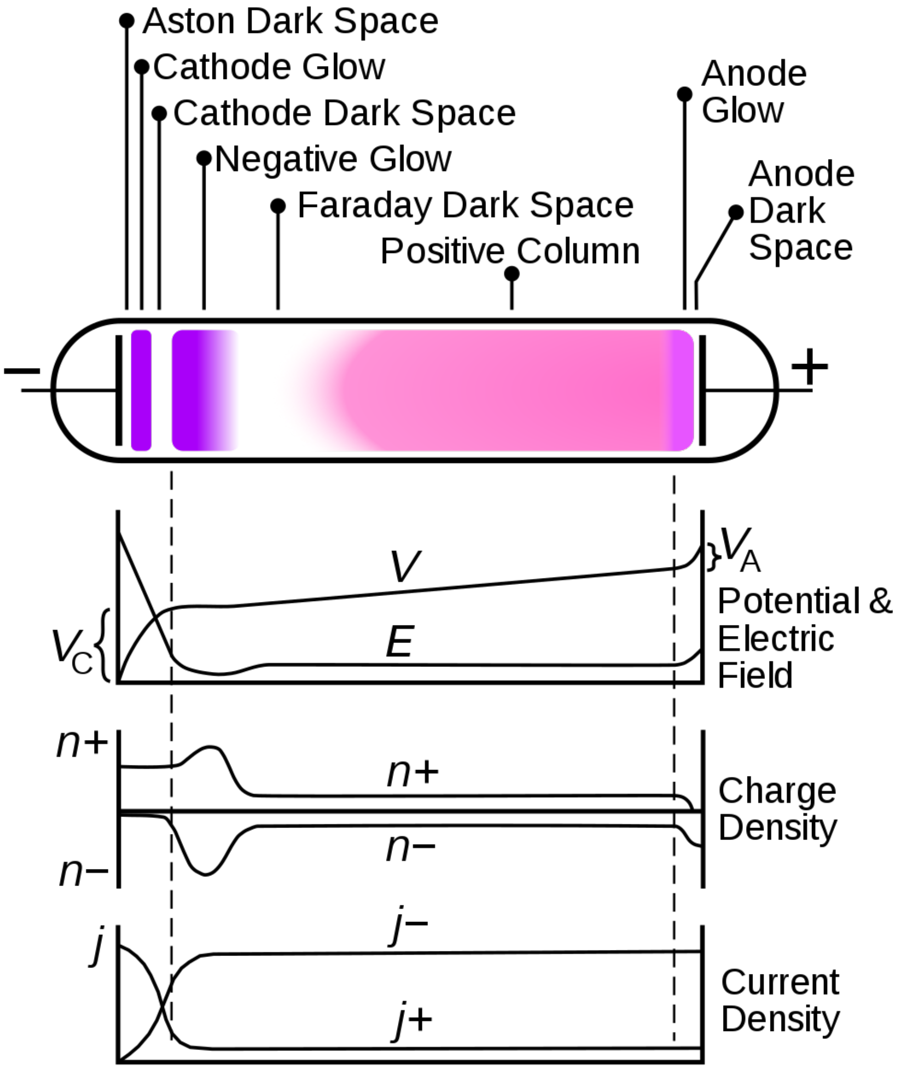

Aalto-yliopisto
Teknillinen korkeakoulu

Glow discharge plasma

For PVD
Interesting things happen here

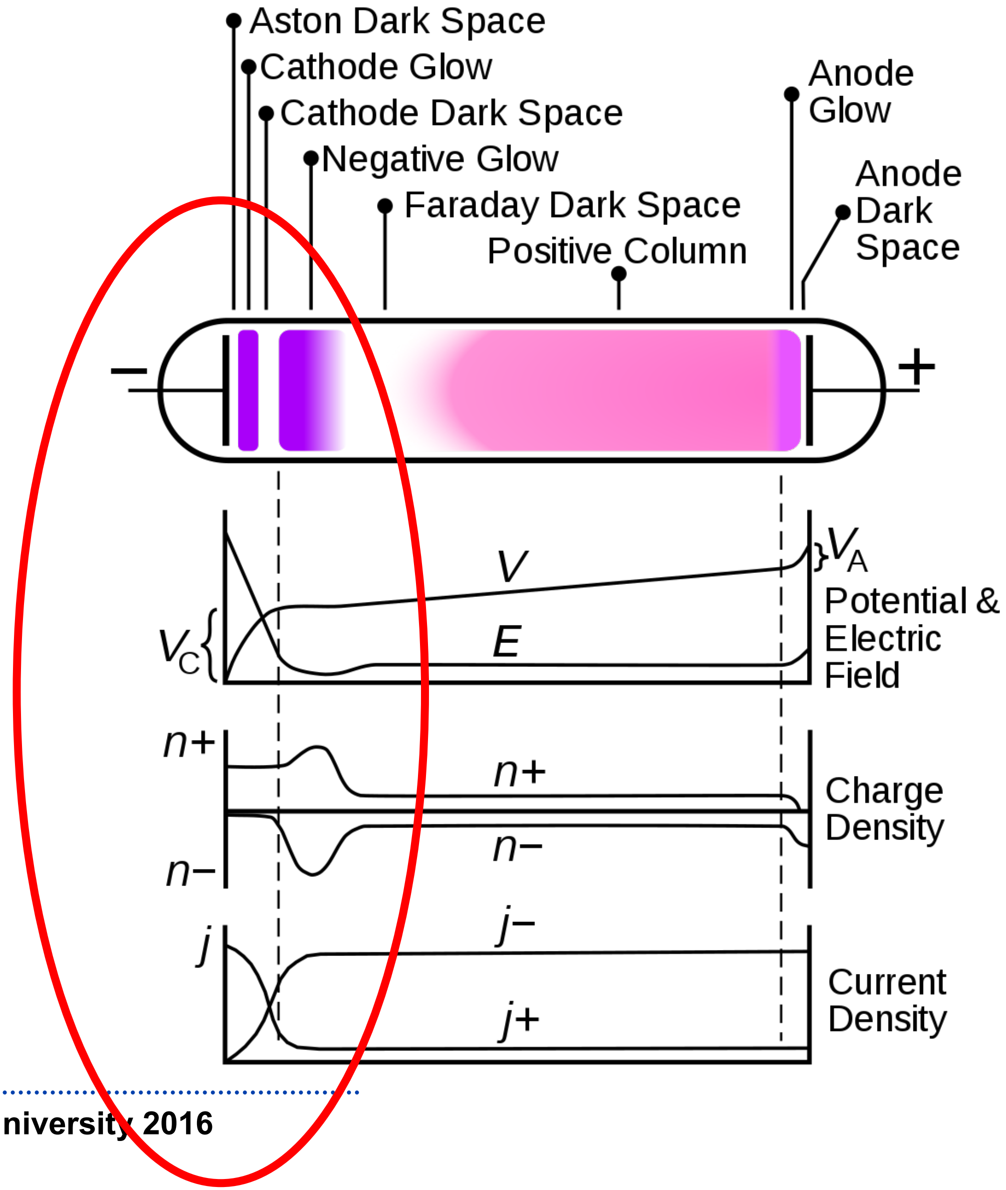

Breakdown voltage
Pasheschen minimum

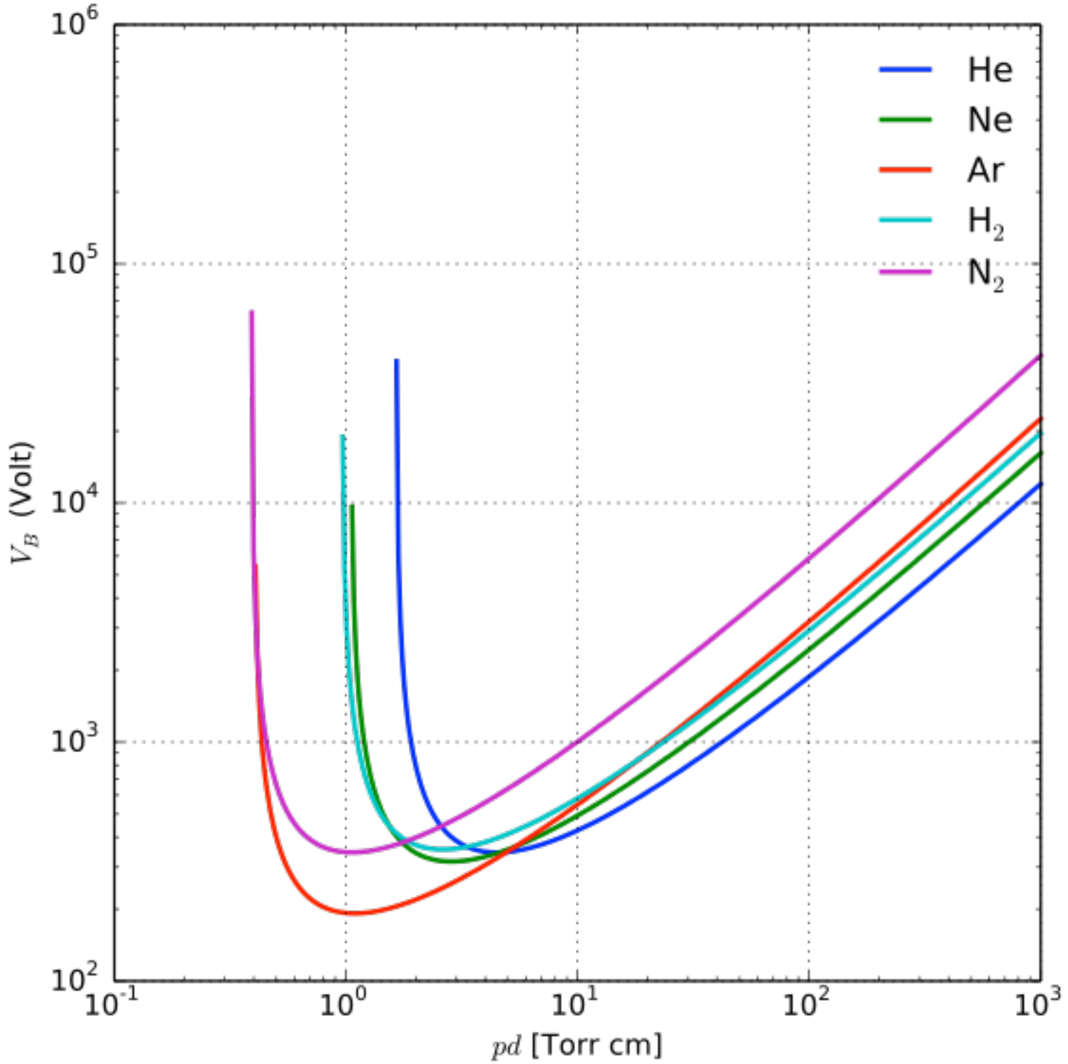

DC plasma

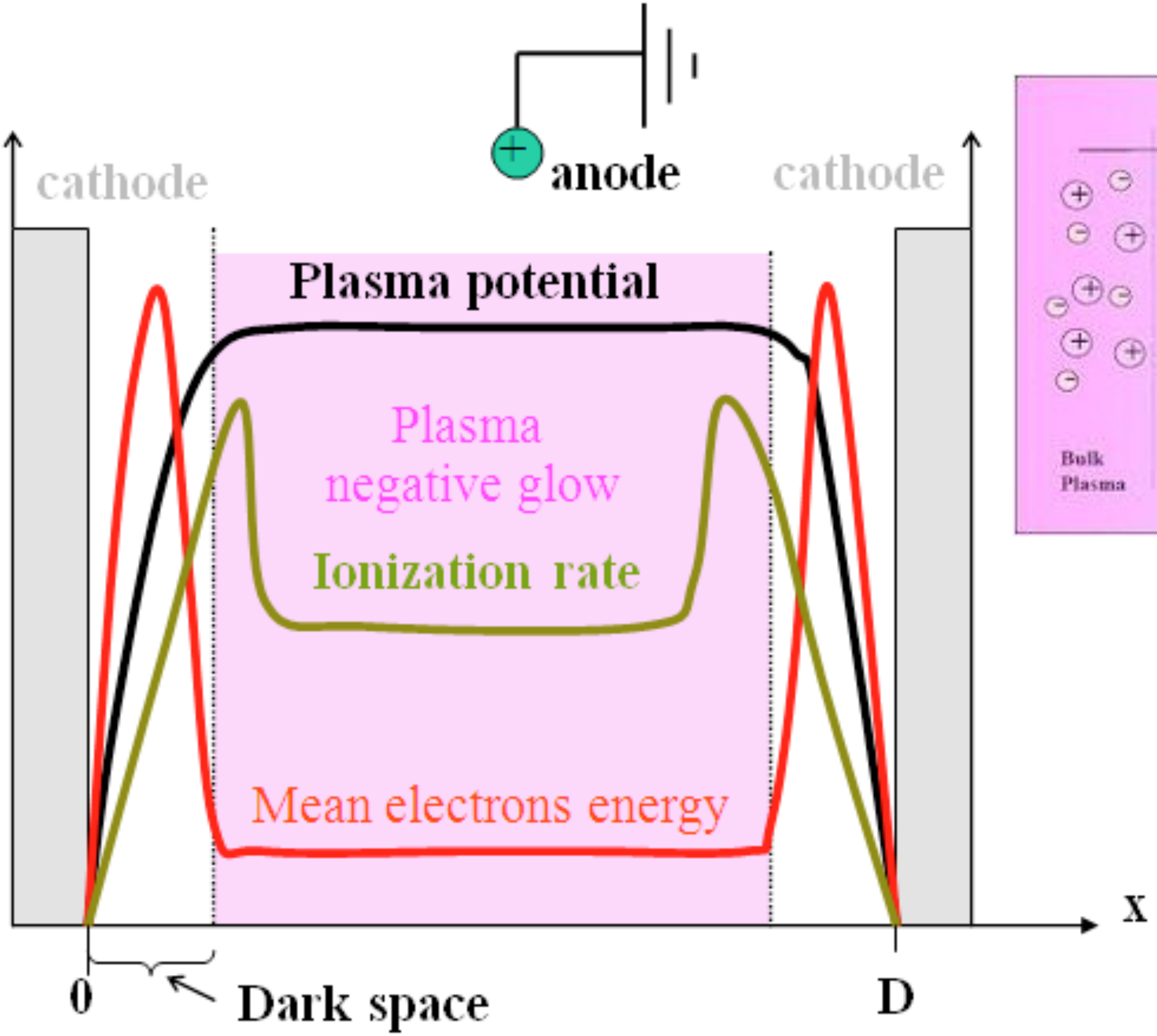
anode
cathode
cathode
Plasma potential
Plasma
negative glow
Ionization rate
Mean electrons energy
X
0
Dark space
D

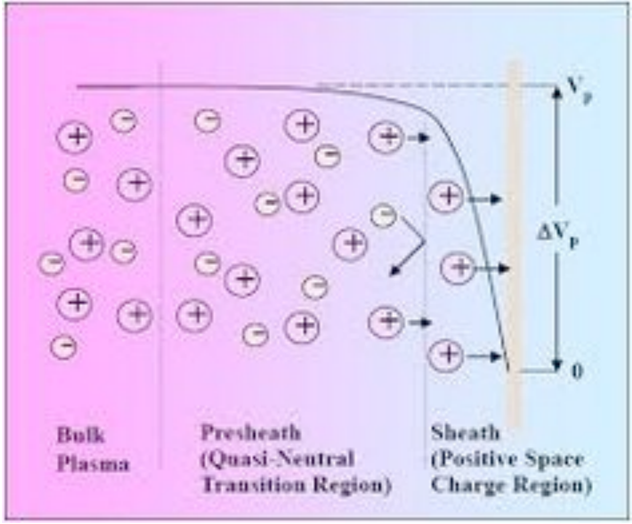
V_p
ΔV_p
0
Bulk
Plasma
Presheath
(Quasi-Neutral
Transition Region)
Sheath
(Positive Space
Charge Region)

Important plasma parameters

- Oscillations
- Debye length
- mean free path
- ionization crossection

Plasma oscillation

Assume: n_0 fixed ions (+) & n_0 moving electrons (–)

Apply a small electric field $\mathbf{E}_1$

→ electrons move:

$$\begin{aligned} n_+ &= n_0 \\ n_- &= n_0 + n_1(\mathbf{r},t) \quad ; \quad n_1 \ll n_0 \end{aligned}$$

Electron continuity equation:

$$\frac{\partial n}{\partial t} + \nabla \cdot (n\mathbf{u}) = 0$$

$$n = n_0 + n_1(\mathbf{r},t) \quad ; \mathbf{u} = \underset{0}{\cancel{\mathbf{u}_0}} + \mathbf{u}_1(\mathbf{r},t)$$

($\mathbf{u}_0 = 0$ ↔ electrons are assumed cold)

$$\underset{0}{\cancel{\frac{\partial n_0}{\partial t}}} + \frac{\partial n_1}{\partial t} + \nabla \cdot ((n_0 + n_1)\mathbf{u}_1) = 0 \quad \Rightarrow \quad \frac{\partial n_1}{\partial t} + n_0 \nabla \cdot \mathbf{u}_1 + \nabla \cdot (\underset{0 \text{ 2nd order}}{\cancel{n_1 \mathbf{u}_1}}) = 0$$

Linearized continuity equation (1st order terms only):

$$\frac{\partial n_1}{\partial t} + n_0 \nabla \cdot \mathbf{u}_1 = 0 \quad !!$$

Force: $\mathbf{F} = q\mathbf{E} \Rightarrow m_e \frac{\partial \mathbf{u}_1}{\partial t} = -e\mathbf{E}_1$

1st Maxwell: $\nabla \cdot \mathbf{E}_1 = -en_1/\epsilon_0$

$$\Rightarrow \quad \frac{\partial^2 n_1}{\partial t^2} + \left(\frac{n_0 e^2}{\epsilon_0 m_e}\right) n_1 = 0$$

$$\omega_{pe}^2 = \frac{n_0 e^2}{\epsilon_0 m_e} \quad \boxed{\text{plasma frequency}}$$

Hannu Koskinen Univ of Helsinki

Debye screening

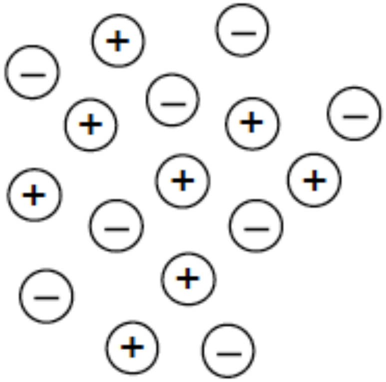

Coulomb potential of each charge: $\varphi = \frac{q}{4\pi\epsilon_0 r}$

Assume thermal equilibrium (Boltzmann distribution)

$$n_\alpha(\mathbf{r}) = n_{0\alpha} \exp\left(-\frac{q_\alpha \varphi}{k_B T_\alpha}\right)$$

α labels the particle populations (e.g., e, p)

Introduce a test charge q_T. What will be its potential?

Home exercise: $\varphi = \frac{q_T}{4\pi\epsilon_0 r} \exp\left(-\frac{r}{\lambda_D}\right)$; $\lambda_D^{-2} = \frac{1}{\epsilon_0} \sum_\alpha \frac{n_{0\alpha} q_\alpha^2}{k_B T_\alpha}$

Debye length: $\lambda_D \propto \sqrt{\frac{T}{n}}$

Plasma parameter: $\Lambda = n_0 \lambda_D^3 \gg 1$

Number of particles in a Debye sphere: $N = \frac{4\pi}{3} n_0 \lambda_D^3$

"Definition of plasma"

$$\frac{1}{\sqrt[3]{n_0}} \ll \lambda_D \ll L$$

L is the size of the system

Collisions

Cross section: σ (m^2) Mean free path: $l_{mfp} = 1/(n\sigma)$

Collision frequency: $\nu_c = n\sigma v$

Hannu Koskinen Univ of Helsinki

n = density of atoms (and ions)

Total collistion cross section:

$\sigma_{total} = \sigma_{exitation} + \sigma_{ion} + \sigma_{attachment} + \sigma_{other}$

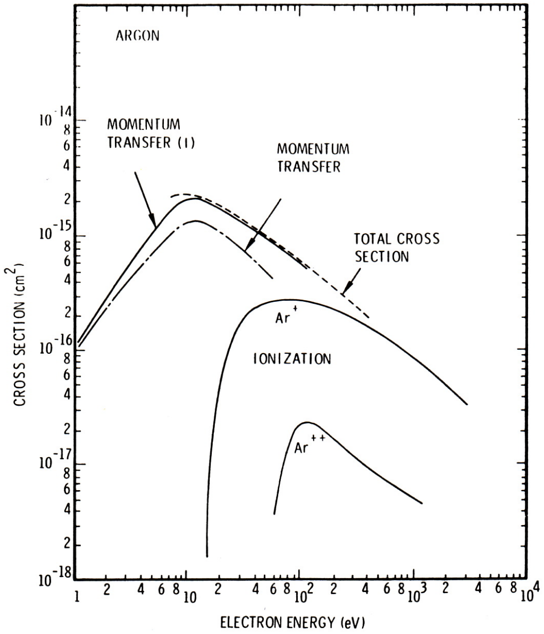

Figure 2.1. Collision cross sections for electrons in Ar gas (from Ref. 1).

Bunshah, Handbook of Deposition Technologies for Films and Coatings Noyes

Different types of plasmas

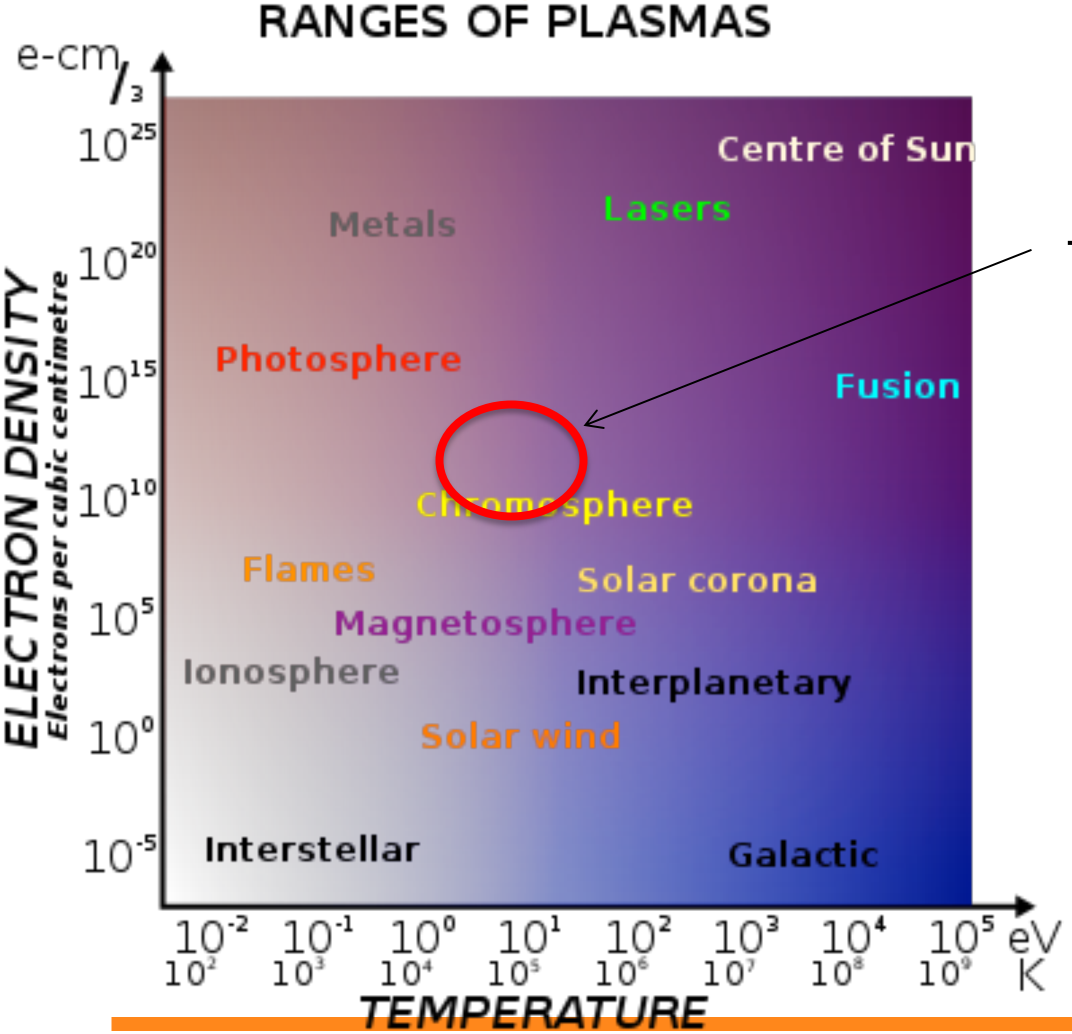

Thin film plasma processes

Wikipedia

Aalto University
School of Chemical
Technology

Electron temperature

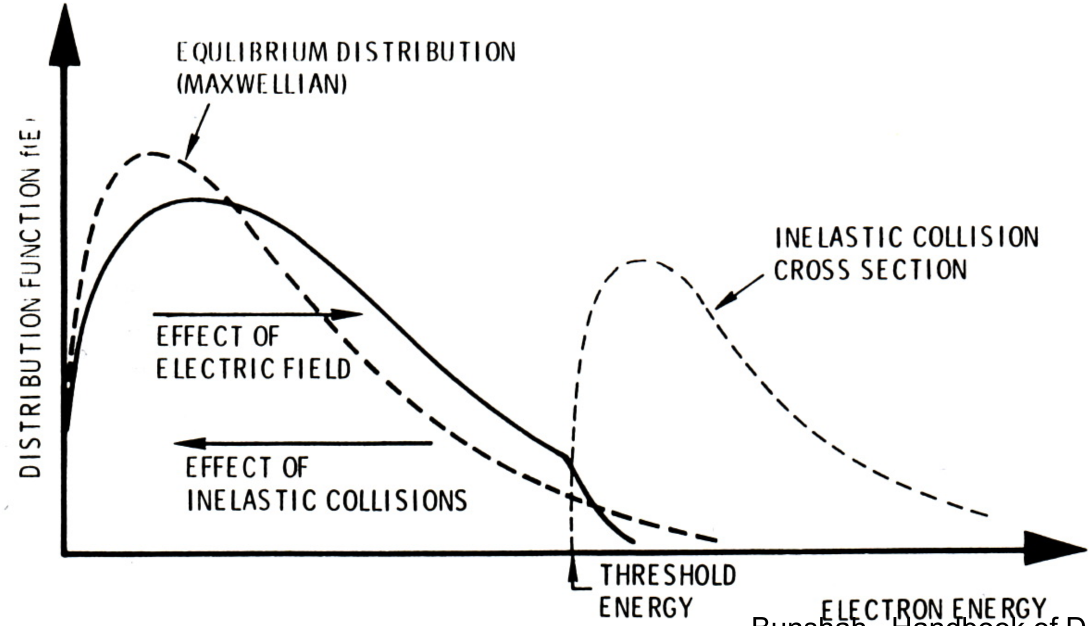

Bunshah, Handbook of Deposition Technologies for Films and Coatings Noyes

Figure 2.4. Schematic illustration of electron energy distribution function and inelastic collision cross section.

Electron and ion temperature

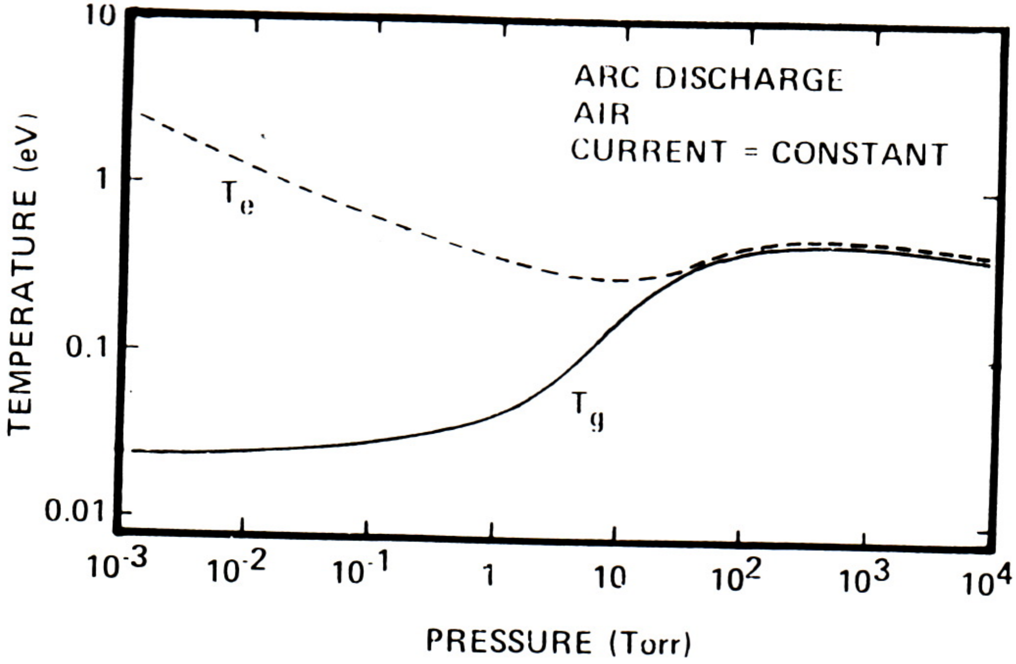

Figure 2.3. Electron (T_e) and gas temperatures (T_g) in an air arc as a function of pressure (from Ref. 5).

Bunshah, Handbook of Deposition Technologies for Films and Coatings Noyes

Plasma sheath

Sheath thickness $d_s \sim$ constant* λ_D
constant $\approx 5 - 40$
Glow discharge $d_s \approx 0.15 - 2$ mm

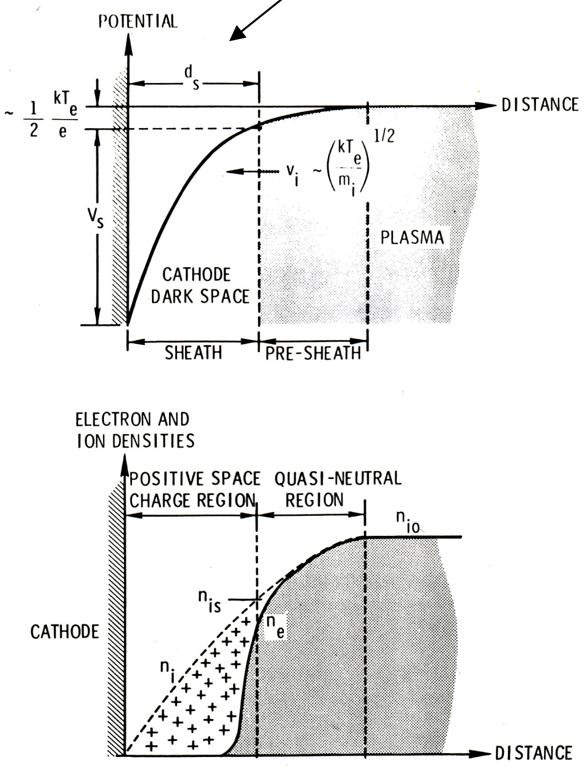

Figure 2.9. Schematic representation of the positive space-charge sheath that develops over a cathode (from Ref. 1).

Bunshah, Handbook of Deposition Technologies for Films and Coatings Noyes

Cold cathode discharge

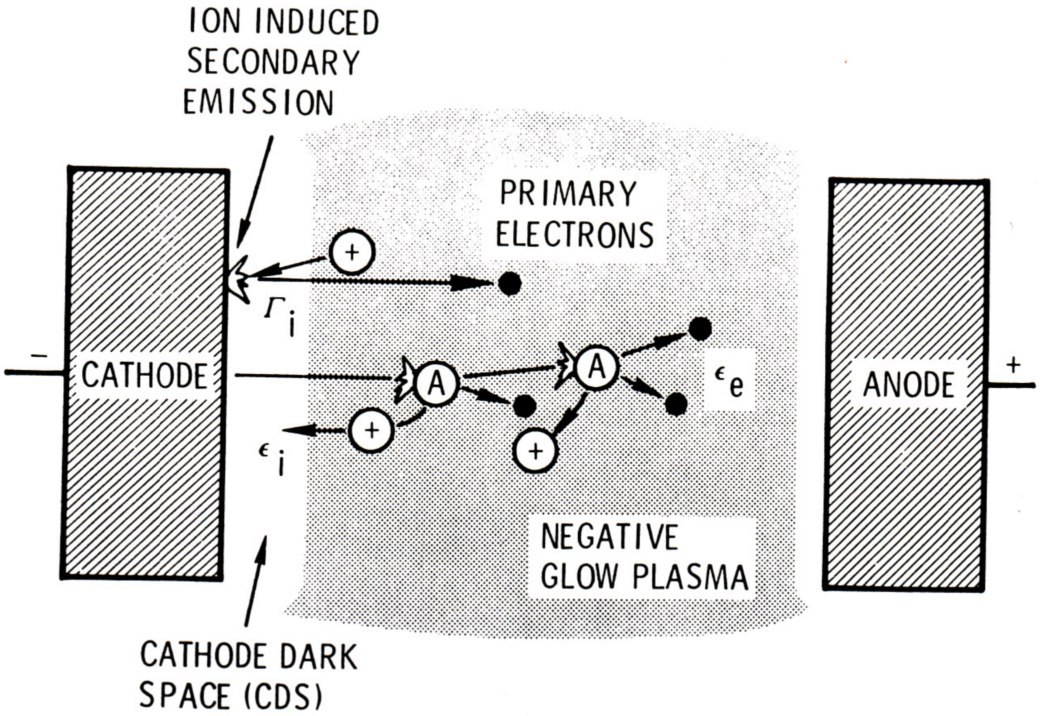

Figure 2.18. Schematic illustration of a cold-cathode discharge.

Bunshah, Handbook of Deposition Technologies for Films and Coatings Noyes

Luminous regions in DC plasma

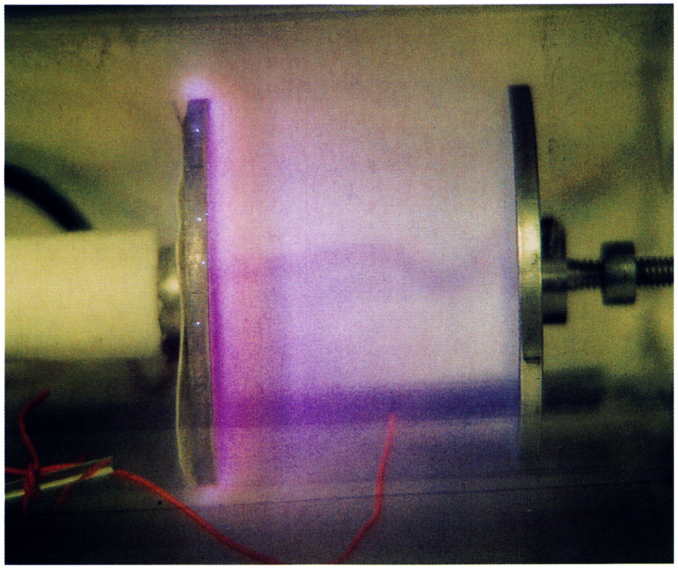

Colorplate VI.18 A DC glow discharge in argon. The anode (grounded) is on the right and the cathode (supported by a white teflon insulator) on the left. The orange wire is a Langmuir probe whose bare tip enters the positive column of the discharge. The positive column is the largest luminous region, which extends about 75% of the way from the anode toward the cathode. The pressure was 100 mtorr and the voltage applied between cathode and anode was 1 kV. The discharge current density was 0.22 mA/cm².

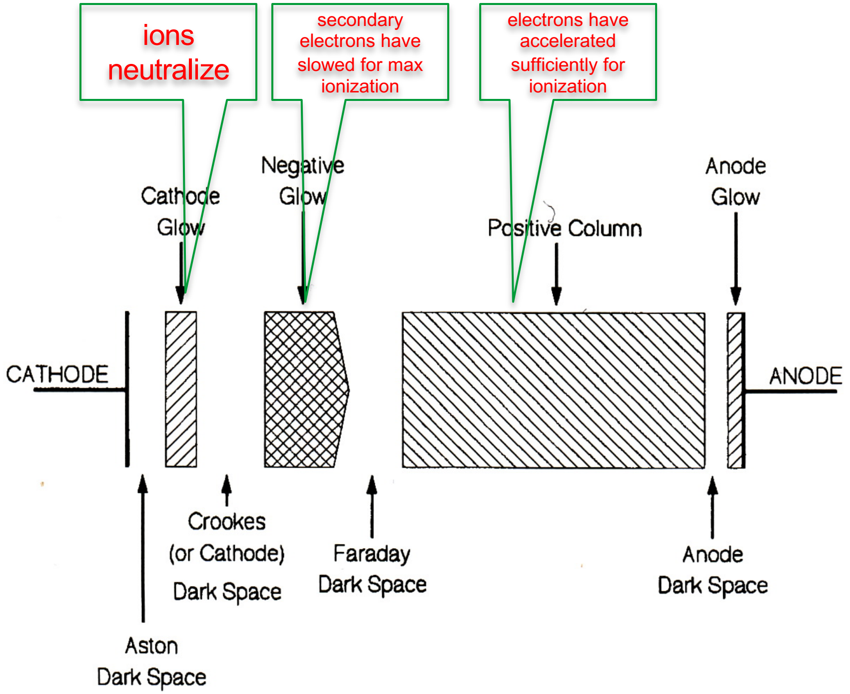

ions neutralize

secondary electrons have slowed for max ionization

electrons have accelerated sufficiently for ionization

Figure VI.17 The classical luminous and dark regions of a DC glow discharge, based on classifications by early researchers [Holland, 1956; Maissel and Glang, 1970; Brown, 1966; Nasser, 1971, Llewellyn-Jones, 1966; Cobine, 1941; von Engel, 1965].

Mahan, Physical Vapor Deposition of Thin Films, Wiley

Practical sputtering plasma -1

- Argon pressure 1 torr
- atom density (n) 3 x 10^{16} cm^{-3}
- n_i=n_e 10^{10} cm^{-3}
- ionization fraction 3 x 10^{-7} (weakly ionized plasma)
- ion temperature T_i 300K
- electron temperature T_e 23,000K

Practical sputtering plasma -2

- VDC 1000V
- Vp 8V
- Current density at cathode 2 mA/cm^2
- Cathode sheath L 2 mm
- mean free path λ 50 μm

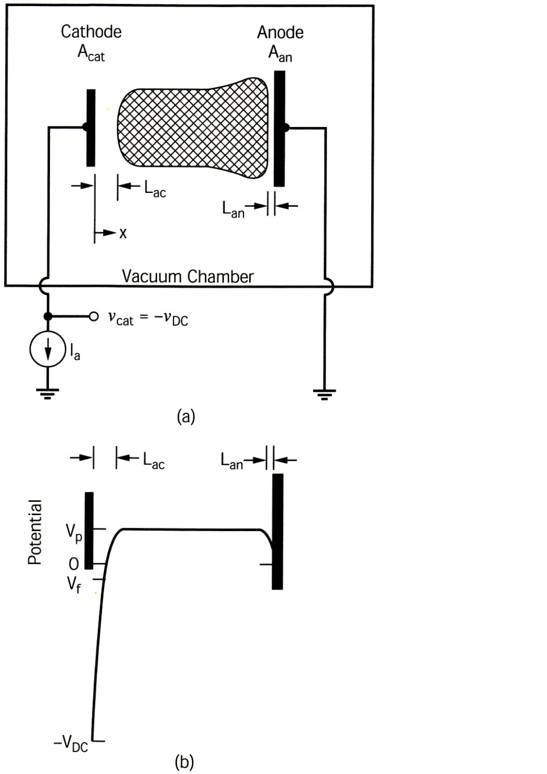

Figure VI.8 (*a*) Schematic diagram of a DC sputtering discharge; (*b*) the potential profile (not to scale, as $V_p - V_f$ is typically much less than V_{DC}).

Mahan, Physical Vapor Deposition of Thin Films, Wiley

Circuit models of DC plasma discharge

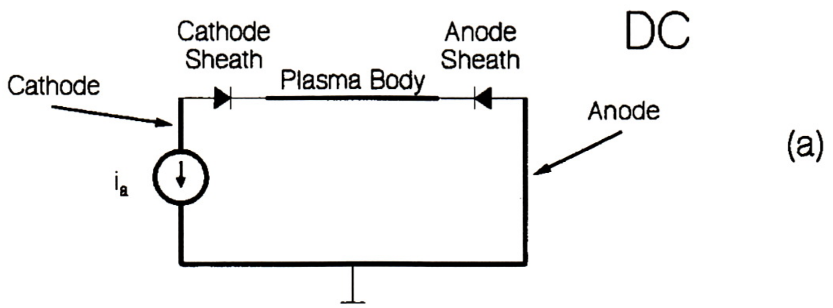

Figure VI.9 Circuit models for (*a*) a DC sputtering discharge and (*b*) a capacitive RF sputtering discharge.

Mahan, Physical Vapor Deposition of Thin Films, Wiley

Ion energy at cathode

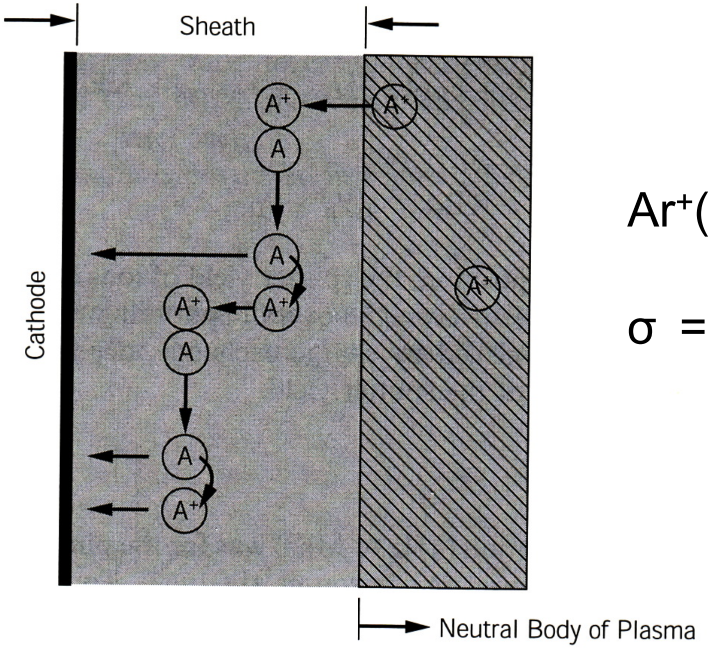

Figure VI.10 The process of symmetric charge exchange within the cathode sheath. When two charge exchange events occur, as shown here, a single ion entering the sheath is converted into two neutrals plus an ion, all of which strike the cathode (but with kinetic energies corresponding to only a fraction of the cathode fall).

$Ar^+(hot) + Ar(cold) \rightarrow Ar(hot) + Ar^+(cold)$

$\sigma = 2.5 \times 10^{-15}\ cm^{-3}$

Mahan, Physical Vapor Deposition of Thin Films, Wiley

AC plasma methods

AC plasma

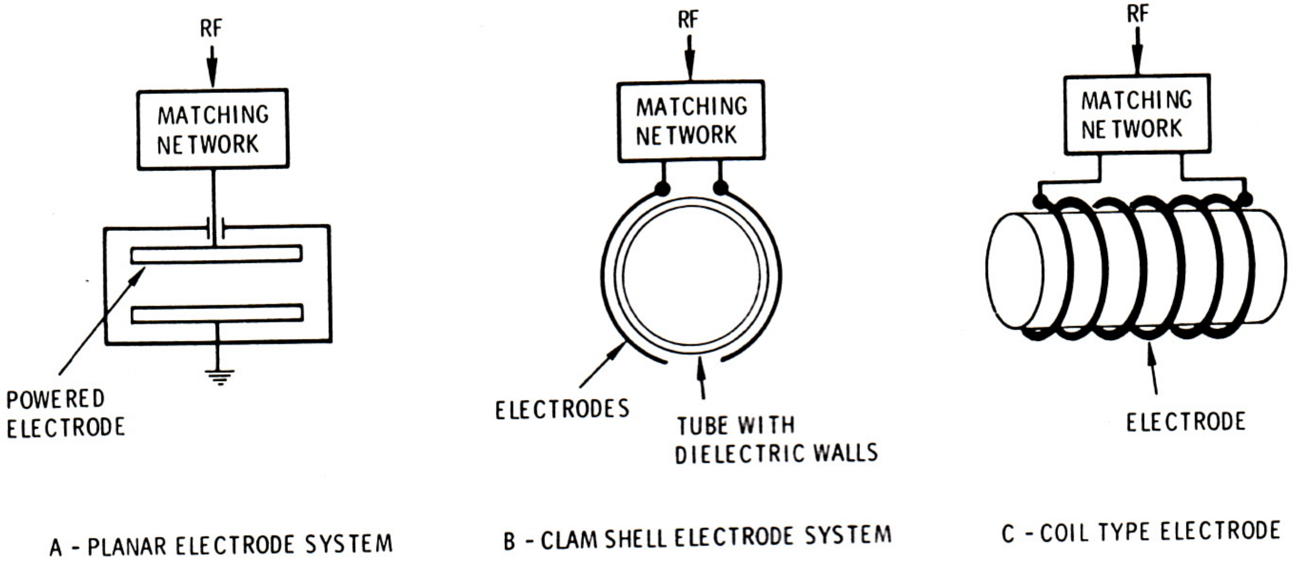

Figure 2.12. Schematic illustration of glow discharge devices commonly used in plasma-assisted materials processing.

Bunshah, Handbook of Deposition Technologies for Films and Coatings Noyes

Forming of self-bias in AC discharge

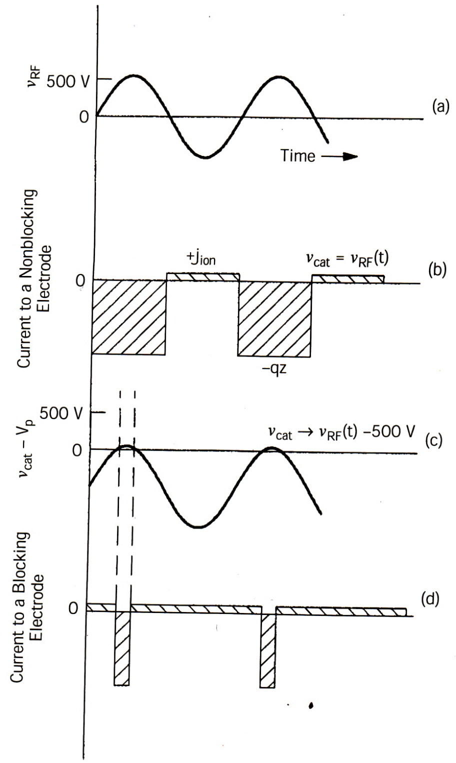

Figure VI.11 DC self-bias. Potentials and currents for RF excitation of (*a*–*b*) nonblocking and (*c*–*d*) blocking electrodes.

Mahan, Physical Vapor Deposition of Thin Films, Wiley

Self bias at electrodes

$$\frac{V_1}{V_2} = \left(\frac{A_2}{A_1}\right)^n$$

n= 4 (sometimes 2)

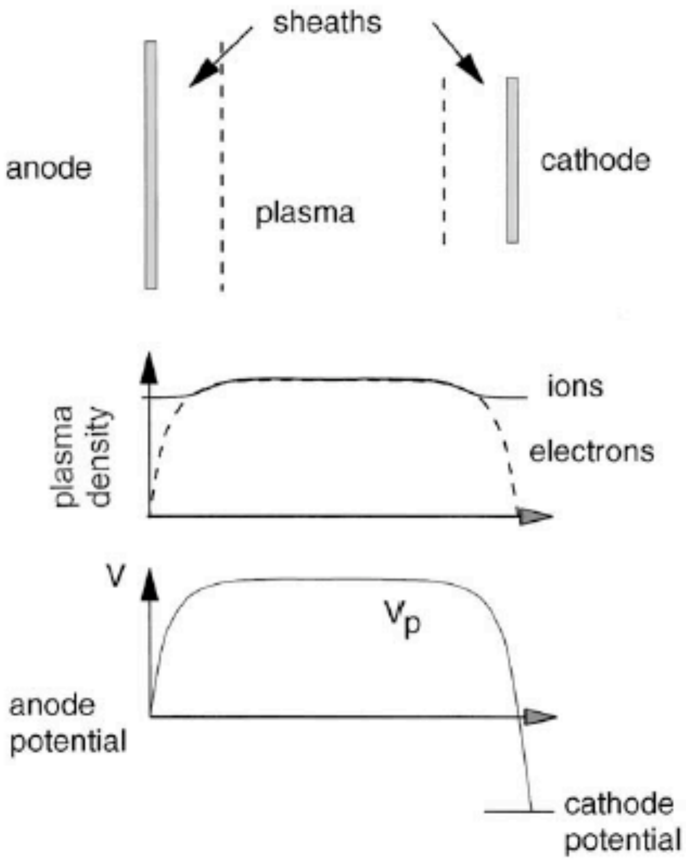

Fig. 7. Electron and ion distributions which create sheaths between the neutral plasma and the walls.

Circuit models of RF plasma discharge

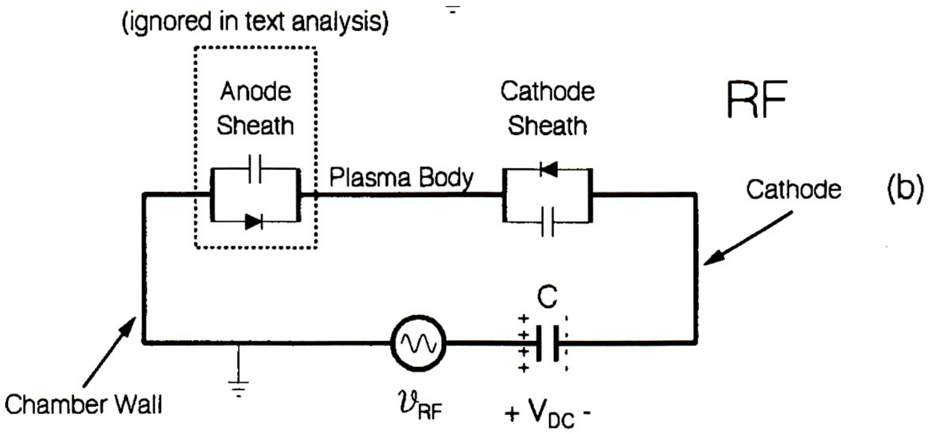

Figure VI.9 Circuit models for (*a*) a DC sputtering discharge and (*b*) a capacitive RF sputtering discharge.

Mahan, Physical Vapor Deposition of Thin Films, Wiley

RF Plasma glow discharge

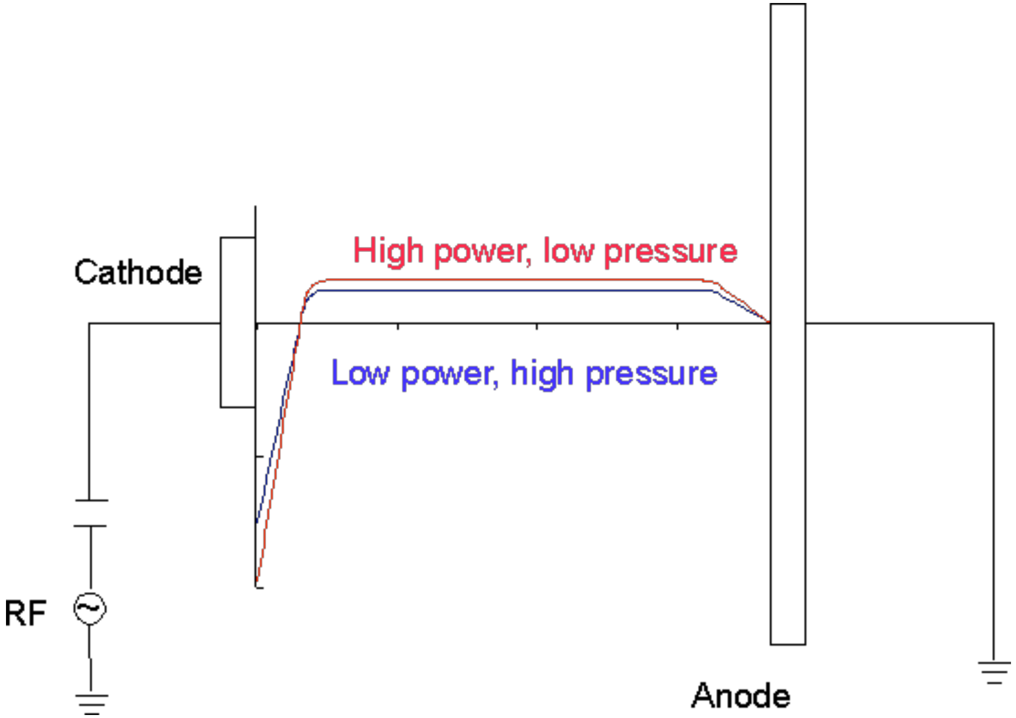

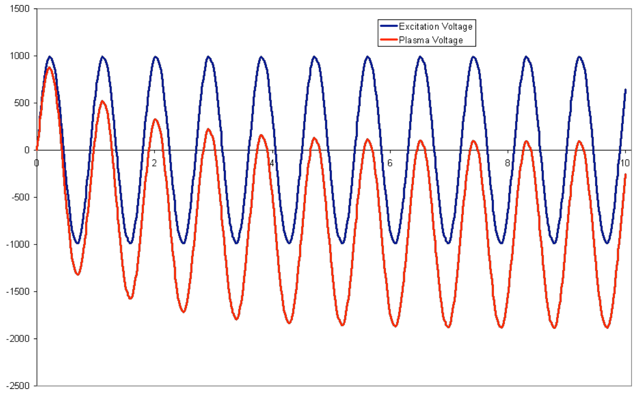

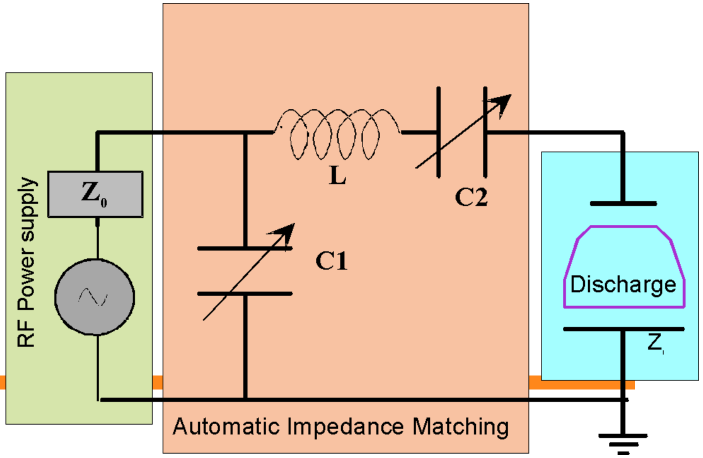

http://www.spectruma.de

Arc plasma

Arc discharge deposition

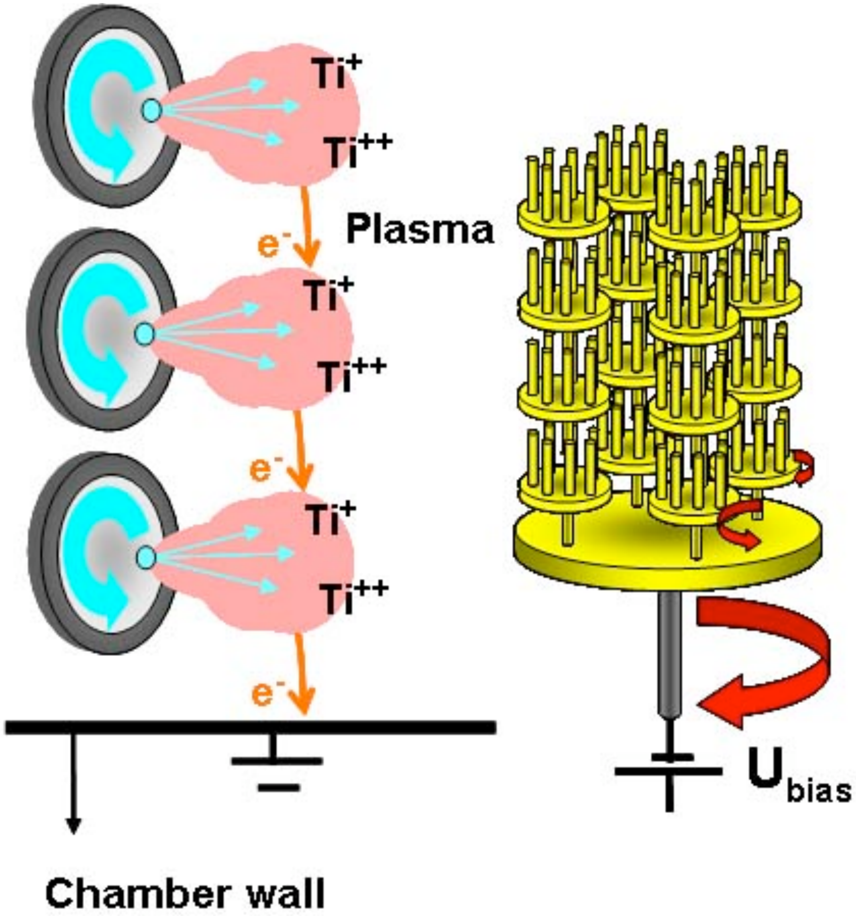

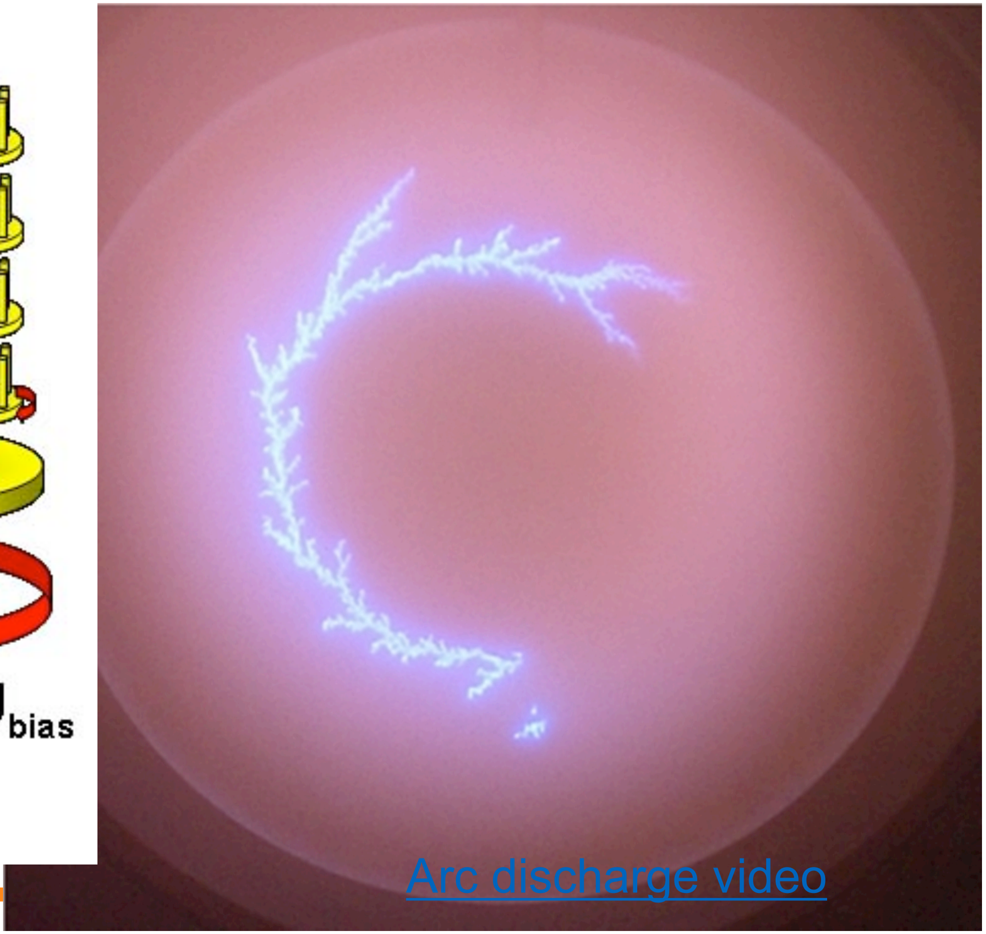

[Arc discharge video](#)

Arc disharge – cathode spot

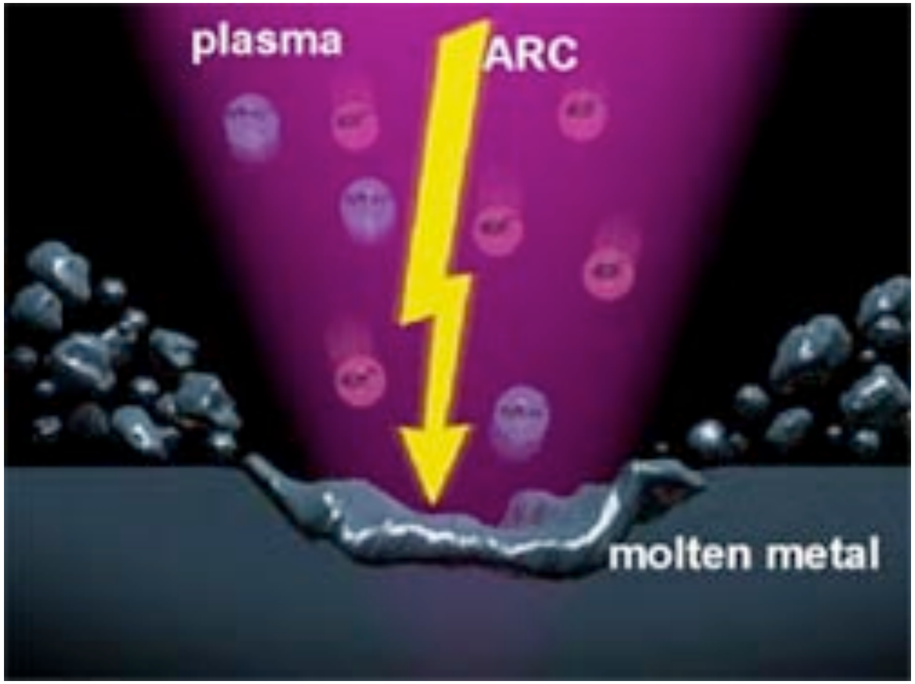

www.shm-cz.cz/files/schema01.jpg

Arc discharge process

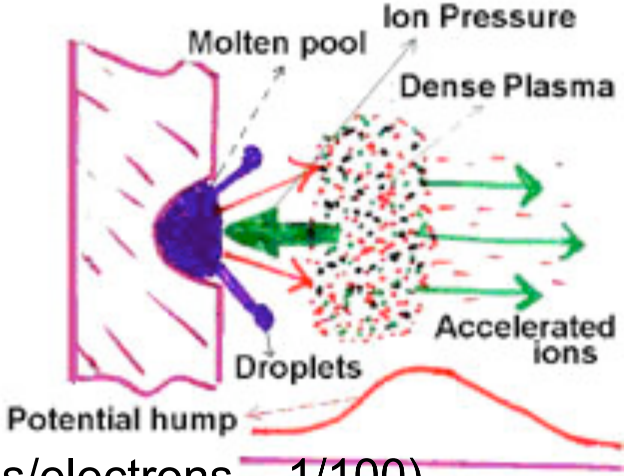

- arc current concentrated into filaments – arcs
- intense electron emission
- intense ion emission due to electron current (atoms/electrons – 1/100)
- ionization of atoms – formation of plasma
- flow of ions to cathode – intense sputtering of atoms
- 10^6 - 10^8 A/m^2
- overlapping thermal spikes
- materials is melted and sublimated in cathode spots
- cathode spots move randomly or could be steered by using magnets
- electons ionize vapor and create more electrons – increase of current
- ions accelerate
  - due to potential difference in plasma
  - due to multiple collisions with fast electrons
- macro particles (up to 10 μm diam.I are formed

Timko, Nordlund simulations
http://prb.aps.org/supplemental/PRB/v81/i18/e184109

Filtered arc

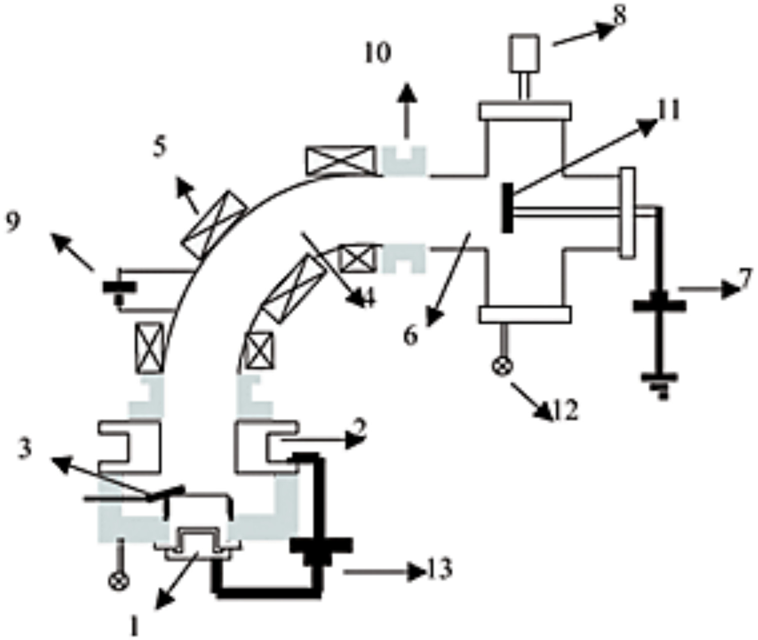

Figure 1. Scheme of the DCF2 device. (1) cathode; (2) anode; (3) trigger; (4) quarter torus magnetic filter; (5) torus coil; (6) deposition chamber; (7) probe bias source; (8) diagnostic port; (9) filter bias source; (10) insulators; (11) collecting probe; (12) vacuum pumping systems; (13) arc source.

PULSED SPUTTERING

Definitions

- DC-sputtering

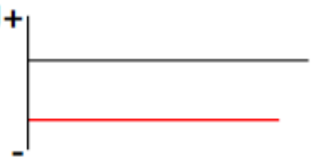

- Pulsed DC

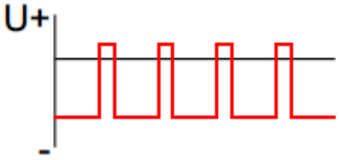

- HiPIMS

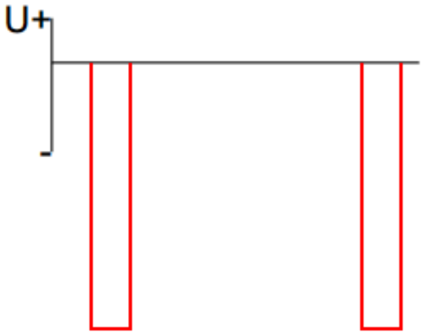

HIPIMS

High Power Pulsed Magnetron Sputtering (HIPIMS)

- Introduced by Kouznetsov et al.*
  - Also known as HIPIMS – High Power Impulse Magnetron Sputtering
- High power pulses of short duration
  - Peak value typically 100 times greater than conventional magnetron sputtering
    - Peak power densities of 1-3 kW/cm²
  - Pulse width of 100 - 150 µsec
  - Discharge voltages of 500-1000 V

*V. Kouznetsov, K. Macák, J. M. Schneider, U. Helmersson, and I. Petrov, "A No Sputter Technique Utilizing Very High Target Power Densities," Surf. Coat. Tec

Pulsed Plasma Diffusion"

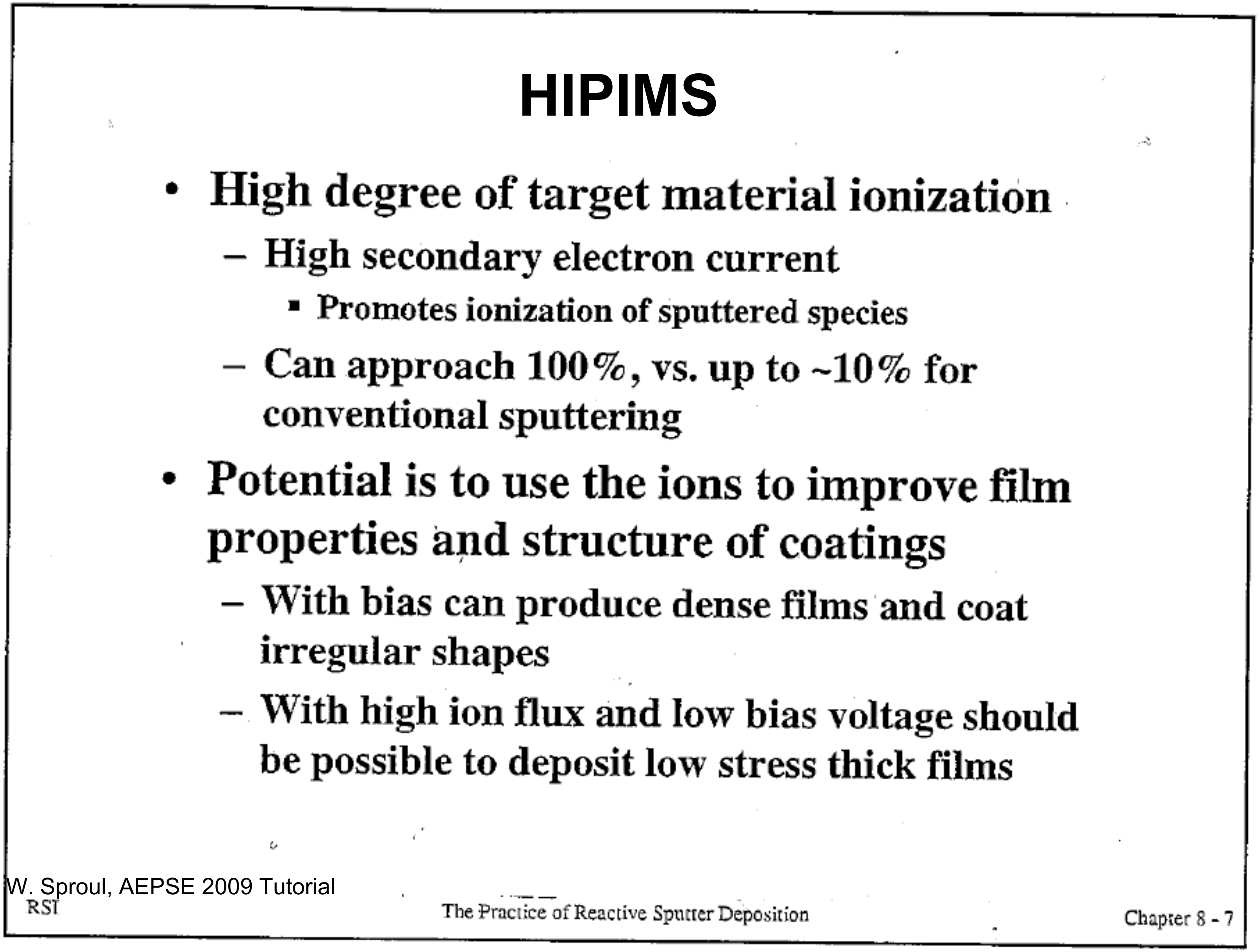

HIPIMS

- High degree of target material ionization
  - High secondary electron current
    - Promotes ionization of sputtered species
  - Can approach 100%, vs. up to ~10% for conventional sputtering
- Potential is to use the ions to improve film properties and structure of coatings
  - With bias can produce dense films and coat irregular shapes
  - With high ion flux and low bias voltage should be possible to deposit low stress thick films

W. Sproul, AEPSE 2009 Tutorial

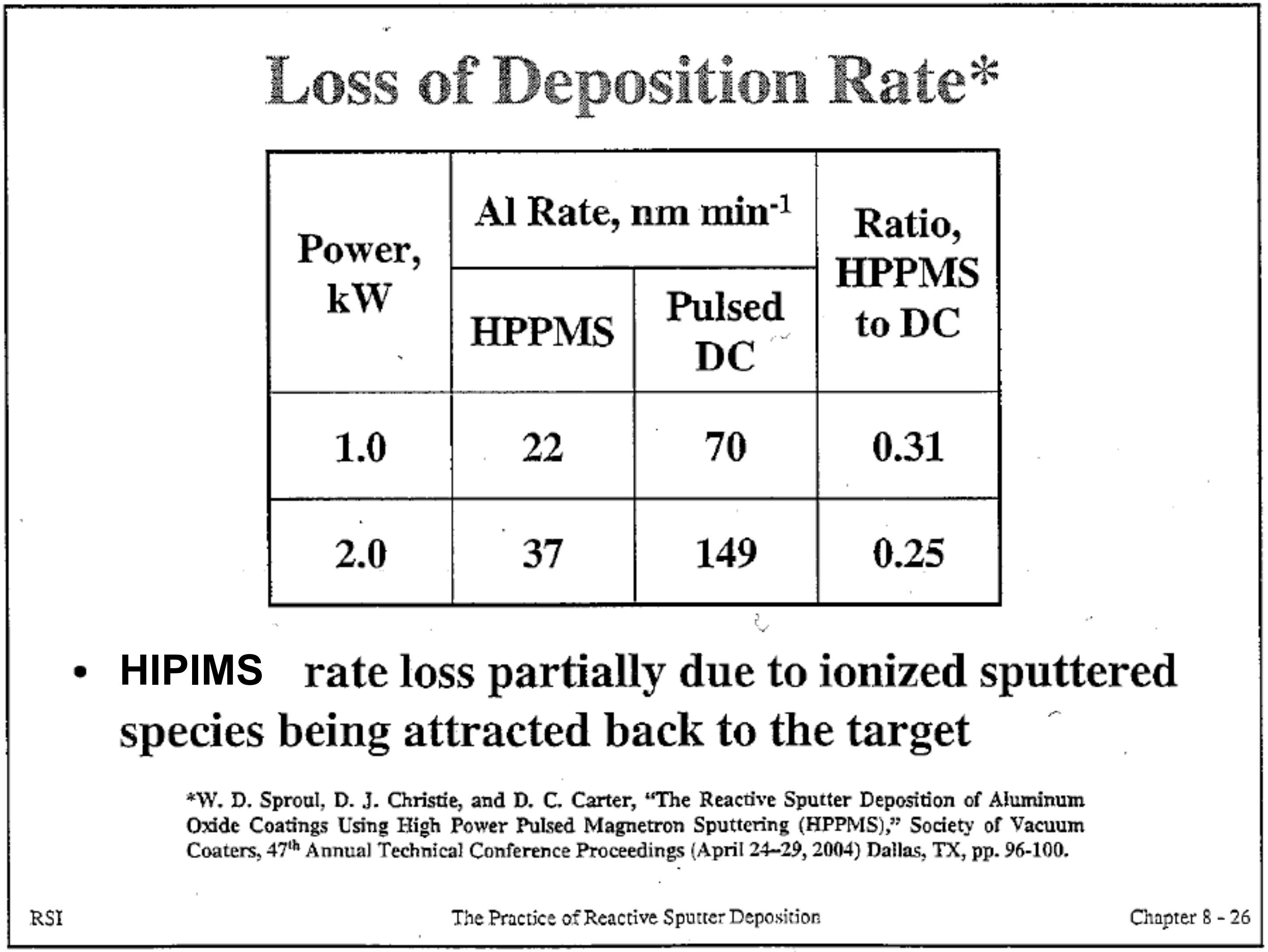

Loss of Deposition Rate*

Power, kW	Al Rate, nm min^{-1}		Ratio, HPPMS to DC
	HPPMS	Pulsed DC	
1.0	22	70	0.31
2.0	37	149	0.25

- **HIPIMS** rate loss partially due to ionized sputtered species being attracted back to the target

*W. D. Sproul, D. J. Christie, and D. C. Carter, "The Reactive Sputter Deposition of Aluminum Oxide Coatings Using High Power Pulsed Magnetron Sputtering (HPPMS)," Society of Vacuum Coaters, 47th Annual Technical Conference Proceedings (April 24–29, 2004) Dallas, TX, pp. 96-100.

W. Sproul, AEPSE 2009 Tutorial

Fluxes of ions in HIPIMS

786 André Anders J. Vac. Sci. Technol. A, Vol. 28, No. 4, Jul/Aug 2010

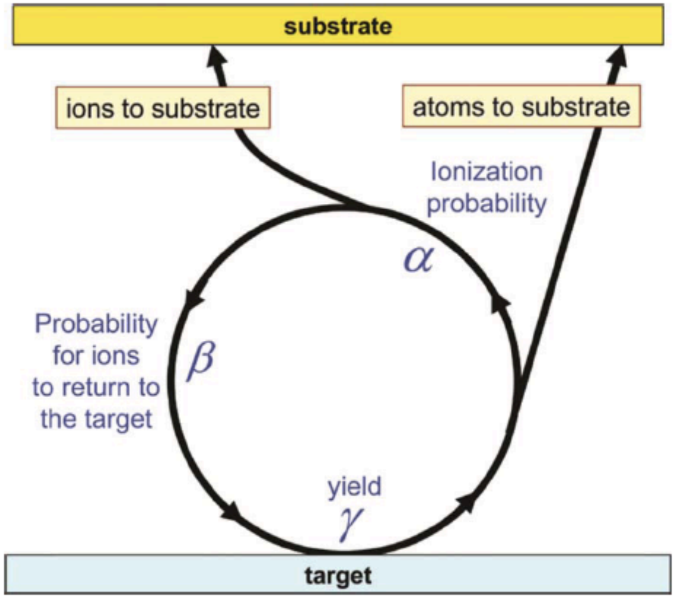

FIG. 2. (Color online) Schematic presentation of the fluxes involved in the deposition by HIPIMS under conditions when the plasma is dominated by metal sputtered from the target; α, β, and γ are the ionization probability, the return probability, and the sputtering yield, respectively; for further explanations see text.

Reactive sputtering

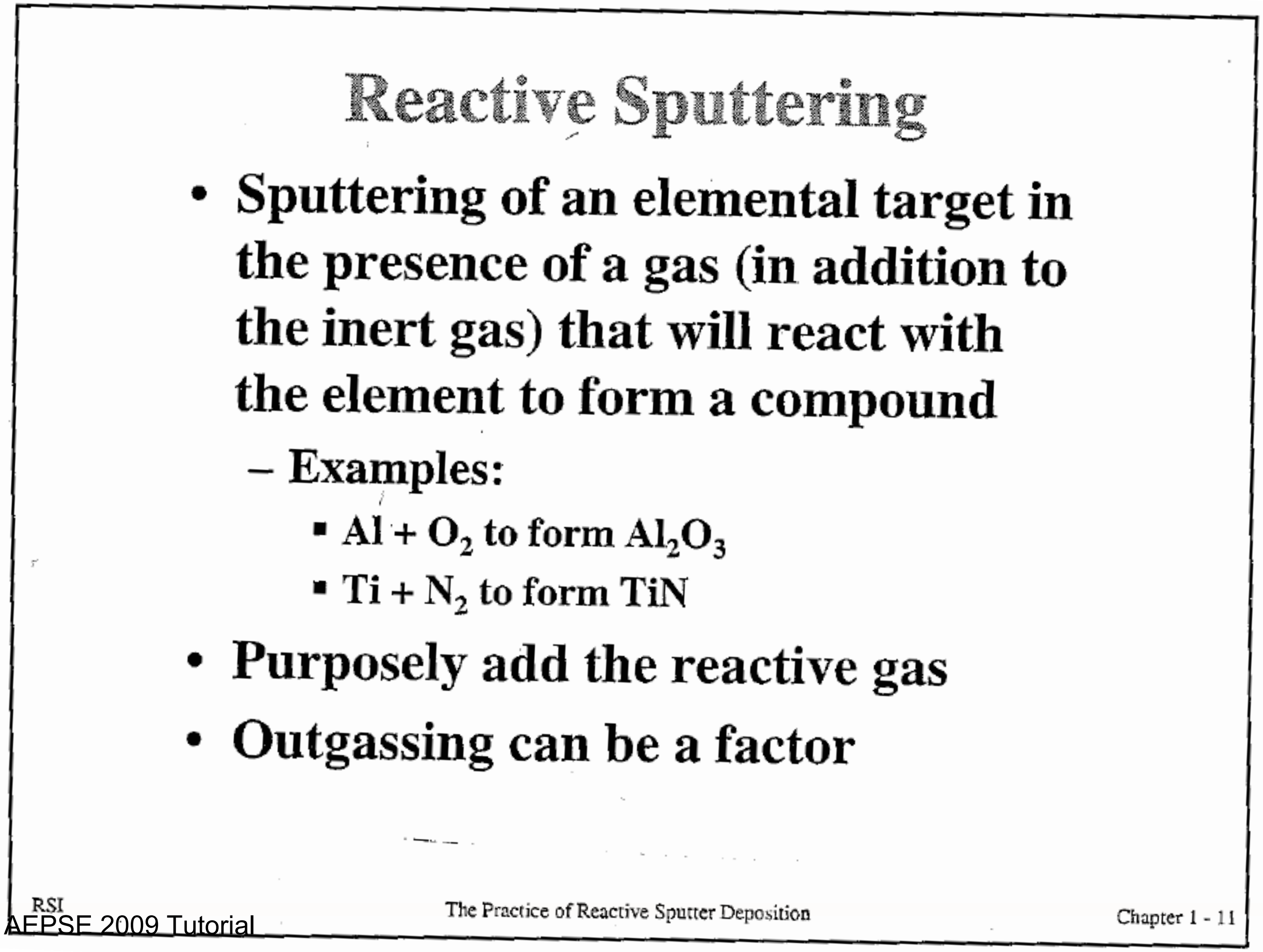

Reactive Sputtering

- Sputtering of an elemental target in the presence of a gas (in addition to the inert gas) that will react with the element to form a compound
  - Examples:
    - Al + O_2 to form Al_2O_3
    - Ti + N_2 to form TiN
- Purposely add the reactive gas
- Outgassing can be a factor

RSI

The Practice of Reactive Sputter Deposition

Chapter 1 - 11

W. Sproul, AEPSF 2009 Tutorial

Reactive sputtering

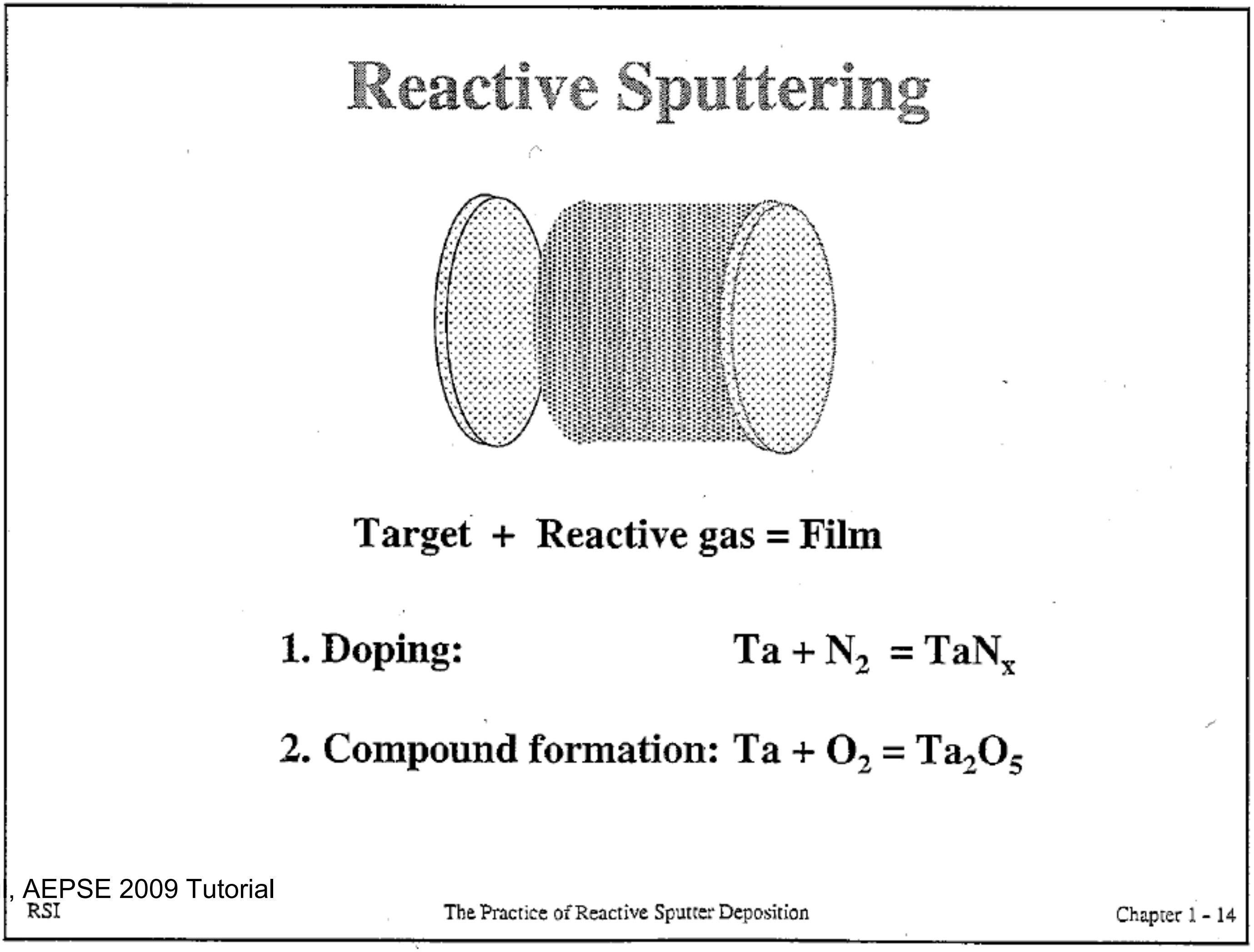

Reactive Sputtering

Target + Reactive gas = Film

1. Doping: $Ta + N_2 = TaN_x$

2. Compound formation: $Ta + O_2 = Ta_2O_5$

RSI The Practice of Reactive Sputter Deposition Chapter 1 - 14

W. Sproul, AEPSE 2009 Tutorial

Reactive sputtering

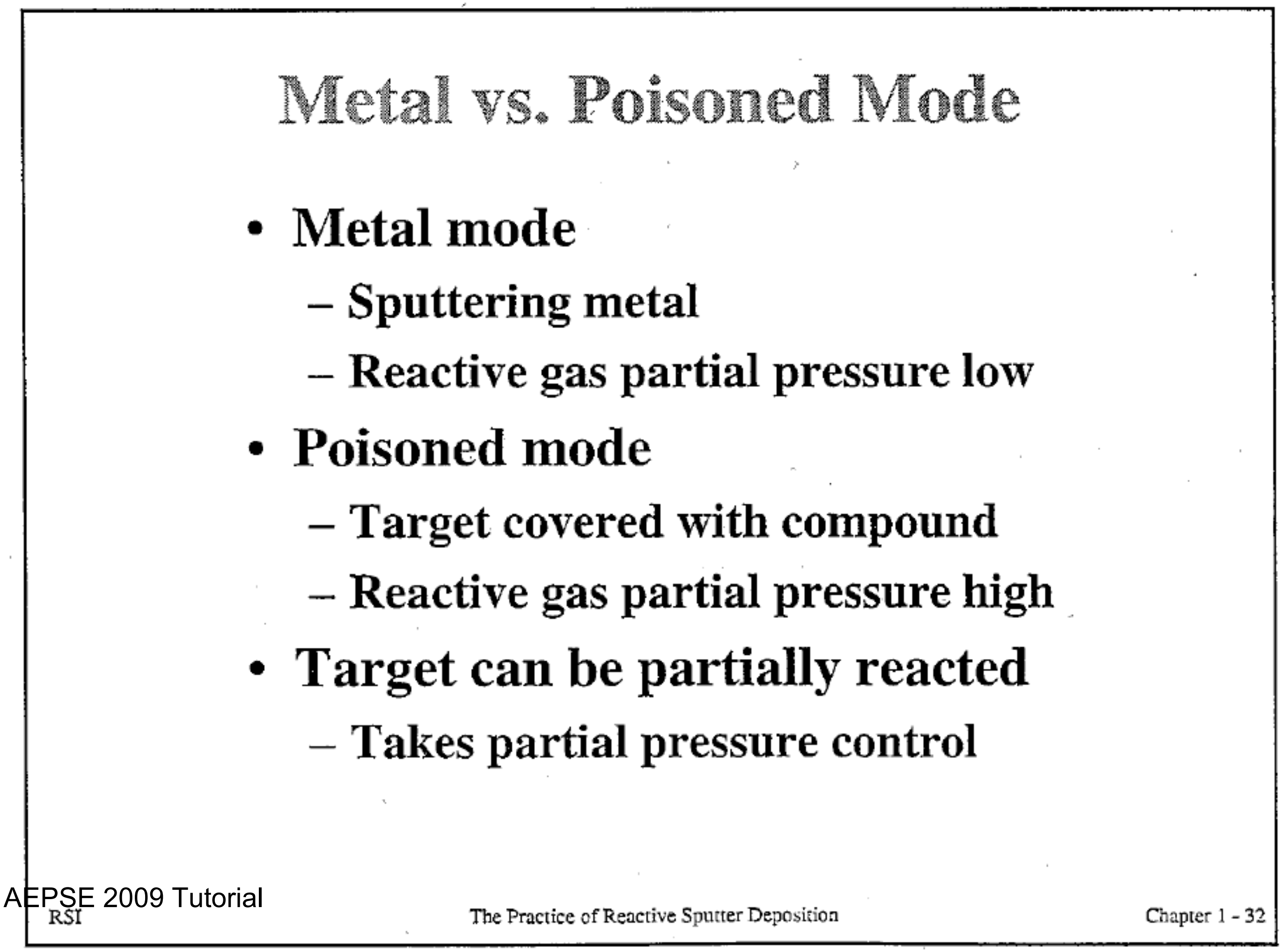

Metal vs. Poisoned Mode

- Metal mode
  - Sputtering metal
  - Reactive gas partial pressure low
- Poisoned mode
  - Target covered with compound
  - Reactive gas partial pressure high
- Target can be partially reacted
  - Takes partial pressure control

W. Sproul, AEPSE 2009 Tutorial

Reactive sputtering

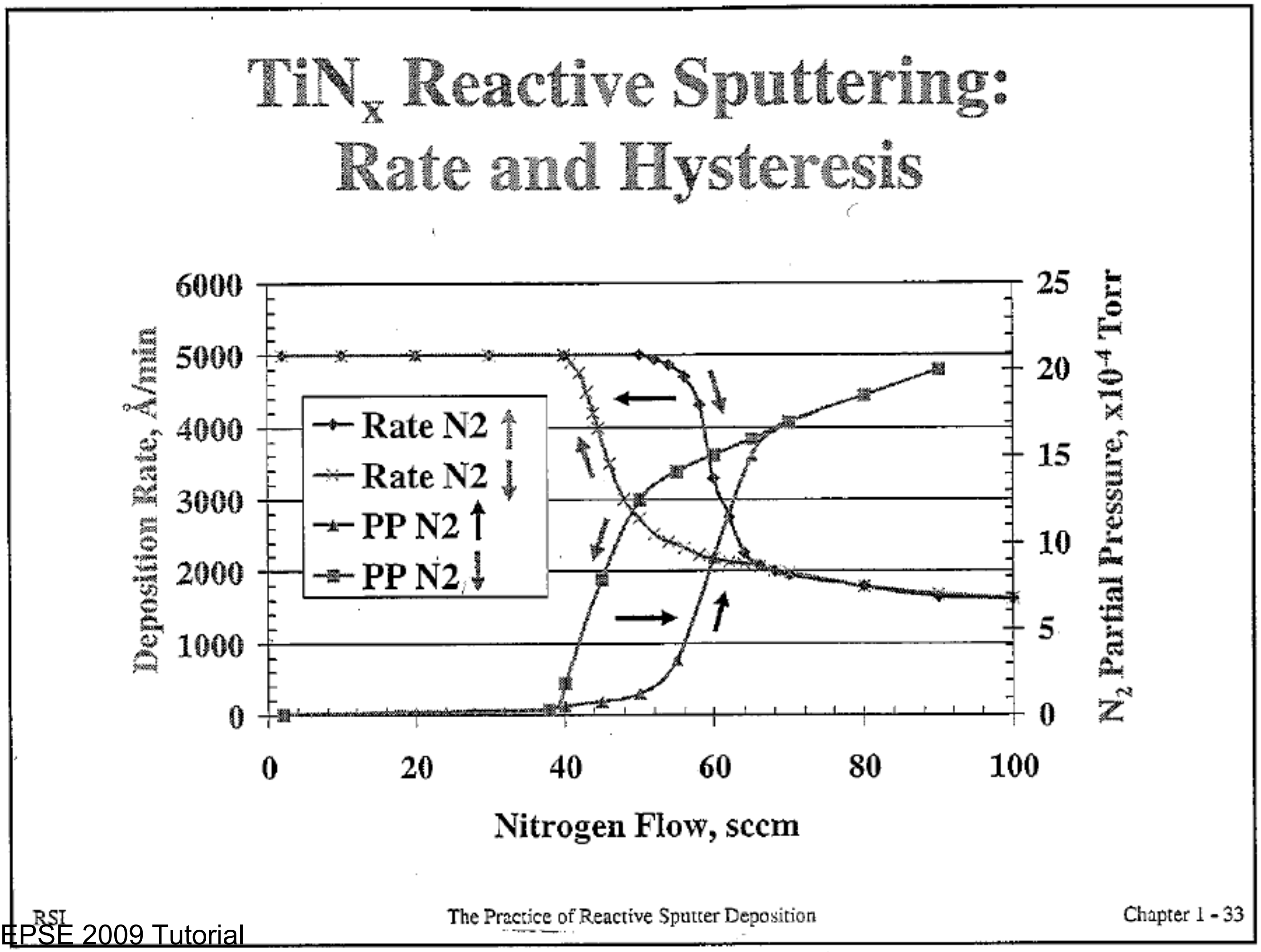

TiN_x Reactive Sputtering: Rate and Hysteresis

RSI

The Practice of Reactive Sputter Deposition

Chapter 1 - 33

W. Sproul, AEPSE 2009 Tutorial

Reactive sputtering

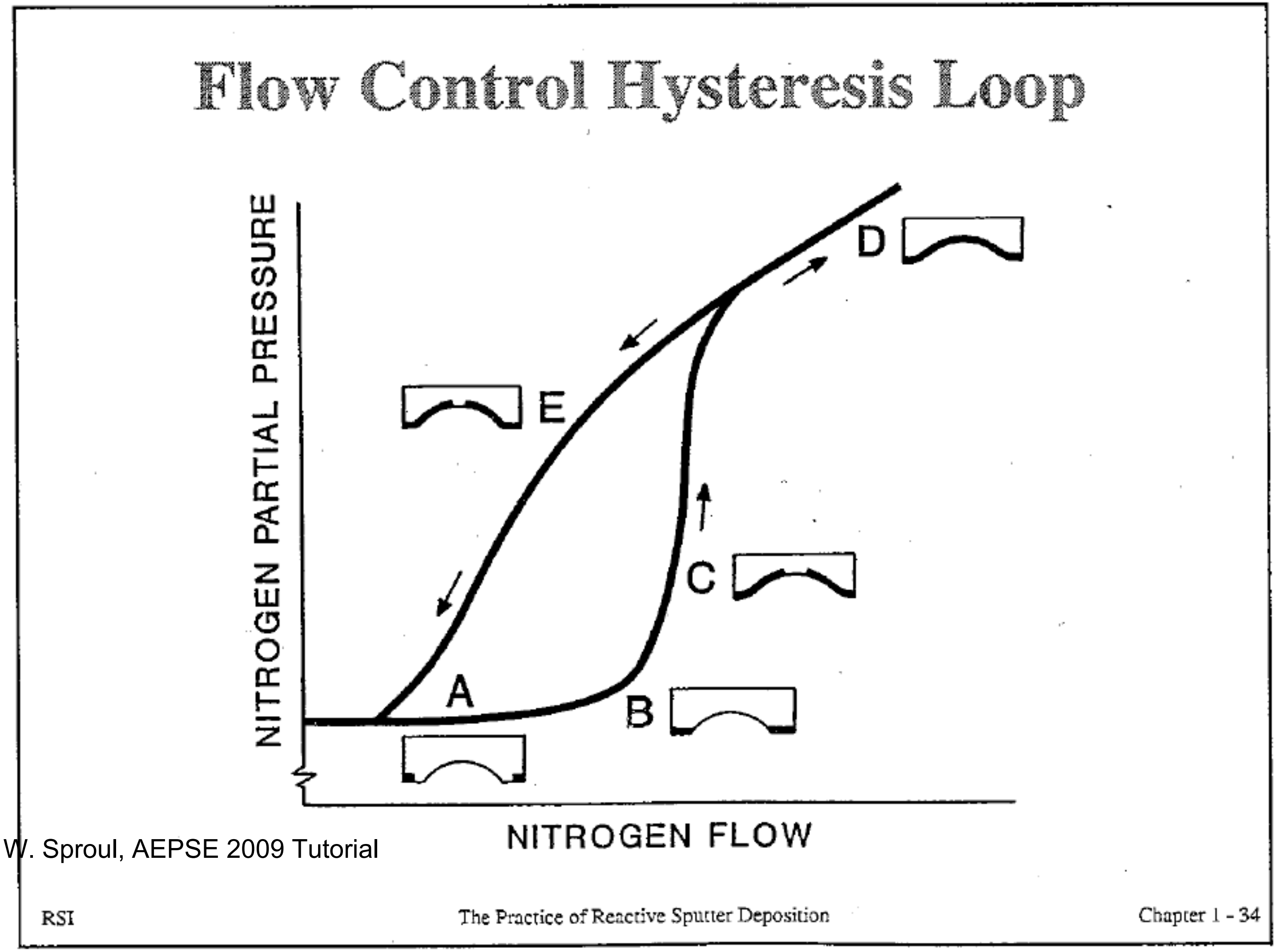

Flow Control Hysteresis Loop

RSI

The Practice of Reactive Sputter Deposition

Chapter 1 - 34

W. Sproul, AEPSE 2009 Tutorial

Reactive sputtering

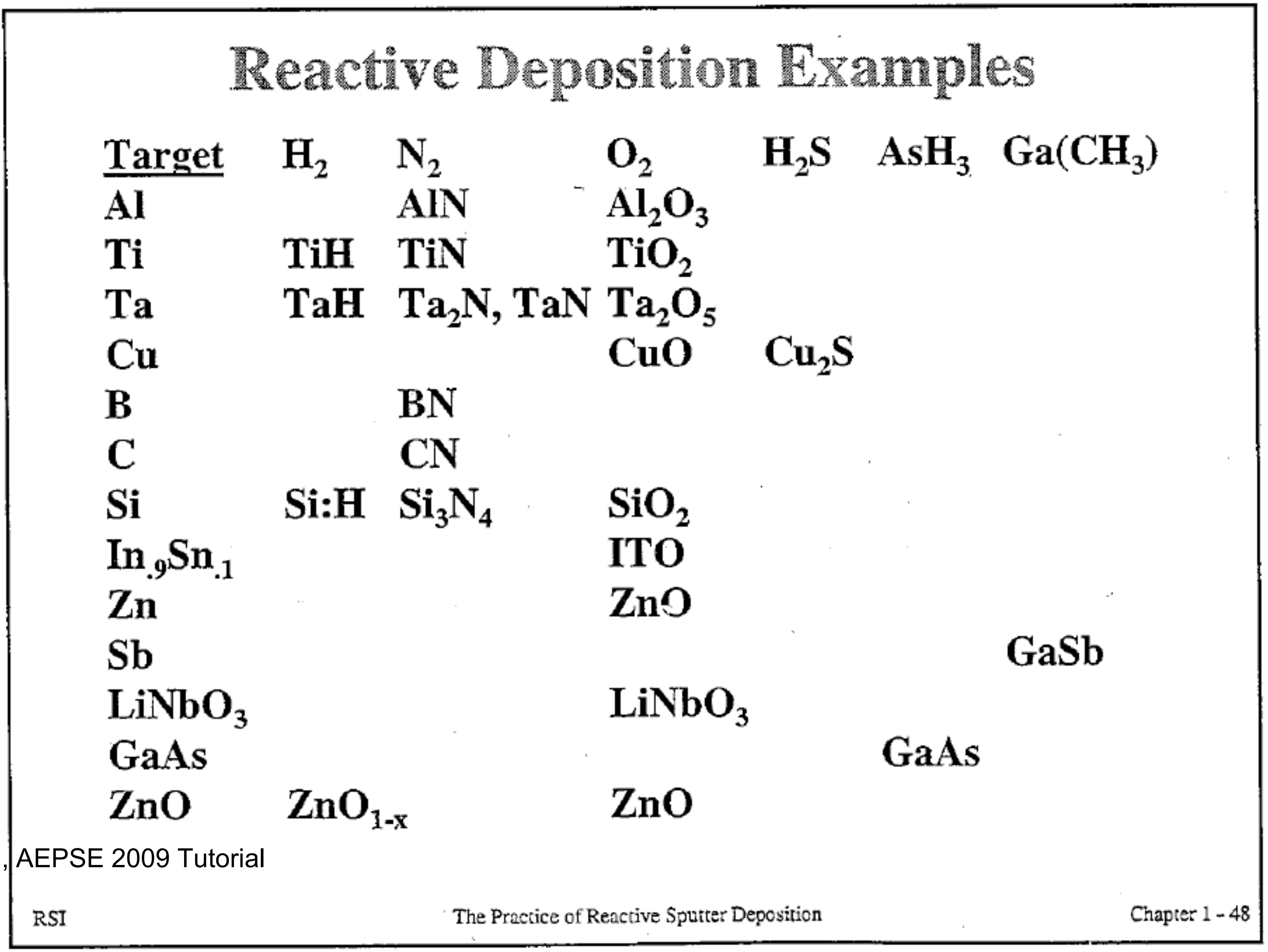

Reactive Deposition Examples

Target	H_2	N_2	O_2	H_2S	AsH_3	$Ga(CH_3)$
Al		AlN	Al_2O_3			
Ti	TiH	TiN	TiO_2			
Ta	TaH	Ta_2N, TaN	Ta_2O_5			
Cu			CuO	Cu_2S		
B		BN				
C		CN				
Si	Si:H	Si_3N_4	SiO_2			
$In_{.9}Sn_{.1}$			ITO			
Zn			ZnO			
Sb						GaSb
$LiNbO_3$			$LiNbO_3$			
GaAs					GaAs	
ZnO	ZnO_{1-x}		ZnO			

RSI The Practice of Reactive Sputter Deposition Chapter 1 - 48

W. Sproul, AEPSE 2009 Tutorial

Ion solid interarctions

Energetic ion surface interactions

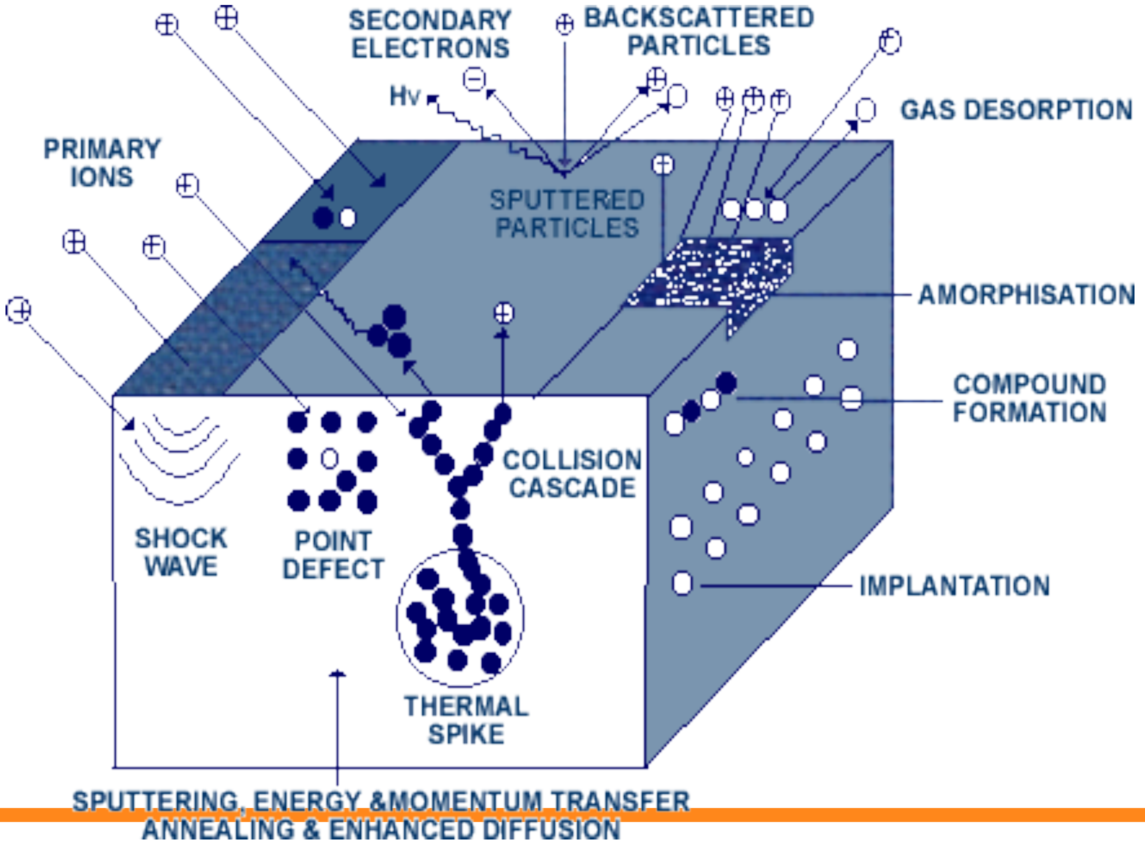

Secondary electrons

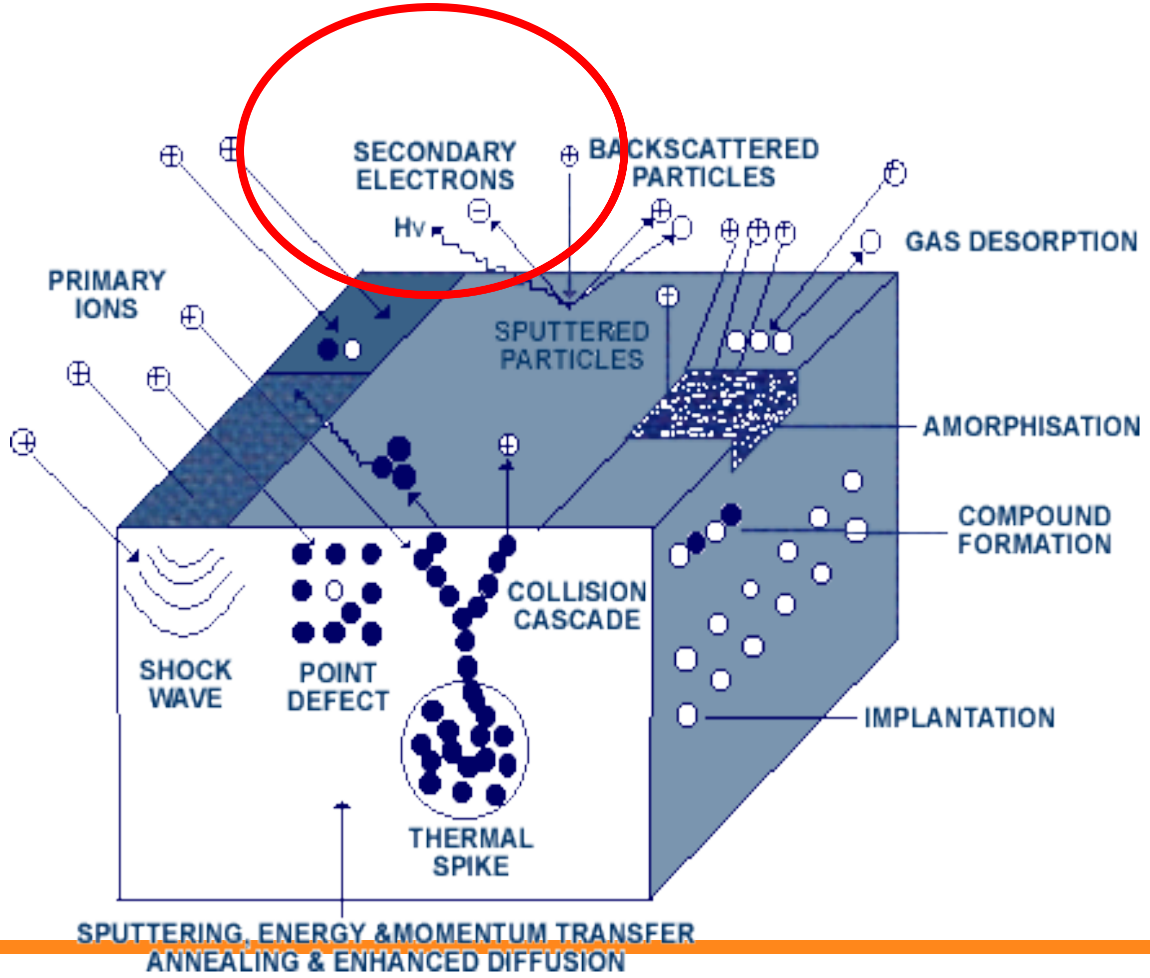

Desorption, cleaning

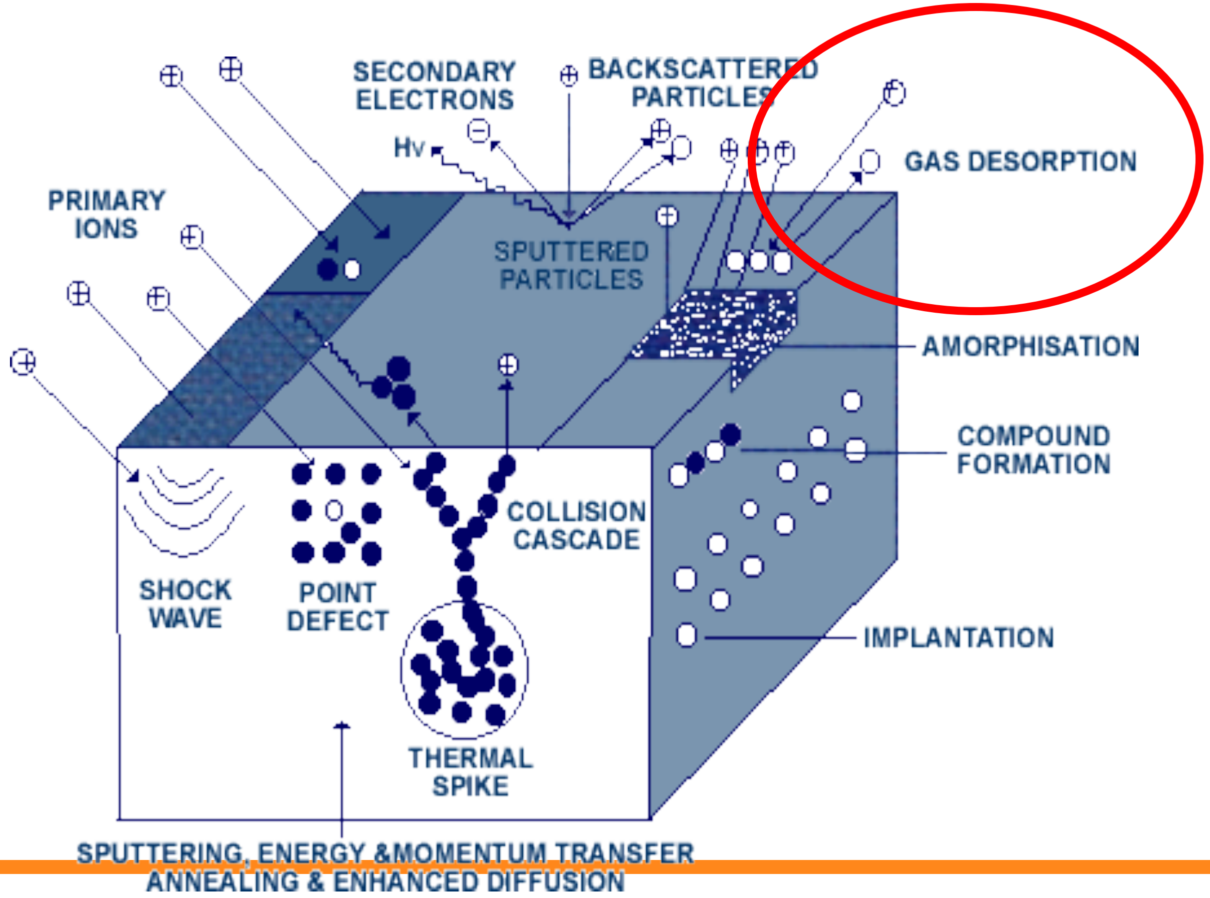

Sputtering

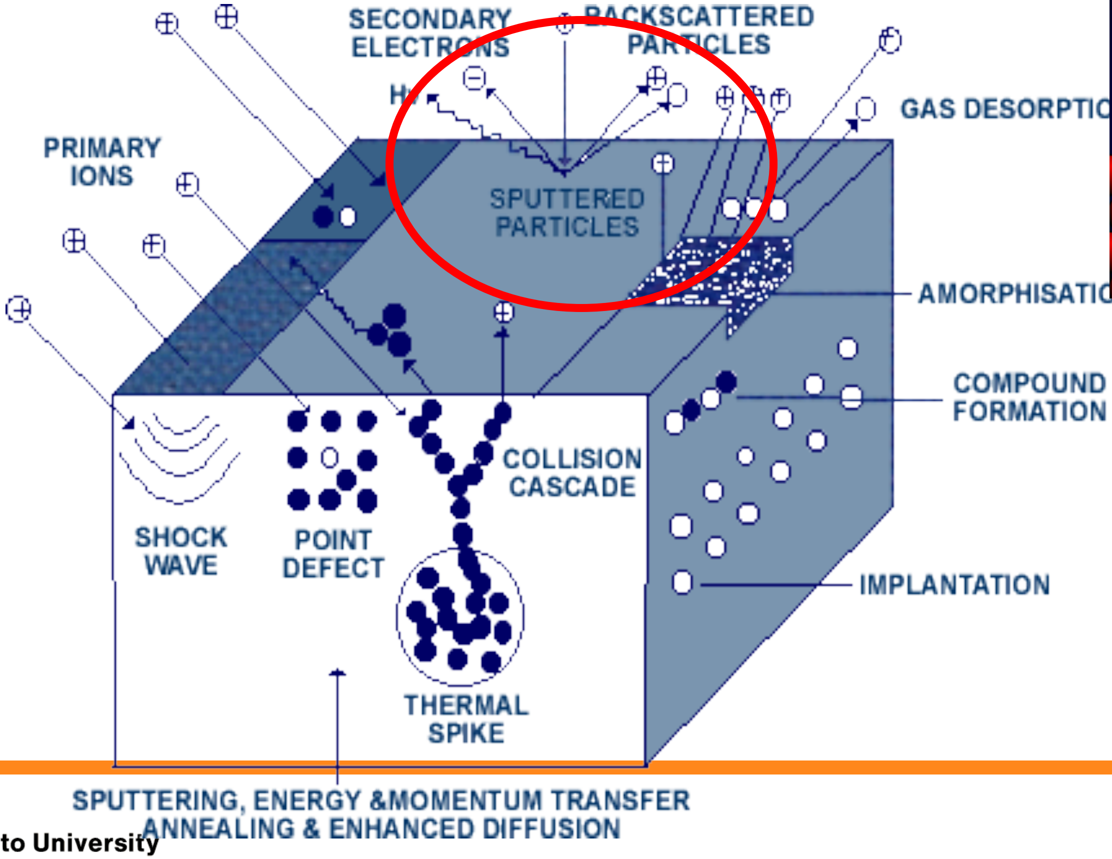
SECONDARY ELECTRONS
BACKSCATTERED PARTICLES
H
GAS DESORPTIO
PRIMARY IONS
SPUTTERED PARTICLES
AMORPHISATIO
COMPOUND FORMATION
COLLISION CASCADE
SHOCK WAVE
POINT DEFECT
THERMAL SPIKE
IMPLANTATION
SPUTTERING, ENERGY &MOMENTUM TRANSFER
ANNEALING & ENHANCED DIFFUSION

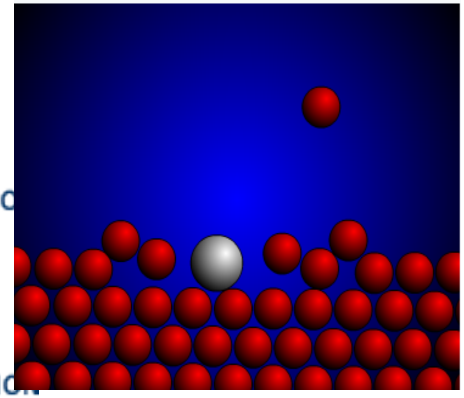

Collision cascade, thermal spike

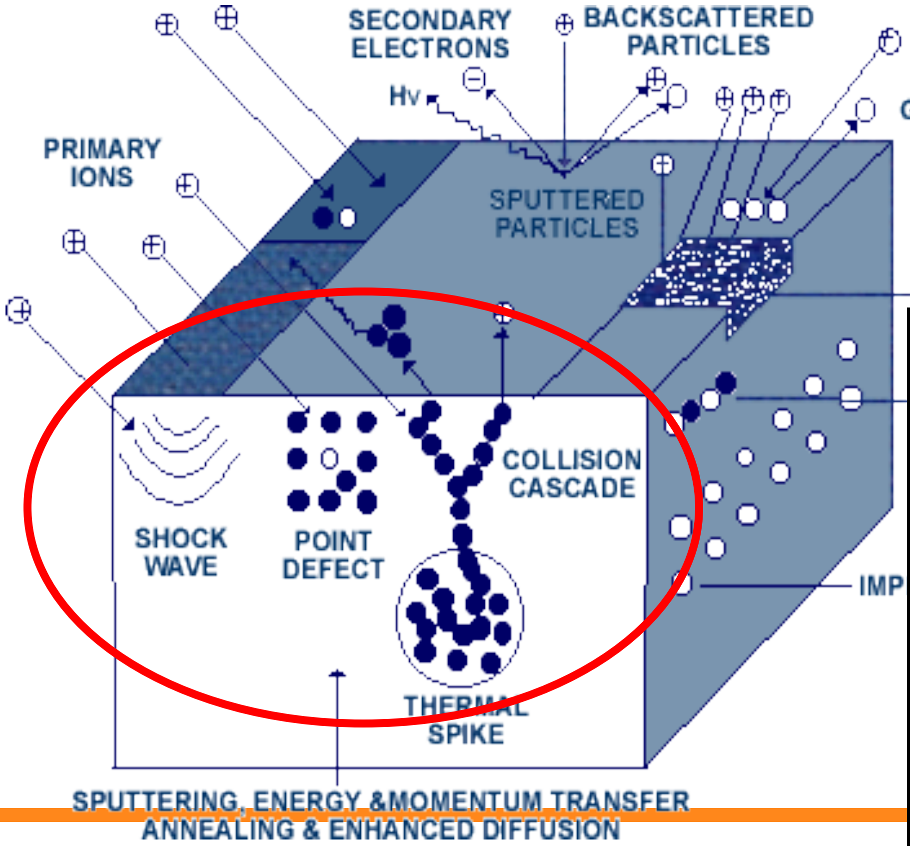

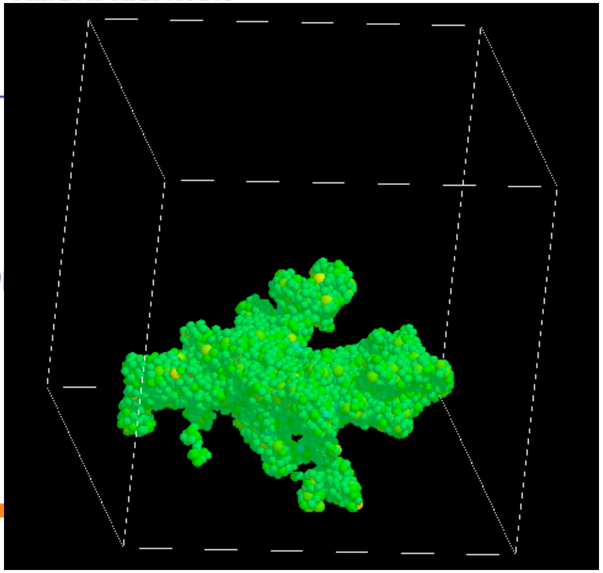

K. Nordlund

doping, compounds

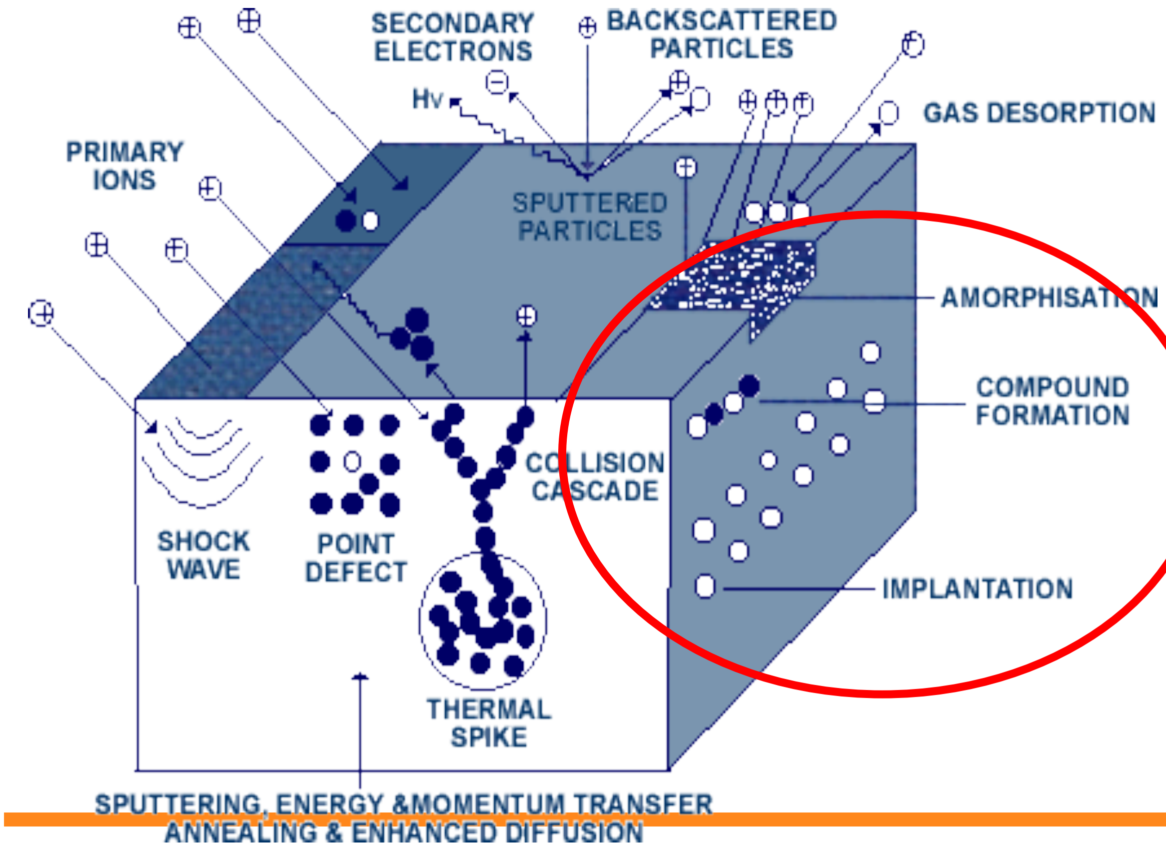

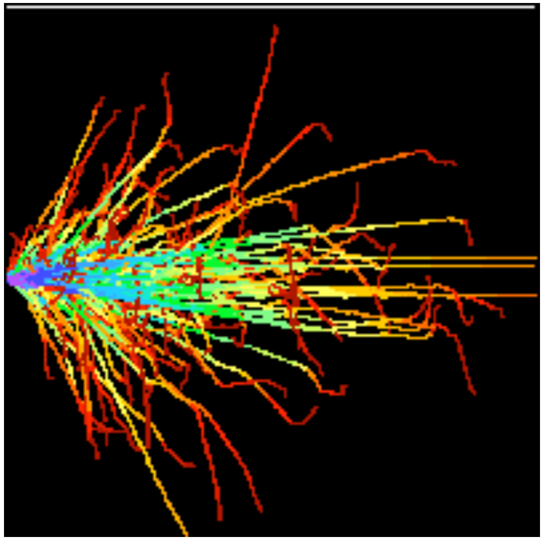

PVD and Ion Assisted Processes

Which role can energetic ions play

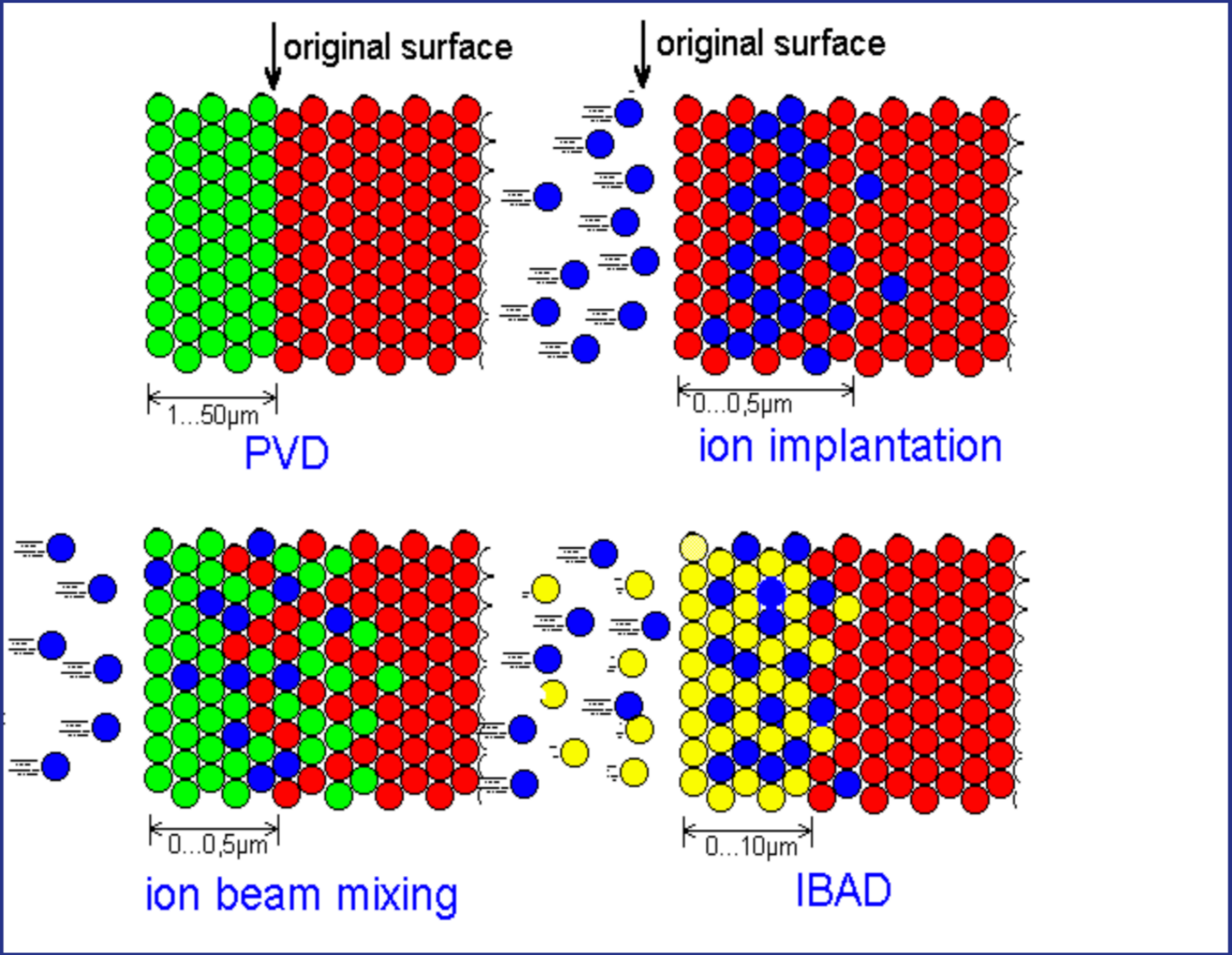

Sputtering

- Source of atoms and ions
- Cleaning: Removing lose atoms, impurities, oxides

Sigmund Theory

$$S = \frac{3\alpha 4 M_1 M_2 E}{4\pi^2 (M_1 + M_2)^2 U_S}$$

Good for low energy (<1keV)

where:

α is a function of M(target)/M(ion) and

incident angle $0.1 > \alpha > 1.4$

but often has a value of 0.2 - 0.4

M1 is the Mass of the ion

M2 is the mass of the target

E is incident ion energy

Us is the binding energy of the target ions

Sputtering yield

18 J. FRANKS

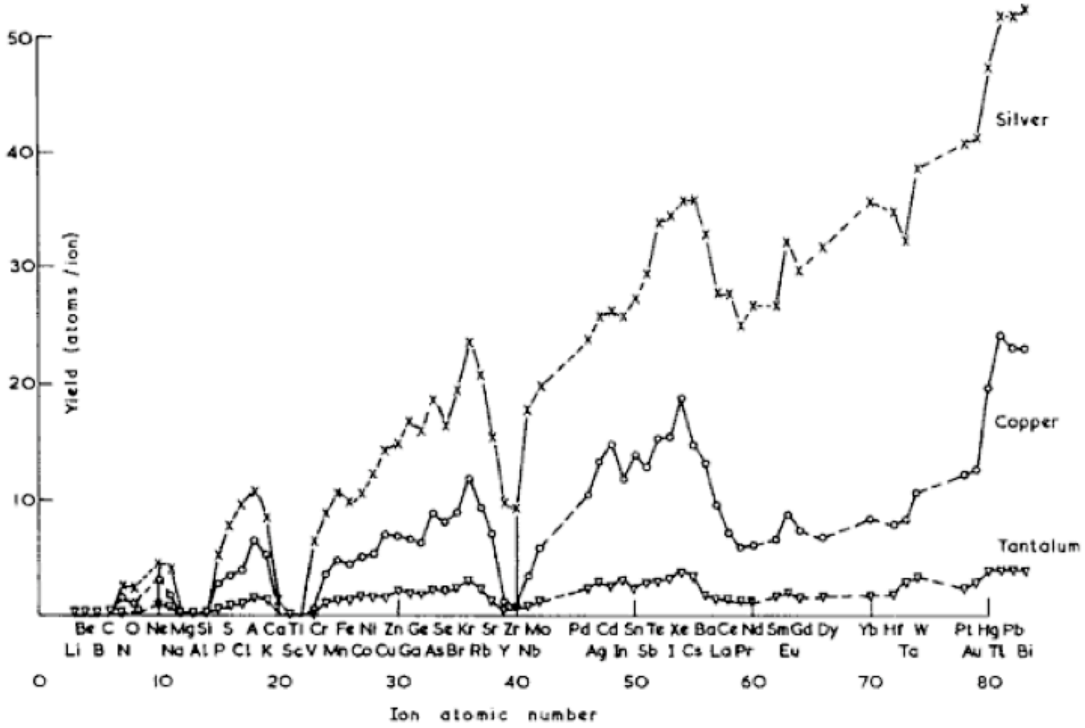

FIG. 15. Sputtering yield of silver, copper, and tantalum as a function of bombarding ion atomic number (Spencer and Schmidt, 1971).

Sputter yield angle dependence

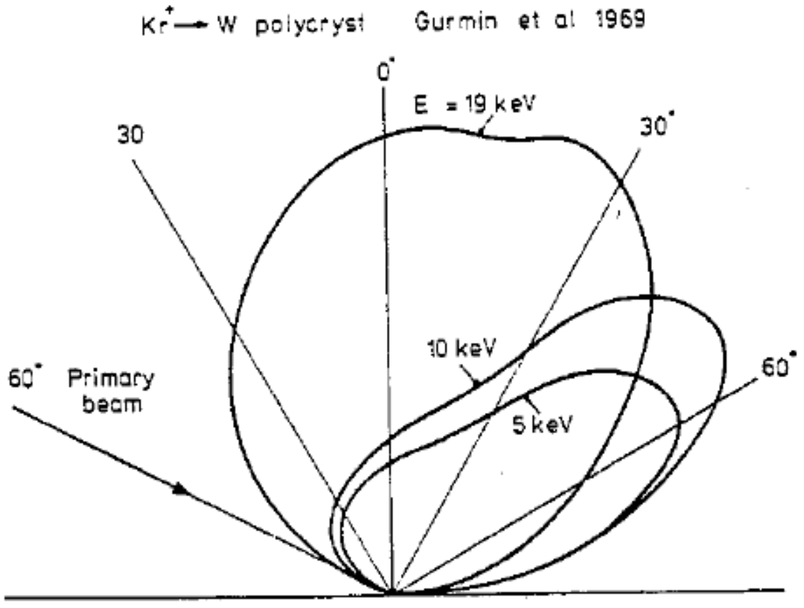

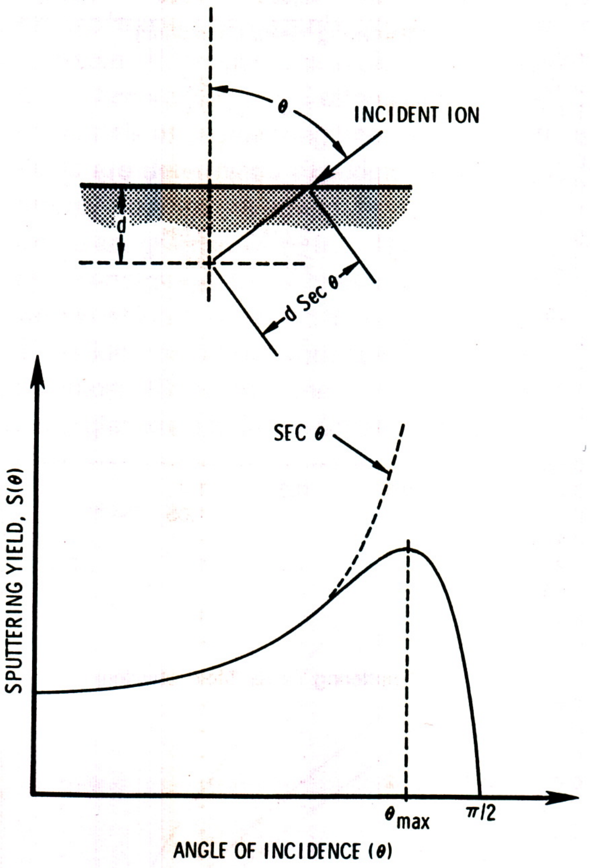

Figure 5.7. Schematic diagram showing variation of the sputtering yield with ion angle of incidence for a constant ion energy.

Sputter yi ibution

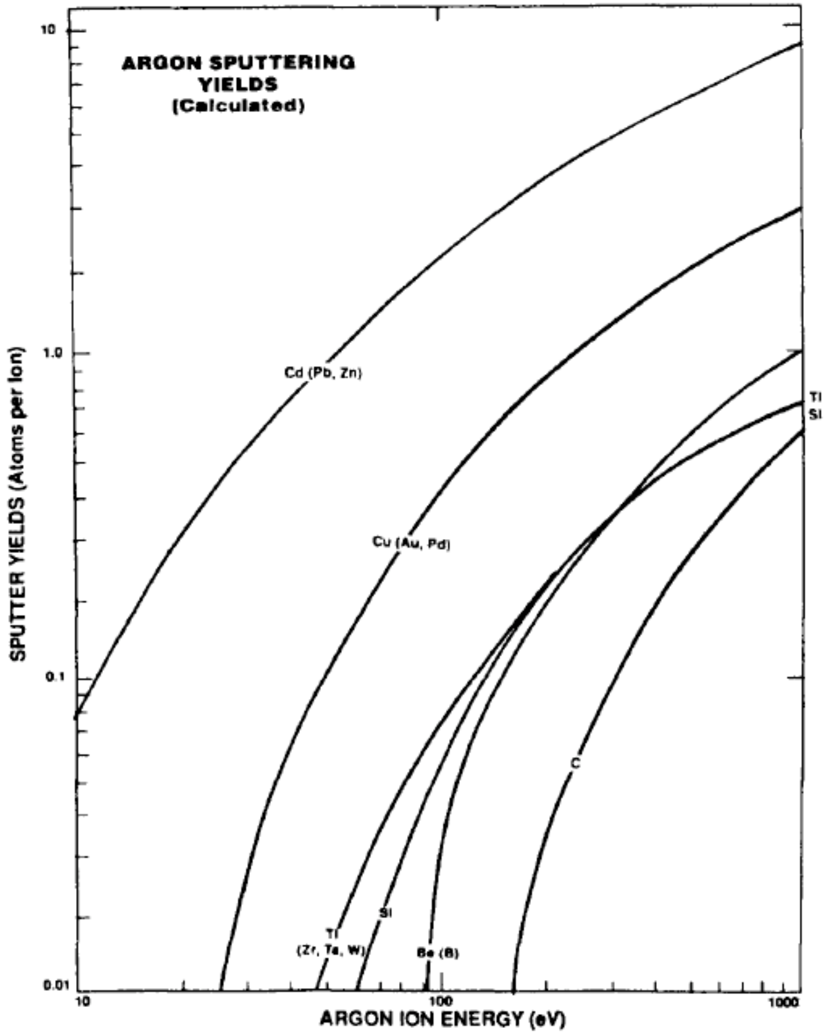

Figure 6-3. Some calculated sputtering yields (adapted from Ref. 20).

Sputter yield angle dependence and energy distribution

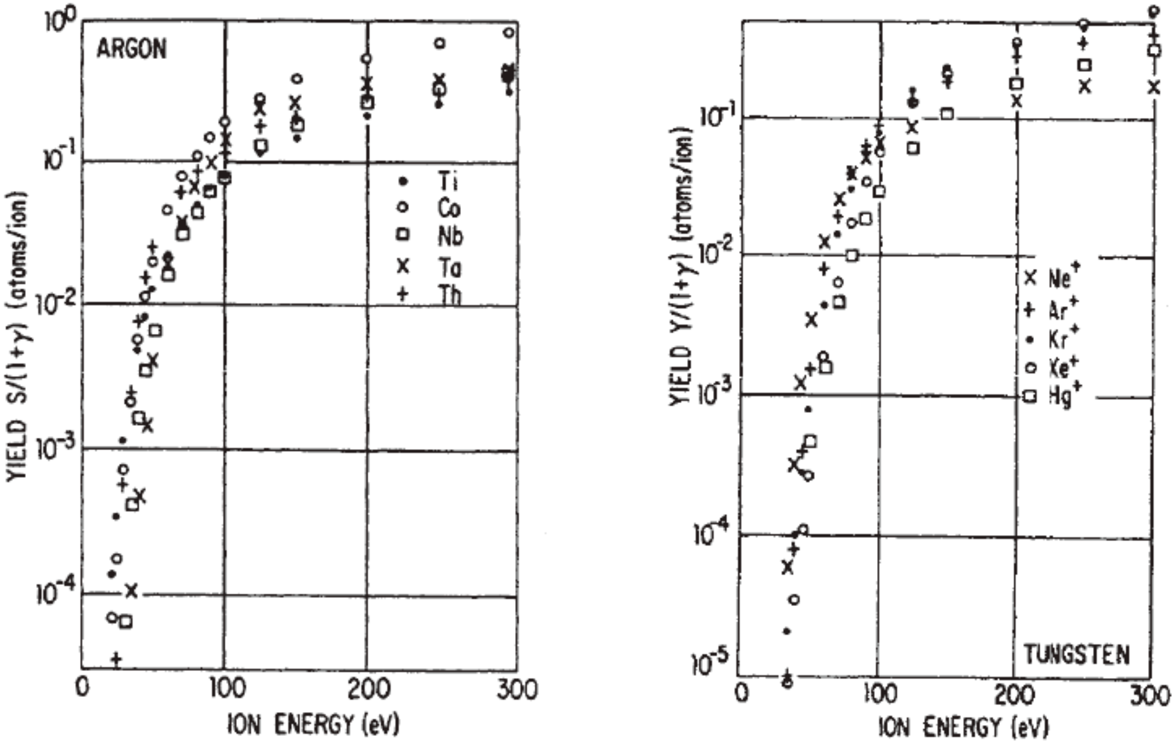

(a) (b)

Figure 3. Sputter yield, *S*, vs ion energy; (*a*) shown for several materials with Ar$^+$ bombardment, and (*b*) for W bombarded by different ion species.[10] *(Reproduced with permission from Maissel and Glang,* Handbook of Thin Film Technology, *McGraw-Hill, 1970.)*

School of Chemical Technology

Preferential sputtering

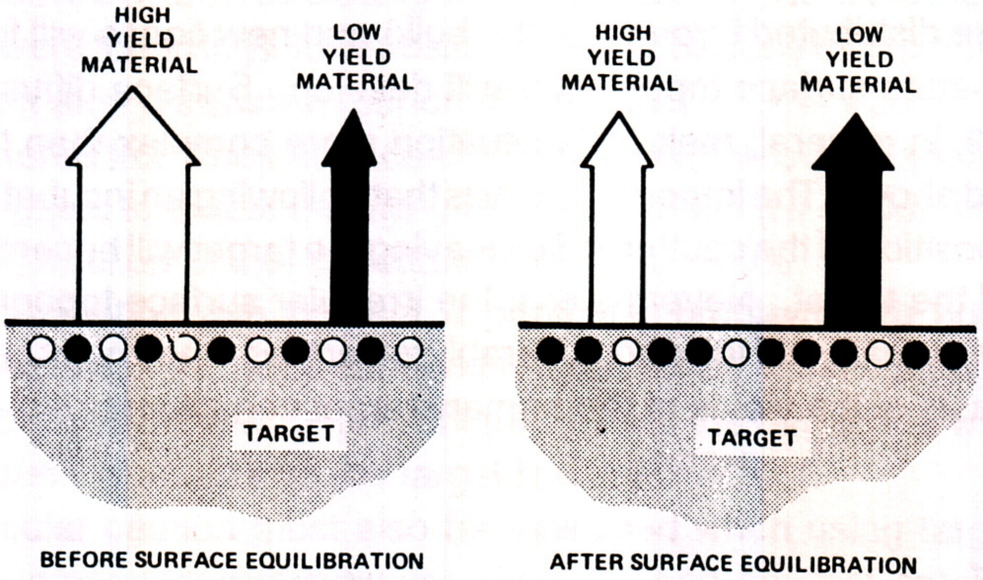

Figure 5.10. Schematic illustration of the surface composition modification which occurs during sputtering of a single-phase alloy.

Adatom nucleation and surface diffusion processes

- Shadowing
- Surface diffusion
- Bulk diffusion
- Desorption

Effecting parameters

- kinetic energy, energy of ions and atoms
- thermal energy
- potential energies
- angle of incidence, topography
- impurities – contamination

Coating structure and plasma parameters

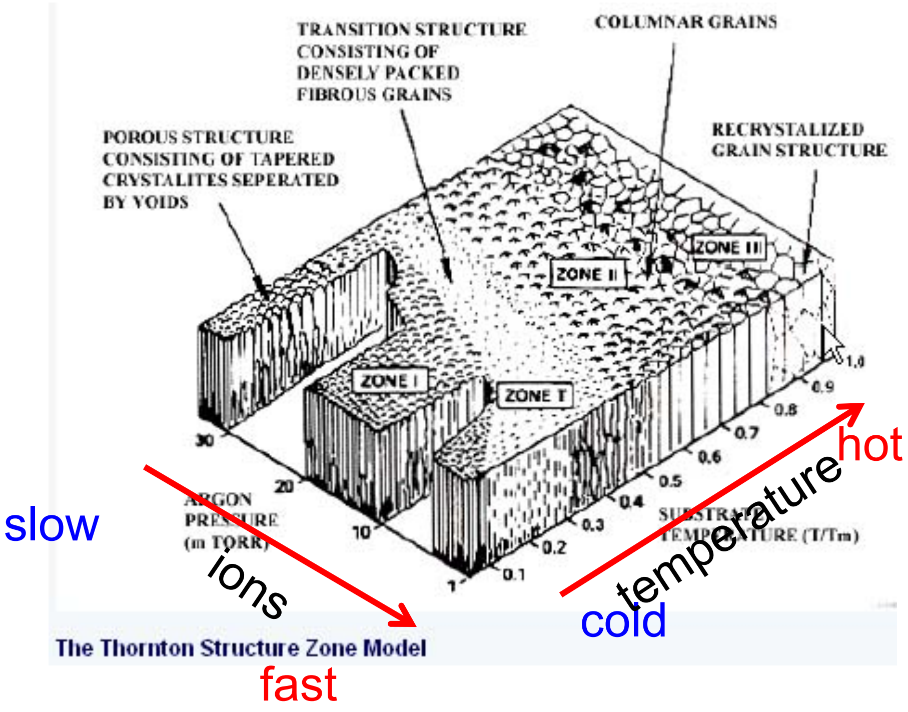

The Thornton Structure Zone Model

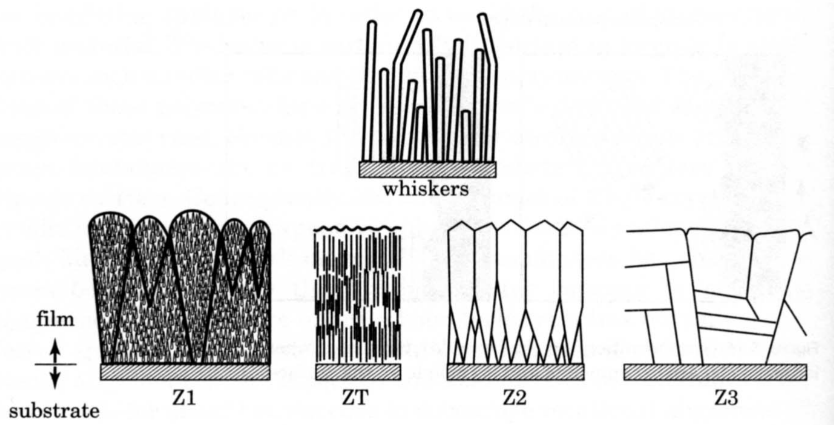

Figure 5.15 Characteristics of the four basic structural zones and of whiskers, in cross section. The ratio of substrate T to film melting T (T_s/T_m) increases in the direction Z1→ZT→Z2→Z3.

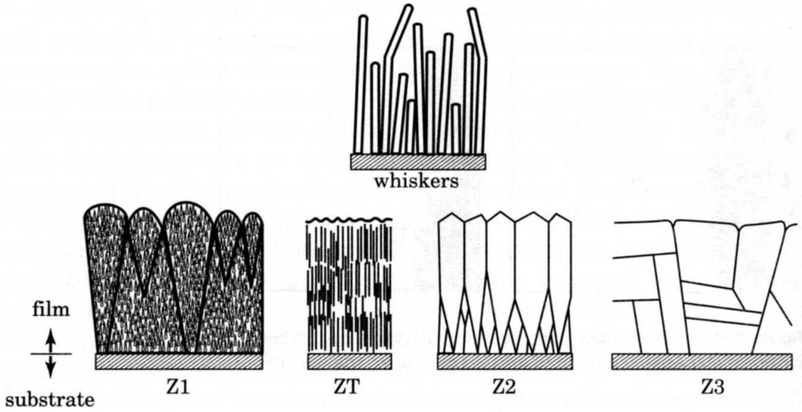

Figure 5.15 Characteristics of the four basic structural zones and of whiskers, in cross section. The ratio of substrate T to film melting T (T_s/T_m) increases in the direction Z1→ZT→Z2→Z3.

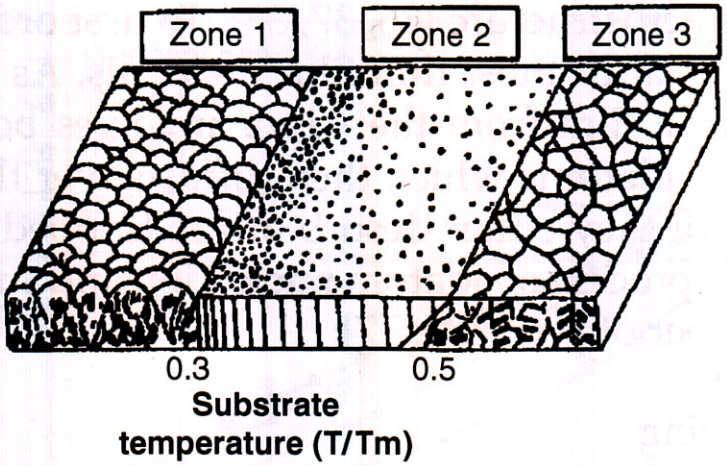

Figure 3.26 Structure zone model of Movechan and Demchishin [39].

Zone 1

- atomic shadowing, low mobility of atoms, continued nucleation
- fibrous grains, pointing at direction of arriving vapor flux, ending with domes shape
- high density of lattice imperfections and pores at grain boundaries
-

Shadow effect

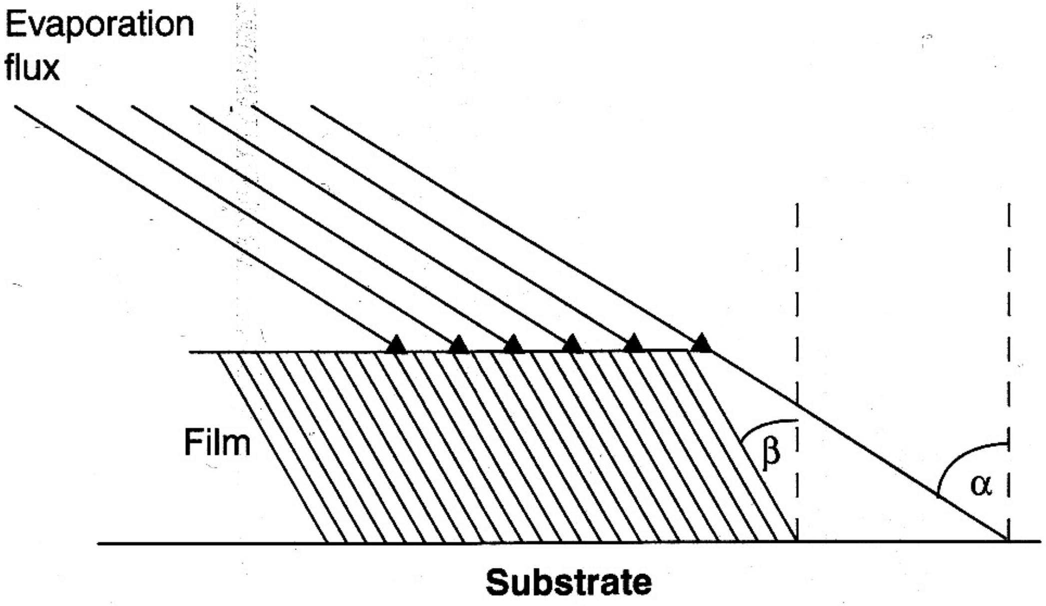

Figure 3.20 Geometry used in the tangent rule [29].

6.2.2012 Koskinen

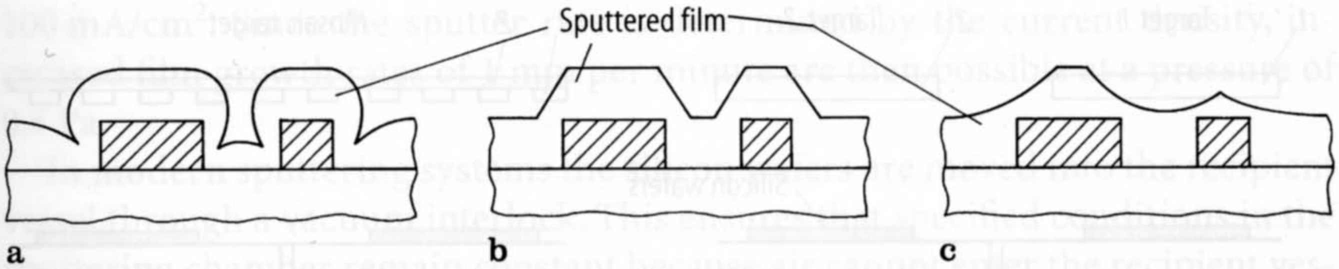

Fig. 3.1.19a-c. Edge coverage of sputtered layers: **a** no bias; **b** moderate bias; **c** heavily biased

Structural hierarchy

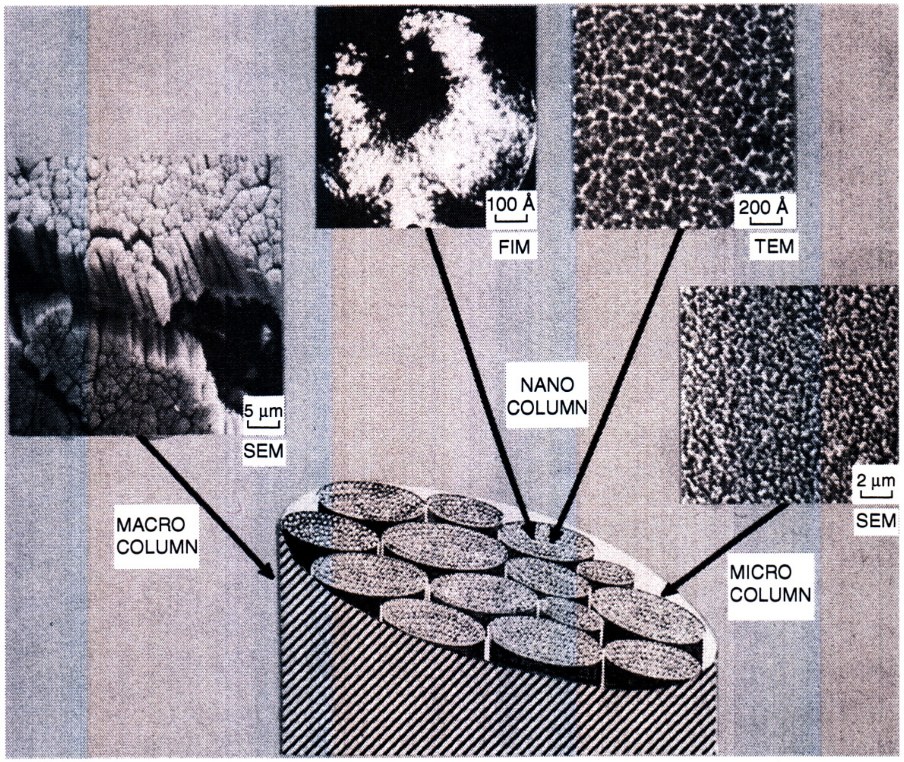

Figure 3.22 Physical structure of nano-, micro and macro columns in a-Ge films [31].

Nodules

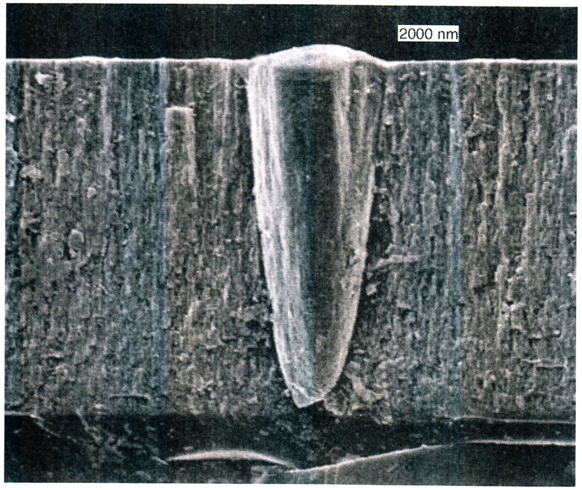

Figure 3.23 Nodule in and AlON rugate filter [28].

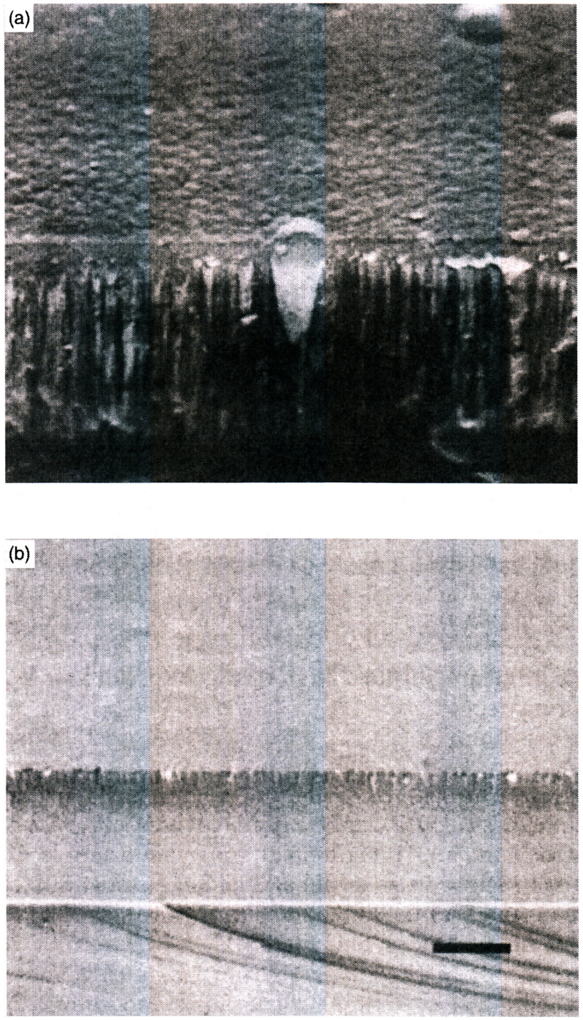

Figure 3.21 SEM micrograph of two SiC films; film (a) had no ion bombardment and film (b) was exposed to ion bombardment [31].

GLAD

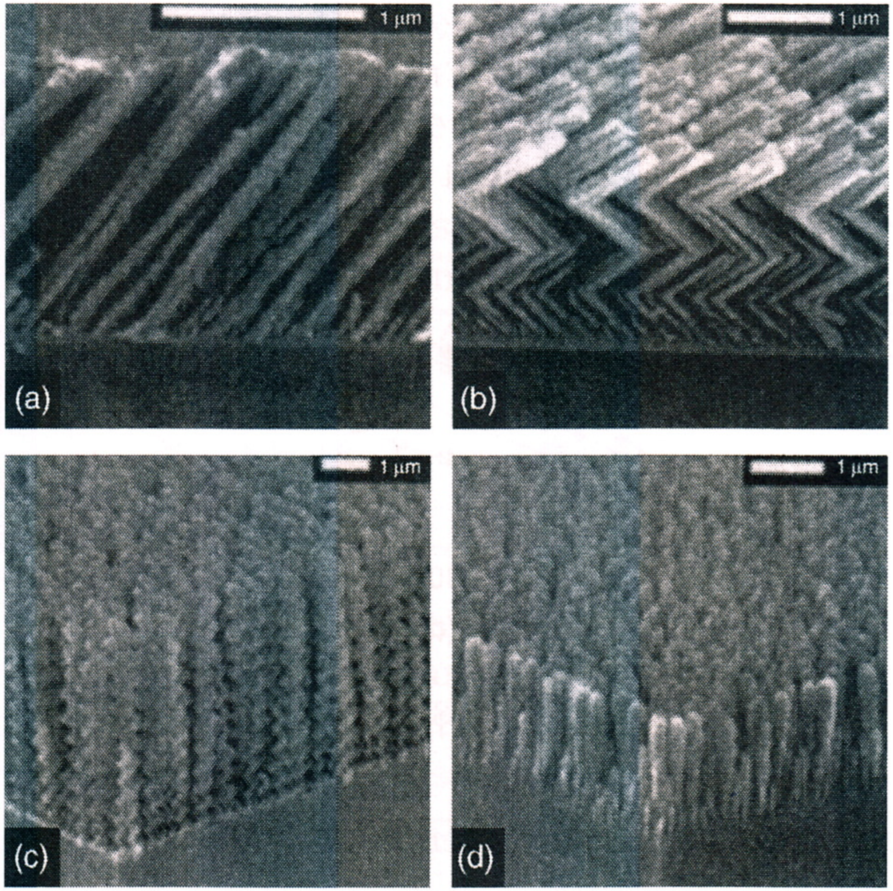

Figure 3.24 Columnar structures fabricated using the GLAD process [32].

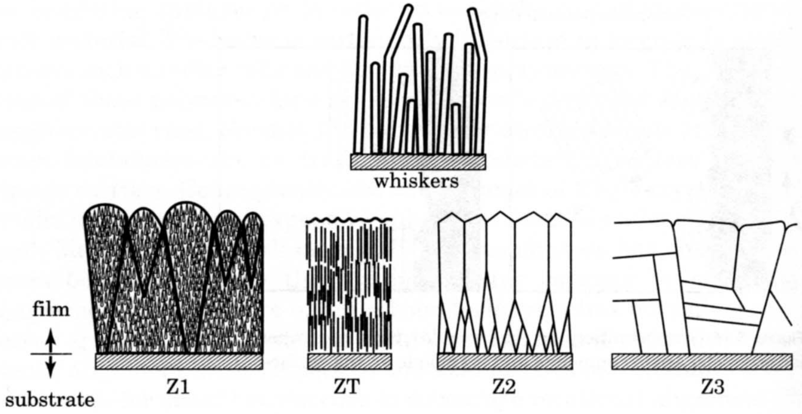

Figure 5.15 Characteristics of the four basic structural zones and of whiskers, in cross section. The ratio of substrate T to film melting T (T_s/T_m) increases in the direction Z1→ZT→Z2→Z3.

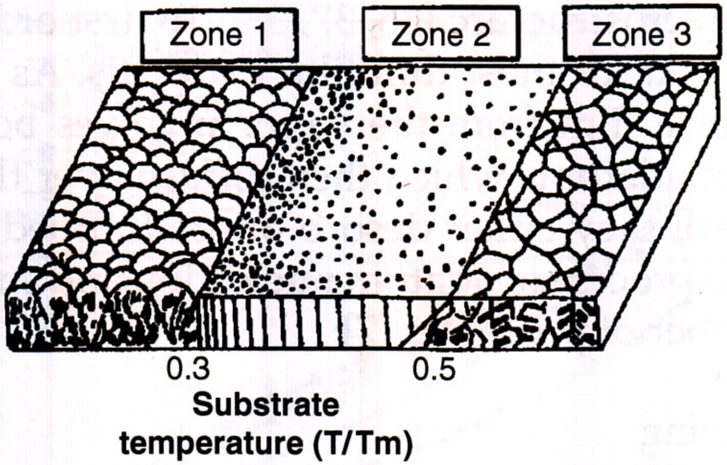

Figure 3.26 Structure zone model of Movechan and Demchishin [39].

Zone 2

- surface diffusion dominates
- uniform columnar grains, grainsize increases with T_h
- faceted surface
- mechanically weak
- electrically favorable e.g. in piezo electrical thin films

Zone T

- transition between zone1 and 2surface diffusion is is “remarkable”
- grain boundary diffusion is limited
- competitive grain growth of V-shaped crystals
- mechanically favorable

Competition of growing crystals

Handbook of Deposition Technologies for Films and Coatings - Science, Applications and Technology (3rd Edition)
Edited by: Martin, Peter M. © 2010 William Andrew Publishing

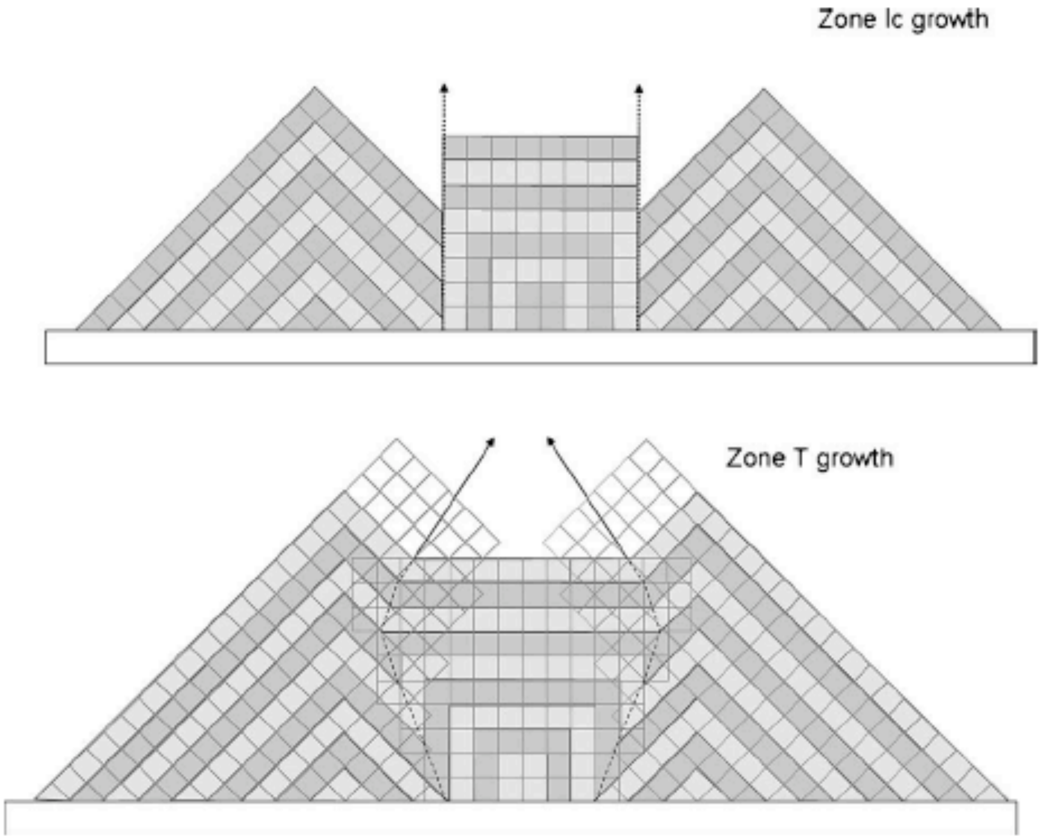

Figure 5.21: Schematic comparison between zone Ic and zone T growth. To indicate the identical normal growth rate of the planes of both grains, alternating coloring is used. In zone T, an overgrowth of one grain by an adjacent grain is observed.

Columnar growth

AlN piezoelectric film

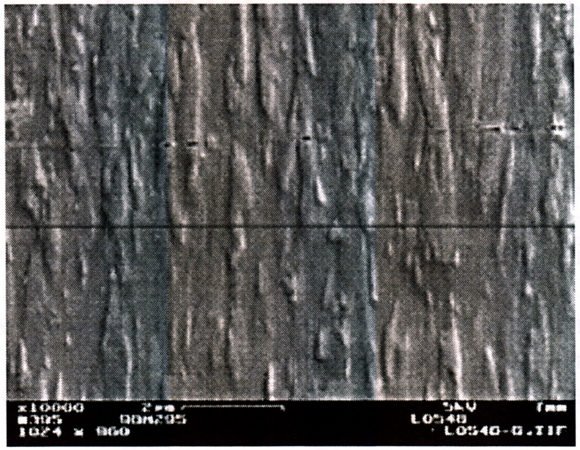

Figure 3.18 SEM picture of well-behaved columnar thin film microstructure.

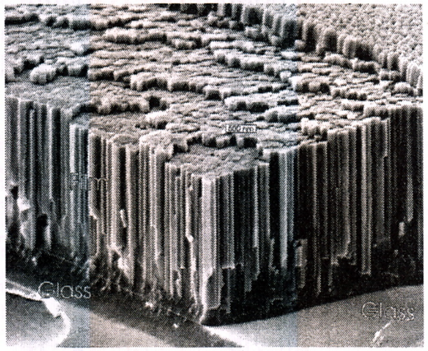

Figure 3.19 Columnar structure in an RF sputtered ALON film [28].

Columnar crystals

15.4.2011 Koskinen

Columnar crystals

15.4.2011 Koskinen

Aalto University
School of Chemical
Technology

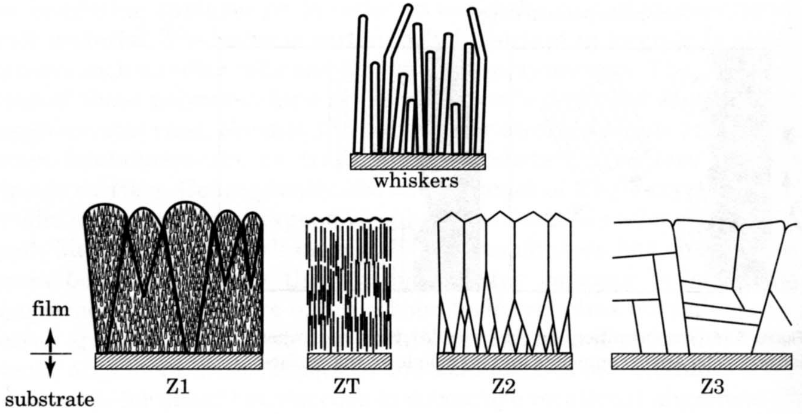

Figure 5.15 Characteristics of the four basic structural zones and of whiskers, in cross section. The ratio of substrate T to film melting T (T_s/T_m) increases in the direction Z1→ZT→Z2→Z3.

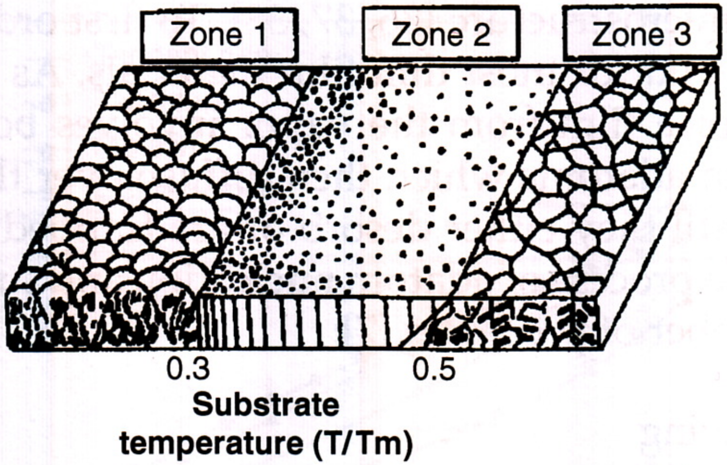

Figure 3.26 Structure zone model of Movechan and Demchishin [39].

Zone 3

- bulk diffusion dominates
- recrystallization of large crystals

Effect of ion energy

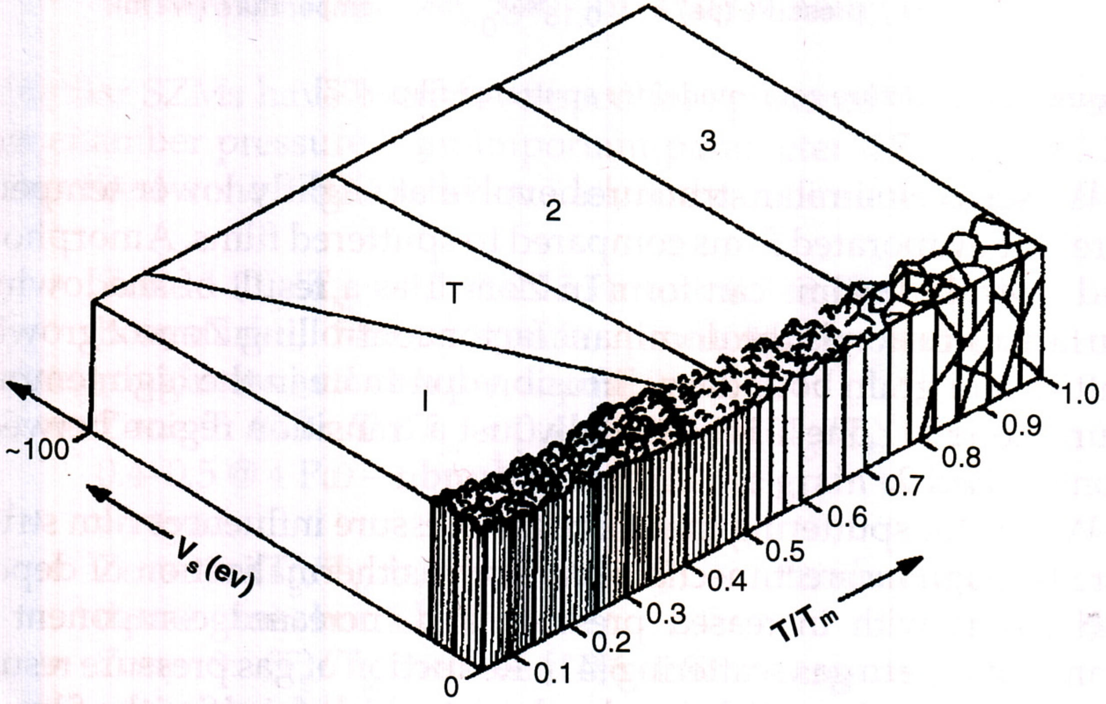

Figure 3.28 Revised SZD for RF sputtering, including ion bombardment.

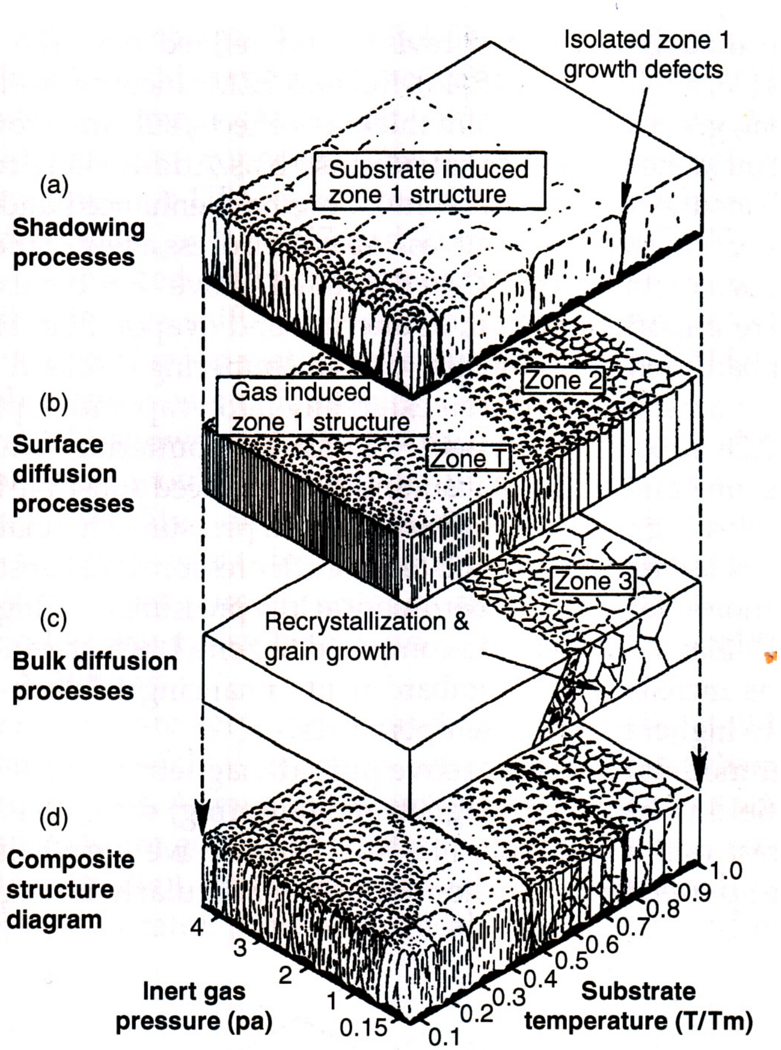

Figure 3.27 Structure zone model for sputtered films [37].

Generalize parameters to all PVD processes

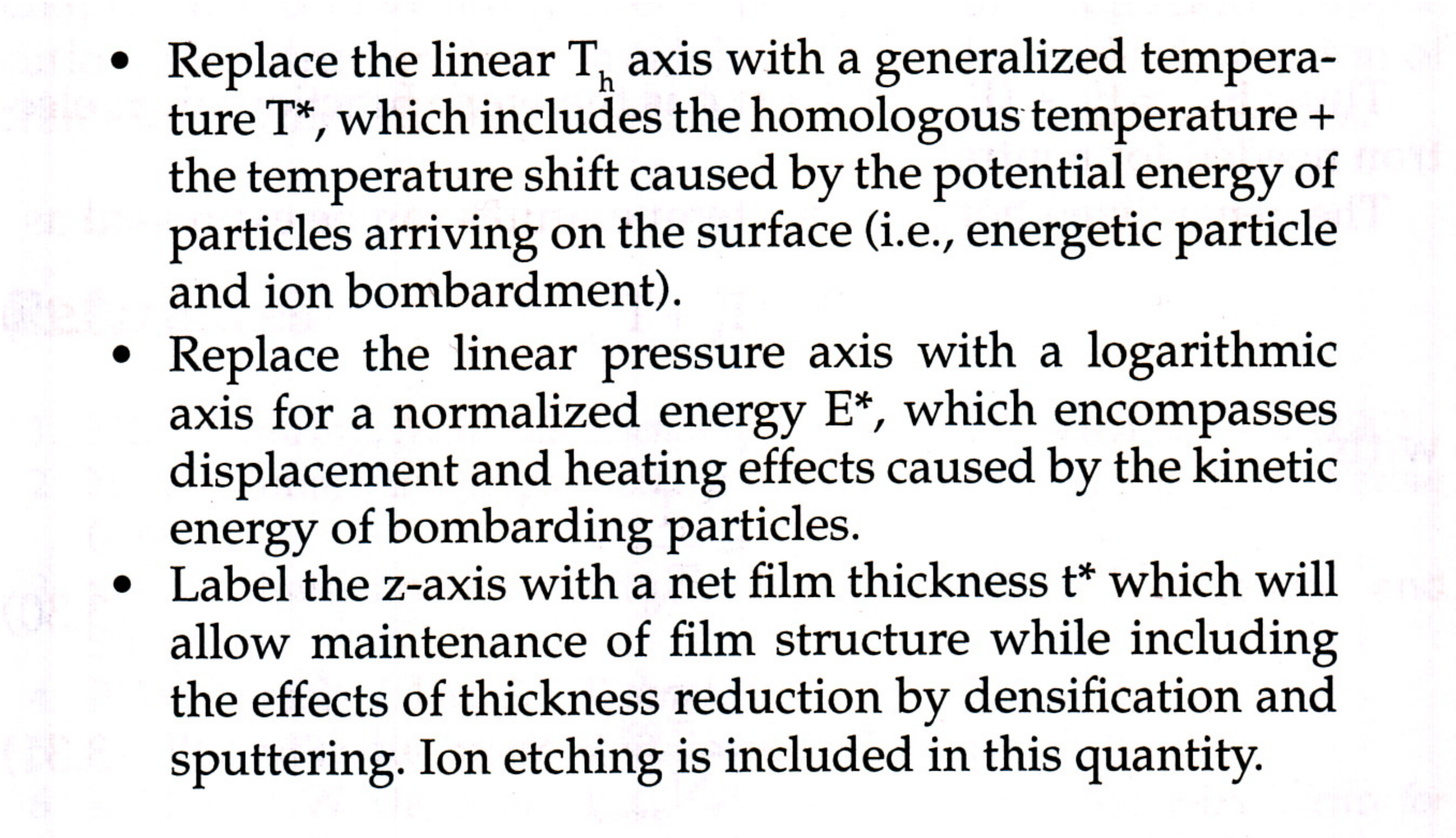

- Replace the linear T_h axis with a generalized temperature T*, which includes the homologous temperature + the temperature shift caused by the potential energy of particles arriving on the surface (i.e., energetic particle and ion bombardment).
- Replace the linear pressure axis with a logarithmic axis for a normalized energy E*, which encompasses displacement and heating effects caused by the kinetic energy of bombarding particles.
- Label the z-axis with a net film thickness t* which will allow maintenance of film structure while including the effects of thickness reduction by densification and sputtering. Ion etching is included in this quantity.

Modified Thorton diagram

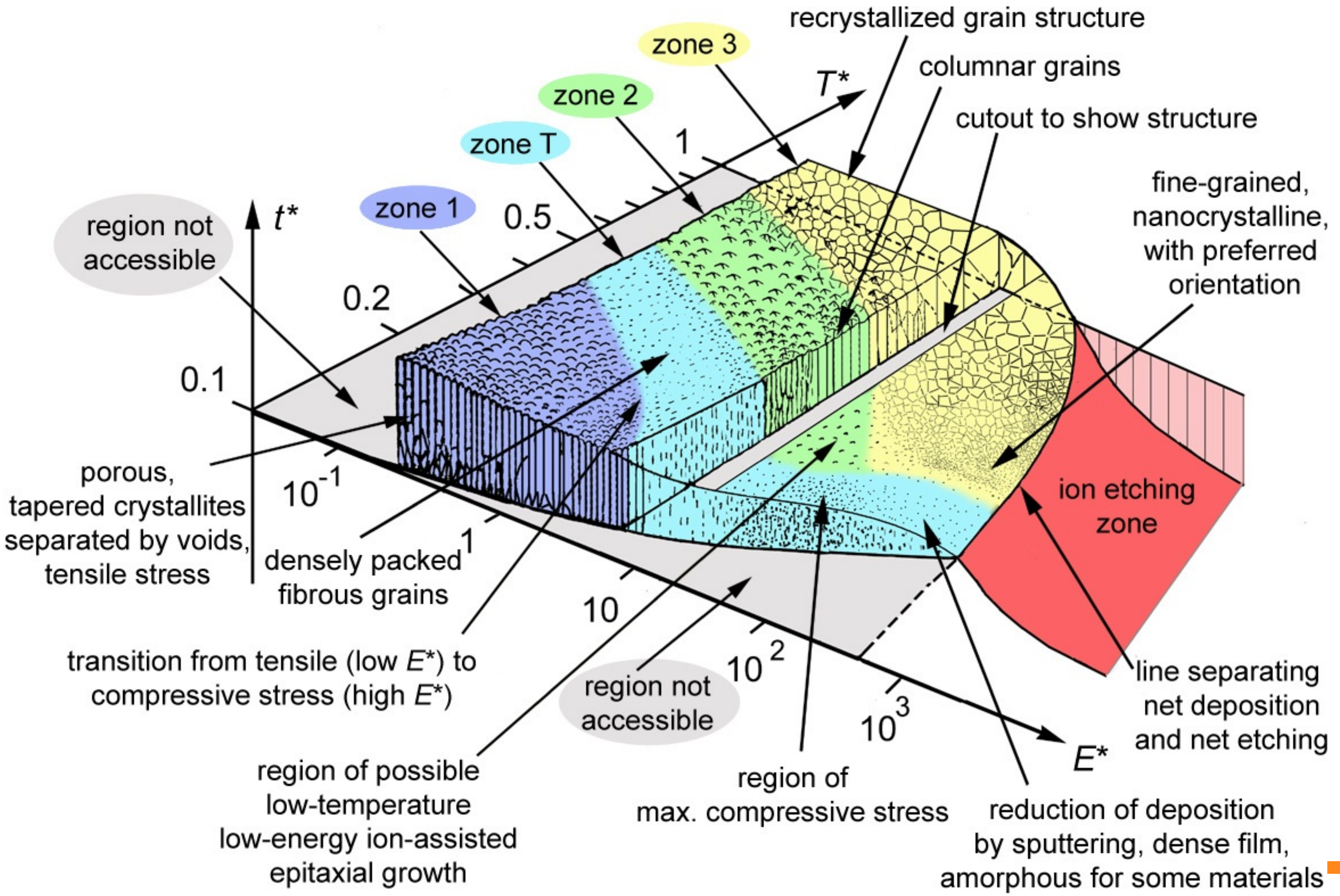

A. Anders, Thin Solid Films 518 (2010) 4087–4090

Reduced parameters SZD

- $T^* = T_h + T_{pot}$
- $T_h = T_s/T_m$
- $E_{pot} = E_c + (E_i - ø)$
- $E_{kin} = E_o + QeV_{sheath}$
- $T_{pot} = E_{pot}/kN_{moved}$
- t^* = thickness

$$E^* = \sum_\alpha \frac{E_{kin,\alpha}}{E_c}\frac{m_\alpha}{m_s}J_\alpha \Big/ \sum_\alpha J_\alpha .$$

- T_s, substrate temperature
- T_m, melting temperature
- E_c heat of sublimation or cohesive energy (1 – 9 eV/atom)
- E_i ionization energy (4 – 10 eV/atom)
- E_{kin} ion kinetic energy
- E_o plasma potential
- V_{sheath} sheath potential
- ø electron work function (c. 4 eV)
- J_a, flux of species a
- m_a, mass of incoming atom
- m_s, mass of surbstrate
- k, Bolzmann constant
- N_{moved}, number of rearranged atoms

A. Anders / Thin Solid Films 518 (2010) 4087–4090

TRIM and SRIM simulations

http://www.srim.org/SRIM/SRIM%2008.pdf

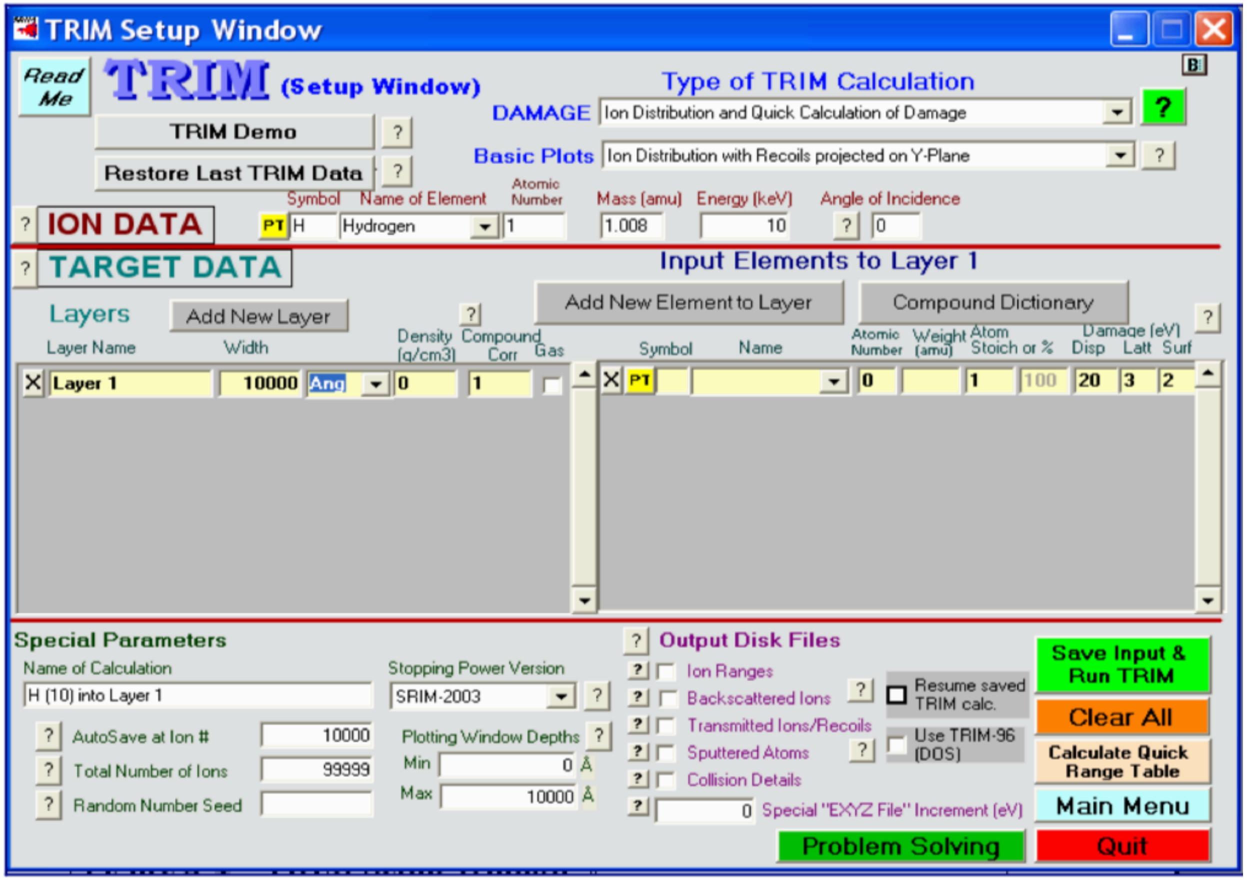

DAMAGE: Ion Distribution and Quick Calculation of Damage

Basic Plots: Ion Distribution with Recoils projected on Y-Plane

ION DATA

Symbol	Name of Element	Atomic Number	Mass (amu)	Energy (keV)	Angle of Incidence
H	Hydrogen	1	1.008	10	0

TARGET DATA

Layer Name	Width	Density (g/cm3)	Compound Corr	Gas
Layer 1	10000 Ang	0	1	☐

Symbol	Name	Atomic Number	Weight (amu)	Atom Stoich	or %	Damage (eV) Disp	Latt	Surf
		0		1	100	20	3	2

Special Parameters

Name of Calculation: H (10) into Layer 1

Stopping Power Version: SRIM-2003

AutoSave at Ion #: 10000

Total Number of Ions: 99999

Random Number Seed:

Plotting Window Depths: Min 0 Å, Max 10000 Å

Output Disk Files

- ☐ Ion Ranges
- ☐ Backscattered Ions
- ☐ Transmitted Ions/Recoils
- ☐ Sputtered Atoms
- ☐ Collision Details
- 0 Special "EXYZ File" Increment (eV)

☐ Resume saved TRIM calc.

☐ Use TRIM-96 (DOS)